

SOME DIELECTRIC AND SPECTROSCOPIC STUDIES
ON HYDROGEN BONDING

by

© M.A. Enayetullah

Submitted in partial fulfillment of
the requirements for the degree of
Master of Science

Thesis Advisor: Professor S. Walker

Department of Chemistry
Lakehead University
Thunder Bay, Ontario, Canada

February 1984

ProQuest Number: 10611699

All rights reserved

INFORMATION TO ALL USERS

The quality of this reproduction is dependent upon the quality of the copy submitted.

In the unlikely event that the author did not send a complete manuscript and there are missing pages, these will be noted. Also, if material had to be removed, a note will indicate the deletion.



ProQuest 10611699

Published by ProQuest LLC (2017). Copyright of the Dissertation is held by the Author.

All rights reserved.

This work is protected against unauthorized copying under Title 17, United States Code
Microform Edition © ProQuest LLC.

ProQuest LLC.
789 East Eisenhower Parkway
P.O. Box 1346
Ann Arbor, MI 48106 - 1346

ABSTRACT

Dielectric relaxation studies were carried out principally on some hydroxy compounds (e.g., phenols) and some carboxylic acids in polystyrene (PS) matrices and, in some cases, in compressed solids (CS). The hydroxy compounds in PS showed at least one absorption each corresponding to the molecular relaxation. In CS and, in some cases, in PS, a second absorption process due to the O-H group relaxation was observed in some of these compounds. The relaxation parameters as well as the Eyring activation parameters for both the molecular relaxation and group relaxation were found to be significantly influenced by hydrogen bonding in several cases.

In general, carboxylic acids showed two families of absorptions. The common absorption process observed for all the acid molecules was attributed to the O-H group relaxation in cyclic acid dimers which has to be preceded by the breakage of hydrogen bonds in the cyclic structures. The other absorption process for a number of the acid molecules was attributed to the molecular relaxation and/or segmental motion. In case of ester molecules a common process due to O-R group reorientation was observed.

One of the goals of the dielectric relaxation studies was to detect the possible involvement of proton tunneling in some compounds of interest; such a process, however, was not detected in the experimental domain.

Infrared absorption and nuclear magnetic resonance studies were carried out on some hydroxy compounds (in CCl_4 solution) in order to supplement the results of dielectric relaxation studies. In alkylphenols the extent of hydrogen bonding was found to be greatly influenced by the steric hindrance of the alkyl groups. NMR results on some alkylphenols were analyzed to obtain the association constants, K_n (for $n=2,3$ and 4) for these molecules. The nature and extent of inter- and/or intramolecular hydrogen bonding in halogenophenols and other hydroxy compounds were revealed by the ir results.

ACKNOWLEDGEMENTS

The experimental work presented in this thesis was carried out at Lakehead University, Thunder Bay, Canada, during the period of Fall 1979 to Summer 1981. The author would like to express his sincere gratitude to Professor S. Walker for his profound interest, continuous encouragement, invaluable guidance, and most important, his patience and understanding without which this work could hardly be completed.

The Graduate School and Chemistry Department of Lakehead University provided financial assistance which the author appreciates very much.

The author would like to thank Dr. M. Desando, Mr. D.L. Gourlay and Dr. S. Qutubuddin for their help in the computer work. He greatly acknowledges the active cooperation and indispensable technical assistance of Mr. B.K. Morgan. Finally, the author would like to thank Mrs. J. Parnell for her encouragement and superb typing.

The thesis is dedicated to the author's parents.

CONTENTS

	Page
CHAPTER I:	
INTRODUCTION.....	1
Outline and Aim.....	2
Basic Theory.....	6
Dielectric Study.....	6
Infrared Absorption Study.....	15
Proton Magnetic Resonance Study.....	18
References.....	20
CHAPTER II:	
EXPERIMENTAL.....	24
Introduction.....	25
The Instruments.....	26
The General Radio (G.R.) Bridge.....	26
The Spectrometers.....	32
Preparation of the Samples.....	32
Analysis of Results.....	36
References.....	42
CHAPTER III:	
INFRARED STUDIES ON SOME PHENOLS AND THEIR H-BONDED COMPLEXES, AND ON SOME OTHER RELATED HYDROXY COMPOUNDS.....	43
Introduction	44
Experimental.....	50
Results.....	51
Discussion.....	51
Alkylsubstituted Phenols and 2-Phenylphenol	51
Halogenophenols.....	58
Hydrogen-bonded Complexes of Phenols...	64
Other Hydroxy Compounds.....	69
References.....	78

	Page
CHAPTER IV: PROTON N.M.R. STUDIES ON HYDROGEN- BONDING EQUILIBRIA OF PHENOL AND SOME HINDERED PHENOLS.....	87
Introduction.....	88
Method of Analysis.....	92
Results and Discussion.....	95
References.....	106
CHAPTER V: DIELECTRIC RELAXATION STUDIES OF SOME PHENOLS AND RELATED COMPOUNDS.....	126
Introduction.....	127
Experimental Results.....	136
Discussion.....	137
References.....	164
CHAPTER VI: DIELECTRIC RELAXATION STUDIES OF SOME CARBOXYLIC ACIDS, ESTERS, AND SOME H- BONDING ACID-BASE SYSTEMS.....	183
Introduction.....	184
Experimental Results.....	196
Discussion.....	198
Acid Molecules.....	198
Salicylic Acid and Ester Molecules.....	214
H Bonding Acid-Base Systems.....	225
References.....	234

LIST OF TABLES

	Page
TABLE III-1	Comparative $\Delta\nu_{\frac{1}{2}}\text{O-H}$ -values for phenol and o-alkylphenols..... 53
TABLE III-2	Base parameters of the organic bases used as proton acceptors..... 68
TABLE III-3	Estimated values of H-bond energies ($-\Delta H$) in the H-bonded complexes of alkylphenols with organic bases..... 70
TABLE III-4	Infrared absorption frequencies for O-H stretching in phenol, alkylphenols and in their H-bonded complexes in CCl_4 solution..... 81
TABLE III-5	Infrared absorption frequencies for O-H stretching in halogenophenols and their H-bonded complexes in CCl_4 solution..... 84
TABLE III-6	Infrared absorption frequencies for O-H stretching in some typical hydroxy compounds..... 86
TABLE IV-1	Comparative values of observed chemical shifts and H bond shifts for different phenols..... 98
TABLE IV-2	Results of N.M.R. studies on H bonding equilibria of phenols obtained by SH method..... 99
TABLE IV-3	Observed chemical shifts for phenol at different concentrations and their theoretical values assuming different monomer-polymer equilibria..... 108

TABLE IV-4	Observed chemical shifts for o-cresol at different concentrations and their theoretical values assuming different monomer-polymer equilibria.....	109
TABLE IV-5	Observed chemical shifts for 2-ethylphenol at different concentrations and their theoretical values assuming different monomer-polymer equilibria.....	110
TABLE IV-6	Observed chemical shifts for 2-isopropylphenol at different concentrations and their theoretical values assuming different monomer-polymer equilibria.....	111
TABLE IV-7	Observed chemical shifts for 2-t-butylphenol at different concentrations and their theoretical values assuming different monomer-polymer equilibria.....	112
TABLE IV-8	Observed chemical shifts for 2,4,6-trimethylphenol at different concentrations and their theoretical values assuming different monomer-polymer equilibria.....	113
TABLE IV-9	Observed chemical shifts for 2,6-diisopropylphenol at different concentrations and their theoretical values assuming different monomer-polymer equilibria.....	114
TABLE IV-10	Observed chemical shifts for 2,6-di-t-butylphenol at different concentrations.....	115

	Page
TABLE V-1	Calculated dipole moments for 2,6-dichlorophenol..... 144
TABLE V-2	Eyring analysis results for some phenols and related compounds..... 167
TABLE V-3	Tabulated summary of Fuoss- Kirkwood analysis parameters and effective dipole moments (μ) for phenols and related compounds..... 173
TABLE VI-1	Approximate lengths and ΔH_E -values of several acid and rigid molecules.... 210
TABLE VI-2	Tabulated summary of Fuoss-Kirkwood analysis parameters and effective dipole moments for carboxylic acids.... 237
TABLE VI-3	Tabulated summary of Fuoss-Kirkwood analysis parameters and effective dipole moments for salicylic acid and some esters..... 240
TABLE VI-4	Tabulated summary of Fuoss-Kirkwood Analysis parameters for some H- bonding acid-base systems..... 243
TABLE VI-5	Eyring analysis results for some carboxylic acids..... 247
TABLE VI-6	Eyring analysis results for salicylic acid and some esters..... 248
TABLE VI-7	Eyring analysis results for some H bonding acid-base systems..... 249

TABLE VI-8	Comparative Eyring analysis results for the process I in acid-base systems and for molecular relaxation of some rigid molecules	250
------------	---	-----

TABLE VI-9	Comparative Eyring analysis results for the process II in acid-base systems and for the process A in acids	251
------------	--	-----

LIST OF FIGURES

		Page
FIGURE II-1	Schematic diagram of the electrode assembly.....	29
FIGURE III-1	Infrared spectra of phenol, o-cresol, 2-ethylphenol, 2-isopropylphenol, 2-t-butylphenol and 2-phenylphenol.....	54
FIGURE III-2	Infrared spectra of 2,4,6-trimethylphenol, 2,6-diisopropylphenol, 2,4,6-tri-t-butylphenol and 2,6-di-t-butylphenol.....	57
FIGURE III-3	Infrared spectra of o-chlorophenol, o-bromophenol and o-iodophenol.....	59
FIGURE III-4	Infrared spectra of 2,6-dichlorophenol, 2,4,6-tribromophenol and 2,4,6-tri-iodophenol.....	62
FIGURE III-5	Infrared spectra of 2,4,6-trichlorophenol, 2,4,6-tribromophenol and 2,4,6-tribromophenol and 2,4,6-tri-iodophenol at higher concentrations....	63
FIGURE III-6	Infrared spectra of 2-isopropylphenol and its complexes with methylcyanide, 1,4-dioxane and pyridine.....	66
FIGURE III-7	Infrared spectra of salicylaldehyde, salicylic acid and methylsalicylate....	73
FIGURE III-8	Infrared spectra of tropolone, 2,4-pentanedione and dibenzoylmethane.....	75

FIGURE III-9	Infrared spectra of 1-naphthol, 2-naphthol and 6-bromo-2-naphthol.....	77
FIGURE IV-1	Plots of observed chemical shift (Hz) versus molar concentration for phenol, o-cresol, 2-ethylphenol and 2-isopropylphenol.....	116
FIGURE IV-2	Plots of observed chemical shift (Hz) versus molar concentration for 2-t-butylphenol, 2,4,6-trimethylphenol, 2,6,-diisopropylphenol and 2,6-di-t-butylphenol.....	117
FIGURE IV-3	Plots of observed H bond shift, $\nu - \nu_1$ (Hz) versus log C for o-cresol, 2-ethylphenol and 2-isopropylphenol.....	118
FIGURE IV-4	Plots of experimental and theoretical (n=2, 3 and 4) chemical shifts versus log C for phenol.....	119
FIGURE IV-5	Plots of experimental and theoretical (n=2, 3 and 4) chemical shifts versus log C for o-cresol.....	120
FIGURE IV-6	Plots of experimental and theoretical (n=2, 3 and 4) chemical shifts versus log C for 2-ethylphenol.....	121
FIGURE IV-7	Plots of experimental and theoretical (n=2, 3 and 4) chemical shifts versus log C for 2-isopropylphenol.....	122
FIGURE IV-8	Plots of experimental and theoretical (n=2, 3 and 4) chemical shifts versus log C for 2-t-butylphenol.....	123
FIGURE IV-9	Plots of experimental and theoretical (n=2, 3 and 4) chemical shifts versus log C for 2,4,6-trimethylphenol.....	124

FIGURE IV-10	Plots of experimental and theoretical (n=2, 3 and 4) chemical shifts versus log C for 2,6-diisopropylphenol.....	125
FIGURE V-1	Plots of dielectric loss factor versus log of frequency for 2,6-dichlorophenol at different temperatures.....	174
FIGURE V-2	Plots of dielectric loss factor versus log of frequency for 2-naphthol at different temperatures.....	175
FIGURE V-3	Plots of dielectric loss factor versus log of frequency for tropolone at different temperatures.....	176
FIGURE V-4	Plots of dielectric 3,3-deutero-2,4-pentanedione at different temperatures.	177
FIGURE V-5	Eyring plots of $\log(\tau T)$ versus $1/T$ for 2-ethylphenol and 2-isopropylphenol.....	178
FIGURE V-6	Eyring plots of $\log(\tau T)$ versus $1/T$ for 4-phenylphenol in the compressed solid and the low temperature process in 6-bromo-2-naphthol.....	179
FIGURE V-7	Eyring plots of $\log(\tau T)$ versus $1/T$ for tropolone and 2-t-dichlorophenol.....	180
FIGURE V-8	Eyring plots of $\log(\tau T)$ versus $1/T$ for 2,4-pentanedione and 3,3-deutero-2,4-pentanedione.....	181
FIGURE V-9	Eyring plots of $\log(\tau T)$ versus $1/T$ for dibenzoylmethane.....	182

FIGURE VI-1	Plots of dielectric loss factor (ϵ'') versus log of frequency for acetic acid at different temperatures.....	252
FIGURE VI-2	Plots of dielectric loss factor (ϵ'') versus log of frequency for trichloroacetic acid at different temperatures.....	253
FIGURE VI-3	Plots of dielectric loss factor (ϵ'') versus log of frequency for 2-naphthoic acid at different temperatures.....	254
FIGURE VI-4	Plots of dielectric loss factor (ϵ'') versus log of frequency for methylsalicylate at different temperatures.....	255
FIGURE VI-5	Eyring plots of $\log(\tau T)$ versus $1/T$ for valeric acid, trichloroacetic acid and benzoic acid.....	256
FIGURE VI-6	Eyring plots of $\log(\tau T)$ versus $1/T$ for methylsalicylate in a polystyrene matrix and compressed solid and for biphenylcarboxylic acid.....	257
FIGURE VI-7	Eyring plots of $\log(\tau T)$ versus $1/T$ for low temperature processes in formic acid + pyridine and acetic acid + pyridine.....	258

CHAPTER I: INTRODUCTION

OUTLINE AND AIM

The phenomenon of hydrogen bonding (henceforth written as H bonding) because of its special significance in the fields of chemistry, chemical physics and molecular biology, has been investigated extensively by a variety of spectroscopic and other physical methods; theoretical approaches have also been developed side-by-side in order to interpret experimental findings as well as to explain the origin and nature of this typical bonding force. The extensive study, particularly over the last five decades, is evidenced by the volume of literature devoted to this single phenomenon. Several texts and monographs (1-5) and a number of review articles (6-16) the comprehensive literature on H bonding; besides hundreds of research papers and articles have so far been published in various journals and periodicals, the relevant ones of which will be referred to whenever necessary.

From the survey of the literature dealing with various aspects of H bonding one can apparently draw two broad outlines regarding recent developments in theoretical

and experimental studies on this subject.

- i) With the advent of very high speed computers theoretical methods and techniques have reached a high degree of refinement as a result of which complex problems of mechanism of H bonding and of charge redistribution accompanying H bond formation in a number of molecular systems have been investigated with considerable success. Besides, these methods have been utilized (8,9,17) to predict and to interpret such experimental quantities as energy of complex (H bonded) formation, complex geometry, inter and intramolecular force constants and potential functions, chemical shifts, electronic transitions, and so on.

- ii) Of various experimental methods, infrared absorption and nuclear magnetic resonance spectroscopy have provided very sensitive means of detecting H bond formation and have been extensively employed in both qualitative and quantitative studies of H bonded systems. Nevertheless, these are not the only means available and other techniques such as dielectric and thermochemical measurements and x-ray and neutron diffraction have also provided fruitful results.

Dielectric investigations are becoming increasingly important as a tool for studying the nature of H-bonding. Several texts on H bonding (1,2,5) and books and reviews on dielectric studies (17-20) contain contributions on dielectric phenomenon of H bonding systems. Of particular interest is the application of relaxation kinetics to these systems which has recently become an important and promising experimental approach. Relaxation studies by various techniques on H bonding have been reviewed (21-23) which reveal the potential of these techniques.

This thesis contains some dielectric and spectroscopic (infrared absorption and nuclear magnetic resonance) studies of some potential systems involving H bonding as well as of some related molecules. The main aim has been the investigation of the relaxation behaviour of these systems by dielectric absorption technique. Relaxation kinetic study of molecular systems provide Eyring activation parameters for both molecular and intramolecular motions which, in turn, can reveal molecular size and structure as well as the nature of molecular interactions involved therein.

In recent years dielectric absorption study of polar solutes dispersed in polymer matrices has drawn considerable interest and it has been found to yield reasonably reliable relaxation parameters as compared to other relaxation techniques (n.m.r. and ultrasonic) (24). Advantageous features of polymer matrix technique are: (i) for a system of flexible polar molecule where both molecular and intramolecular processes occur simultaneously, the former can be slowed down or may be eliminated (25) without affecting the other significantly so that either or both of the processes can be studied separately; and (ii) as opposed to limited temperature ranges accessible to solution studies, polystyrene matrix technique permits measurements over much wider ranges of frequency and of temperature.

The major chapters (Ch. V and VI) of this thesis deal with dielectric relaxation studies of molecular systems of our interest dispersed in atactic polystyrene matrices, and, in some cases, in the compressed solid state. Infra-red and n.m.r. studies have been made in order to supplement results of these dielectric studies; these are given in chapters III and IV, respectively.

BASIC THEORY

Dielectric Study

The basic principles and fundamental equations for dealing with dielectric absorptions are well established. Basically the dielectric absorption is related to the frequency-dependence of polarization of the dielectric material. The total polarization (P_T) of a polar molecule is given by the Clausius-Mossotti-Debye theories (26) as:

$$\begin{aligned} P_T &= P_E + P_A + P_O \\ &= \frac{4\pi N}{3} \left(\alpha_E + \alpha_A + \frac{\mu^2}{3kT} \right) = \frac{\epsilon_0 - 1}{\epsilon_0 + 2} \left(\frac{M}{d} \right) \end{aligned} \quad 1.1$$

where α is the polarizability, M the Avogadro number, μ is the electric dipole moment, k the Boltzmann constant, T the absolute temperature, ϵ_0 the static dielectric constant, M the gram molecular weight, and d is the density (g ml^{-1}) of the material. The subscripts E, A and O in P indicate the electronic, atomic and orientation polarizations, respectively.

The Clausius-Mossotti-Debye theories are applicable to gases but are often inadequate when applied to polar

liquids due to the invalidity of the Lorenz field used in these theories as a measure of the local field in a dipolar dielectrics.

The dielectric constant or permittivity may be expressed in terms of polarizability. In order to obtain a relation between permittivity and dipole moment which should have wider range of validity including liquids and solids Onsager (26) developed the equation:

$$\frac{(\epsilon_0 - \epsilon_\infty)(2\epsilon_0 + \epsilon_\infty)}{\epsilon_0(\epsilon_\infty + 2)^2} \cdot \frac{M}{\bar{d}} = \frac{4\pi N \mu^2}{9KT} \quad \text{I-2}$$

where ϵ_∞ is the optical dielectric constant at very high frequencies when the orientation polarization vanishes. Equation I-1 then becomes:

$$\frac{\epsilon_\infty - 1}{\epsilon_\infty + 2} \cdot \frac{M}{\bar{d}} = \frac{4\pi N}{3} (\alpha_E + \alpha_A) \quad \text{I-3}$$

Combinations of equations I-1 and I-3 gives the Debye equation:

$$\frac{3(\epsilon_0 - \epsilon_\infty)}{(\epsilon_0 + 2)(\epsilon_\infty + 2)} \cdot \frac{M}{\bar{d}} = \frac{4\pi N \mu^2}{9kT} \quad \text{I-4}$$

Equations I-2 and I-4 allow a comparison of the values of μ^2 obtained from Onsager and Debye equations thus:

$$\frac{\mu^2(\text{Onsager})}{\mu^2(\text{Debye})} = \frac{(2\varepsilon_0 + \varepsilon_\infty)(\varepsilon_0 + 2)}{3\varepsilon_0(\varepsilon_\infty + 2)} \quad \text{I-5}$$

For gases at low pressures ε_0 and ε_∞ are practically identical, and obviously the Onsager equation then reduces to the Debye equation.

Polarizability is dependent on the frequency of the applied field, and all types of molecular polarization can reach their equilibrium values up to certain frequency limit which, for simple polar molecules in nonpolar solvents, is of the order of 10^8 Hz. In this lower frequency range the dielectric constant is numerically equal to that obtained when a static field is employed. But as the frequency is increased beyond this limit, the reorientation of molecular dipoles, at some point, lag behind field oscillation, and polarization falls off producing less and less contribution to the total permittivity. The resulting phase displacement (δ) leads to a dissipation of energy, as joule heating, in the medium, the measure of which is given by dielectric loss (ε'') defined as:

$$\epsilon'' = \epsilon' \tan \delta \quad \text{I-6}$$

where ϵ' is the real part of the dielectric constant and $\tan \delta$ is the loss tangent or the energy dissipation factor. In this frequency region the dielectric constant becomes a complex quantity ϵ^* given by:

$$\epsilon^* = \epsilon' - i\epsilon'', \quad (i = \sqrt{-1}) \quad \text{I-7}$$

The frequency dependence of the complex permittivity is given by:

$$\frac{\epsilon^* - \epsilon_\infty}{\epsilon_0 - \epsilon_\infty} = \frac{1}{1 + i \omega \tau} \quad \text{I-8}$$

where ϵ_0 and ϵ_∞ are the low and high frequency limiting values of ϵ^* , respectively, ω is the angular frequency in rads s^{-1} , and τ is the characteristic relaxation time in seconds which is defined (27) as the time required for the polarization to decay to $\frac{1}{e}$ times its original value. A combination of equations I-7 and I-8 followed by separation into real and imaginary parts lead to the following equations due to Debye and Pellat:

$$\frac{\epsilon' - \epsilon_{\infty}}{\epsilon_0 - \epsilon_{\infty}} = \frac{1}{1 + (\omega\tau)^2} \quad \text{I-9}$$

$$\frac{\epsilon''}{\epsilon_0 - \epsilon_{\infty}} = \frac{\omega\tau}{1 + (\omega\tau)^2} \quad \text{I-10}$$

The quantity ϵ'' in equation I-10 becomes maximum when $\omega\tau=1$, and this permits evaluation of the relaxation time from the known frequency of maximum absorption. Elimination of $\omega\tau$ from equations I-9 and I-10 gives the following equation:

$$\left(\epsilon' - \frac{\epsilon_0 + \epsilon_{\infty}}{2}\right)^2 + \epsilon''^2 = \left(\frac{\epsilon_0 - \epsilon_{\infty}}{2}\right)^2 \quad \text{I-11}$$

This is the equation of a semi-circle which leads to a Cole-Cole plot when ϵ'' is plotted against ϵ' in a complex plane at the same frequency. The values of ϵ_0 and ϵ_{∞} are obtained from the intersections on the ϵ' axis in this plot.

The foregoing equations of permittivity apply (28) to both solids and liquids and are valid for systems involving a single relaxation process characteristic of

the Debye behaviour. Many solids show dielectric absorption wider than normal Debye curves due to the presence of a range of relaxation times, and these are frequently represented by Fuoss-Kirkwood equation (29).

$$\epsilon''_{\text{obs}} = \epsilon''_{\text{max}} \operatorname{sech} \beta \ln \frac{f_{\text{obs}}}{f_{\text{max}}} \quad \text{I-12}$$

where f_{obs} is the frequency in Hz, f_{max} is the frequency at which maximum absorption occurs, and β is an empirical constant known as the distribution parameter, which measures absorption width and may have values between unity for a single relaxation and zero for an infinite range.

Assuming a continuous relaxation time about the most probable values τ_0 , Cole and Cole developed the general dispersion equation:

$$\frac{\epsilon^* - \epsilon_\infty}{\epsilon_0 - \epsilon_\infty} = \frac{1}{1 + (i\omega\tau_0)^{1-\alpha}} \quad \text{I-13}$$

where α is the distribution parameter which varies between zero to unity. Equation I-13 can be rationalized to give:

$$\frac{\epsilon'_0 - \epsilon'_\infty}{\epsilon_0 - \epsilon_\infty} = \frac{1 + (\omega\tau_0)^{1-\alpha} \sin(\alpha\pi/2)}{1 + 2(\omega\tau_0)^{1-\alpha} \sin(\alpha\pi/2) + (\omega\tau_0)^{2(1-\alpha)}} \quad \text{I-14}$$

and

$$\frac{\epsilon''_0}{\epsilon_0 - \epsilon_\infty} = \frac{(\omega\tau_0)^{1-\alpha} \sin(\alpha\pi/2)}{1 + 2(\omega\tau_0)^{1-\alpha} \sin(\alpha\pi/2) + (\omega\tau_0)^{2(1-\alpha)}} \quad \text{I-15}$$

For $\alpha = 0$, the equations I-13-15 reduce to Debye-Pellat equations I-8-10 respectively.

Further modified equation was given by Davidson and Cole (31) for systems for which the complex plane plot is not symmetrically semicircular, i.e. a skewed arc; this equation is:

$$\frac{\epsilon^* - \epsilon_\infty}{\epsilon_0 - \epsilon_\infty} = \frac{1}{(1 + i\omega\tau_0)^h} \quad \text{I-16}$$

where h is again as constant, $0 < h < 1$, with $h=1$ corresponding to Debye-Pellat equation I-9.

The modified equations mentioned above have been applied to account for a distribution of a range of relaxation times in Debye process. In some cases, however, dielectric absorptions are characterized by more than one discrete relaxation process each of which independently shows Debye behaviour. For such systems Budó developed the following equation which sums up the Debye terms:

$$\frac{\epsilon^* - \epsilon_\infty}{\epsilon_0 - \epsilon_\infty} = \sum_{k=0}^N \frac{C_k}{1 + 2\omega\tau_k} \quad \text{I-17}$$

where τ_k is the relaxation time for the k th mode of relaxation and C_k is a factor (called weight factor) representing the proportion of contribution of the k th mode to the total dispersion. Thus, for systems having two discrete processes with relaxation times τ_1 and τ_2 the following equations can be deduced:

$$\frac{\epsilon' - \epsilon_\infty}{\epsilon_0 - \epsilon_\infty} = \frac{C_1}{1 + (\omega\tau_1)^2} + \frac{C_2}{1 + (\omega\tau_2)^2} \quad \text{I-18}$$

$$\frac{\epsilon''}{\epsilon_0 - \epsilon_\infty} = \frac{C_1 \omega\tau_1}{1 + (\omega\tau_1)^2} + \frac{C_2 \omega\tau_2}{1 + (\omega\tau_2)^2} \quad \text{I-19}$$

where C_1 and C_2 are weight factors and $C_1 + C_2 = 1$. The relative magnitudes of τ_1 and τ_2 in such cases can be obtained from the complex plane plot and the weight factors, but may often be approximated by a sector of the semicircle (23).

The common practice in the dielectric experiments is to employ one or the other of the several empirical relationships discussed above for the analysis of experimental results. Most commonly used equations are those due to Cole-Cole, Cole-Davidson and Fuoss-Kirkwood. Each of these equations have been found suitable for certain types of systems but not for others, so that one has to make proper choices for one's system of interest.

Infrared Absorption Study

The formation of hydrogen bonds (X-H...Y) gives rise to the following prominent effects in the infrared spectra of the systems:

- i) the stretching mode (ν_{X-H}) and its harmonics are shifted to lower wavenumbers.
- ii) the bandwidth of the fundamental is increased, sometimes with the appearance of unresolved submaxima.
- iii) the integrated intensity of the fundamental is increased, sometimes by factors of up to ten or more, while the corresponding overtones decrease slightly in intensity.

These features are dependent on the phase and medium of the H-bonded complex as well as on temperature.

Basic theories of spectral modifications due to H-bonding have been discussed elsewhere (9,32,33,34,35) and will not be given here; only the brief outlines are as follows:

For a diatomic molecule X-H, a close replica of a harmonic oscillator, the quantum mechanical solution for λ yields the following equation for the vibrational frequency (ω):

$$\Delta E = hc\omega = \frac{1}{2\pi} \left(\frac{k}{\mu}\right)^{\frac{1}{2}} \quad \text{I-20}$$

where h is Plank's constant, c is the velocity of light and μ is the reduced mass. The force constant k may be regarded as a measure of the stiffness of the springlike bond and is directly proportional to the frequency ω .

The lowering of the $\nu_{\text{X-H}}$ frequency was first attributed to the weakening of the X-H bond on the formation of the H-bond. This hypothesis is supported by the observed lengthening of X-H bond by 0.1 to .2 Å in hydrogen-bonded crystal (2,10). Semiempirical calculations (36), however, have shown that the force constant of the X-H bond decreases but not sufficiently to account for the totality of the frequency shift. Another significant factor modifying the frequency has been found to be the change in anharmonicity of the stretching vibration while forming the H-bonded complex (37).

The nature and extent of spectral modifications caused by H-bond formation can, in turn, affect various chemical and physical properties as well as some molecular parameters. Extensive infrared studies can thus be a valuable means for studying these properties and parameters of H-bonded systems.

Proton Magnetic Resonance Study

Proton magnetic resonance measurements provide a very common and fruitful method for studying H-bonding where the most informative experimental parameter is the chemical shift, in the case of H-bonding, generally shown as H bonding shift or association shift. The formation of hydrogen bond $X-H \cdots Y$ modifies the electron density around the proton of the X-H group resulting, generally, in the downfield shift of the proton involved in the association, with the exception of some cases involving aromatic molecules when a diamagnetic shift is observed due to shielding of the π -electrons (38). The basic principles underlying the association shift are now fairly established and have been discussed by several authors (13,39,40).

There are several contributing factors to the H bonding shift; these are:

- i) the electronegative acceptor group Y tends to draw the H away from the electronic environment of X-H bond; this deshielding of the H causes its resonance signal to occur at lower magnetic fields than in the absence of Y. Generally, this is the principal contri-

bution to the observed association shift.

ii) The electron currents flowing through the Y-system set up a magnetic field which may contribute to the secondary magnetic field at the proton, and if this has a nonzero average, there will be a net contribution to the proton chemical shift. This contribution can be either positive or negative, but will be positive if the principal symmetry axis of Y be along X-H.

iii) Another possible contribution to association shift could be due to the quenching of intramolecular paramagnetic effects of neighbouring atom magnetic anisotropy. This results in a down field shift upon the formation of nonlinear H bonds, because of the loss of axial symmetry.

Thus, obviously the relative position of the resonance signal indicates greater or lesser extent of H bonding, a lower field shift corresponding to greater extent of H bonding. This generalization is fairly approximate, although electronic screening, steric hindrance, and inductive effects should not be ignored completely.

REFERENCES

1. D. Hadzi and H. W. Thompson, Ed., "Hydrogen Bonding", Pergamon Press, Oxford, 1959.
2. G. C. Pimentel and A. L. McClellan, "The Hydrogen Bond", W. H. Freeman and Co., San Francisco, 1960.
3. W. C. Hamilton and J. A. Ibers, "Hydrogen Bonding in Solids", W. A. Benjamin, New York, N.Y., 1968.
4. S. N. Vinogradov and R. H. Linnell, "Hydrogen Bonding", Van Nostrand Reinhold, New York, N.Y., 1971.
5. P. Schuster, G. Zundel and C. Sandorfy, Ed., "The Hydrogen Bond", North Holland Publishing Company, Oxford, 1976.
6. L. Pauling, "The Nature of the Chemical Bond", Cornell University Press, Ithaca, N.Y., 1960.
7. S. Bratoz, Advan. Quantum Chem., 1967, 3, 209.
8. A. S. N. Murthy and C. N. R. Rao, J. Mol. Structure, 1970, 6, 253.
9. P. A. Kollman and L. C. Allen, Chem. Rev., 1972, 72, 283.
10. G. C. Pimentel and A. L. McClellan, Ann. Rev. Phys. Chem., 1971, 22, 347.
11. H. E. Hallam in "Infrared Spectroscopy and Molecular Structure", M. Davis (Ed.), Elsevier Publishing Co., Amsterdam, 1963.
12. A. S. N. Murthy and C. N. R. Rao, Appl. Spectr. Rev., 1968, 21, 1.
13. J. C. Davis, Jr. and K. K. Deb, Adv. Magn. Resonance, 1970, 4, 201.

References continued...

14. C. N. R. Rao and A. S. N. Murthy, *Develop. Appl. Spectroscopy*, 1970, 7B, 54.
15. K. D. Moller and W. G. Rothschild, "Far Infrared Spectroscopy" Ch. 6, Wiley Interscience, 1971.
16. J. Emsley. *Chem. Soc. Rev.*, 1980, 9, 91.
17. (a) M. Remko and J. Polcin, *Adv. Mol. Relax. Processes*, 1977, 11, 249.
(b) B. M. Rode, A. Engölbrecht and W. Jakabetz, *Chem. Phys. Lett.*, 1973, 18, 285.
(c) M. Remko, *Adv. Mol. Relax. Processes*, 1977, 11, 291.
(d) P. Schuster and Th. Franck, *Chem. Phys. Lett.*, 1968, 2, 587.
(e) M. Remko, *Adv. Mol. Relax. Interact. Processes*, 1979, 15, 193.
(f) P. Bosi, G. Zerbi and E. Clementi, *J. Chem. Phys.*, 1977, 66, 3376.
18. N. E. Hill, W. E. Vaughan, A. H. Price and M. Davies, "Dielectric Properties and Molecular Behaviour", Van Nostrand, Reinhold, London, 1969, 320.
19. M. Davis, *Ann. Reports on Progress of Chemistry*, 1970, 67, 65.
20. V. V. Daniel, "Dielectric Relaxation", Academic Press, New York, 1967.
21. E. Jakusek and L. Sobczyk, *Dielect. and Related Mol. Processes*, 1976, 3, 108.
22. (a) H. G. Hertz and M. D. Zeidler in Ref. 5, Vol. III.
(b) J. Crossley, *R. I. C. Reviews*, 1971, 69.

References continued...

23. (a) R. Zana and J. Lang, *Adv. Mol. Relax. Processes*, 1975, 7, 21.
- (b) J. Crossley, *Adv. Mol. Relax. Processes*, 1970, 2, 69.
- (c) J. Emery and S. Gasse, *Adv. Mol. Relax. Interact. Processes*, 1978, 12, 47.
24. S. P. Tay, S. Walker and E. Wyn-Jones, *Adv. Mol. Relax. Interact. Processes*, 1978, 13, 47.
25. M. Davis and J. Swain, *Trans. Faraday Soc.*, 1971, 67, 1637.
26. L. Onsager, *J. Amer. Chem. Soc.*, 1936, 58, 1446.
27. C. P. Smyth, "Dielectric Behaviour and Structure", McGraw Hill Book Co., London, 1955.
28. R. J. Mekins, *Progress in Dielectrics*, 1961, 3, 151.
29. R. M. Fuoss and J. G. Kirkwood, *J. Amer. Chem. Soc.*, 1941, 63, 385.
30. K. S. Cole and R. H. Cole, *J. Chem. Phys.*, 1941, 9, 341.
31. D. W. Davidson and R. H. Cole, *J. Chem. Phys.*, 1951, 19, 1484.
32. N. Sheppard in Ref. 1, p. 85.
33. S. Bratoz and D. Hadzi in Ref. 1, 111.
34. D. Hadzi and S. Bratoz in Ref. 5, Vol. 2, Ch. 12.
35. S. Besnainon, *Adv. Mol. Relax. Interact. Processes*, 1980, 16, 81.

References continued...

36. L. A. Curtiss and J. A. Pople, *J. Mol. Spectrosc.*, 1973, 48, 413.
37. M. Asselin and C. Sandorfy, *J. Mol. Struct.*, 1971, 8, 145.
38. J. W. Emsley, J. Feeney and L. H. Sutcliffe, "High Resolution Nuclear Magnetic Resonance Spectroscopy", Vol. 1, Pergamon Press, New York, 1965.
39. J. A. Pople in Ref. 1, 71.
40. J. A. Pople, W. G. Schneider and H. J. Bernstein, "High Resolution Magnetic Resonance", McGraw Hill Book Co., New York, 1959.

CHAPTER II: EXPERIMENTAL

INTRODUCTION

Dielectric properties of a polar material can conveniently be considered by assuming it to be situated between the parallel plates of a condenser such that the dielectric constant (ϵ) of the material may be defined by the equation:

$$\epsilon = \frac{C}{C_0} \quad \text{II-1}$$

where C and C_0 are the capacitance values for the condenser with the dielectric material and with the vacuum respectively. The dielectric constant is, in fact, a frequency dependent complex quantity as was given in Eqn. I-7. When a sinusoidal potential of amplitude E and frequency ω rad s⁻¹ are applied to the capacitor, the current I flowing through the circuit is given by:

$$I = E\omega C = E\omega C_0(\epsilon' - i\epsilon'') \quad \text{II-2}$$

In this equation the real component $E\omega C_0\epsilon'$, known as charging current is 90° out of phase with the applied potential and therefore does not involve any electrical work. The imaginary component, $E\omega C_0\epsilon''$, known as the loss current, is

however, in phase with the applied potential and is related to the energy dissipated as heat since it causes some electrical work to be done given by the dot product, $EI = E^2 \omega C_0 \epsilon''$. As was given by Eqn. I-6, the resulting phase displacement (δ), i.e. the angle between the total current and charging current, is related to the dielectric loss factor (ϵ'') as:

$$\tan \delta = \frac{\text{loss current}}{\text{charging current}} = \frac{\epsilon''}{\epsilon'} \quad \text{II-3}$$

where ϵ' is the observed dielectric constant according to Eqn. II-1. These are the basic principles of the dielectric measurements.

The basic theories of IR and n.m.r. methods have been discussed in the first chapter.

THE INSTRUMENTS

The General Radio (GR) Bridge

The dielectric measurements for the purpose of

this thesis were carried out with the General Radio 1615A Capacitance bridge which measures the capacitance and conductivity of the capacitor. These quantities are related to the real and imaginary components of the complex permittivity by the following equations(1):

$$\epsilon' = \frac{C}{C_0} \quad \text{II-4}$$

and

$$\epsilon'' = \omega \frac{G}{C_0} \quad \text{II-5}$$

where G is the conductivity of the system and the other terms have their usual meanings. The sample placed between the high and the low electrodes made the capacitor of the system for which the measurement of C_0 was very difficult since it would require the electrodes to be arranged exactly the way they were when containing the sample. However, this quantity can be calculated from the relation (2):

$$C_0 = \frac{0.2244A_1}{d_1} \quad \text{II-6}$$

where A_1 is the effective area of the electrode plates in in.², d is the spacing of the plates in , and C is the capacitance in picofarads. For convenient handling of the experimental data Eqns. II-4-6 can be combined to give the equations:

$$\epsilon' = \frac{Cd_1}{0.2244A_1} \quad \text{II-7}$$

and

$$\epsilon'' = \frac{\epsilon'G}{\omega CC} \quad \text{II-8}$$

where G is in picomhos.

The effective area of the electrode plates, A_1 , was determined from the measured capacitance of the cell containing a standard quartz disc of diameter 2.0 ins. and thickness 0.0538 ins. (supplied by the Rutherford Research Products Co., New Jersey, U.S.A.) and with a dielectric constant of 3.819.

The electrode assembly was a three terminal system,

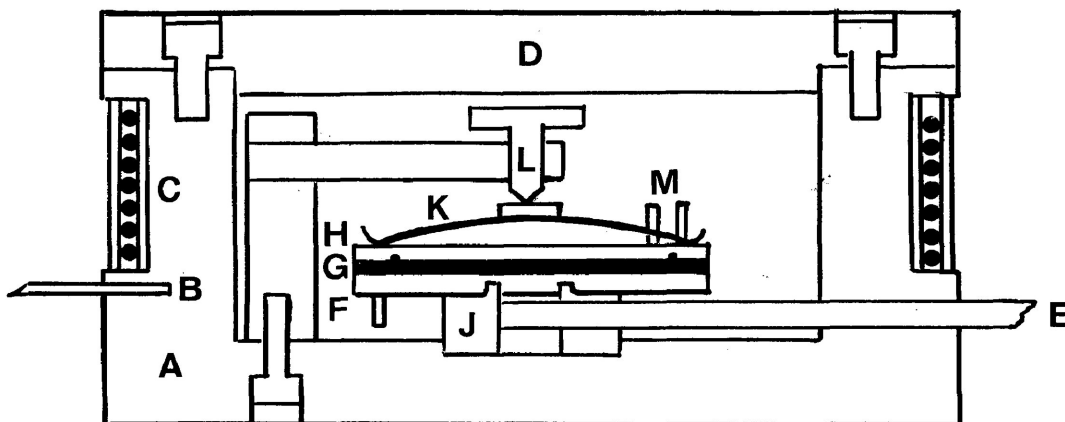


FIGURE II-1:- Schematic diagram of the electrode assembly

- | | |
|---|--|
| A | Aluminum Case |
| B | Controller Thermocouple |
| C | Insulated Heater |
| D | Flat Lid |
| E | Digital Pyrometer Probe |
| F | Low Electrode |
| G | Sample |
| H | High Electrode |
| J | Glass Ceramic Insulator |
| K | Three Prong Spring Clamp |
| L | Clamp Screw |
| M | Terminals (The lead wires are not shown) |

a schematic diagram of which is shown in Fig. II-1. The high electrodes, made of brass, had a diameter of 2.0 ins. while the low electrode of 1.5 ins. diameter was made of copper. The low electrode was surrounded by a guard ring (also made of copper) having an outer diameter of 2 ins. which would reduce any error due to fringing of the electric field at the edges.

The electrode assembly was mounted in an aluminum airtight temperature-controlled container having an inlet-outlet system for purging the chamber with dry nitrogen gas. Holes in the container enabled placement of a thermo-couple connected to a Beckman/RIIC model TEM-1 temperature controller as well as a probe for a digital pyrometer (Newport 264-3). The aluminum container having 0.5 ins. thick wall had a flat top which could be easily affixed by screws. A container of liquid nitrogen placed on this top was used for cooling. Both the containers were surrounded by 1.5 ins. thick styrofoam heat insulation.

Temperature could be made accurate to $\pm 0.1^{\circ}\text{C}$

by connecting the thermocouple to the nichrome wire heating coil surrounding the cell. A particular temperature was maintained by inserting an appropriate number of sheets of paper in between the two containers so that the heater current was about 2 amps corresponding to a power of about 8 watts.

The temperature range which could be attained with the system was from 80 to 333 K. These two extremes corresponds to near liquid nitrogen temperature and the glass transition temperature of polystyrene respectively. With compressed crystalline solid discs the temperature range could be extended up to the melting point of the solid but not beyond 373 K, which is near the melting point of the styrofoam cell insulation.

The General Radio bridge allowed dielectric measurements at frequencies ranging from 50 Hz to 10^5 Hz when used in conjunction with model 1310-A oscillator and model 1232-A tuned amplifier and null detector, both manufactured by the same General Radio Company.

The Spectrometers

Infrared absorption spectra were obtained with a Beckman IR-12 Spectrometer while a Bruker WP-80 FT-NMR Spectrometer was used for PMR studies.

PREPARATION OF THE SAMPLES

The capacitors measured by the GR bridge were solid discs consisting of the polar solutes dispersed in atactic polystyrene matrices. The discs were prepared using a procedure similar to that described by Davis and Swain (3). The desired amount of the solid (~ 0.2 to 0.4 g) and polystyrene pellets (nearly 4.0 g to make about 5 mol per cent of the solute) was dissolved in ~ 10 g. of a non polar solvent, usually trans-1,2-dichloroethylene (b.P. 320.7 K) in a porcelain crucible. The weight of the solute was roughly determined from the knowledge of its dipole moment, solubility in the solvent used, and taking into account its effect on the glass transition temperature of the polymer. The mixture was stirred thoroughly and then dried by evaporation in a drying oven at $\sim 90^{\circ}\text{C}$. After sufficient evaporation, when the mixture appeared to be extremely

thick, the crucible was removed from the oven and allowed to cool so that the solid mass could be gently pried away from the crucible walls with the help of a stainless steel spatula. The mass was rolled into a flat disc and then placed on a teflon sheet in a vacuum oven at 85°C, the pressure being reduced by a single-stage rotary pump and finally dried to a constant weight such that the least amount (<1%) of solvent remained in the mass.

The matrix material was placed in a stainless steel die equipped with polished tungsten carbide faces of 2 ins. diameter. The die was heated by a heating sleeve surrounding it up to a temperature of around 110°C so as to melt the material. The mass was then pressed by applying a pressure of five tons to the moving element of the die and allowed to cool down while under pressure. The glass-like circular disc was then pressed out after dismantling the die. The disc was trimmed around its edges with a sharp knife blade, and its average thickness was measured with a micrometer. The weight of the disc was also noted in order to determine the molar concentration of the solute in the matrix using the formula given

by Tay and Walker (4) as:

$$\text{Molar concentration } c = \frac{\text{Wt. of solute}}{\text{Mol. Wt. of solute}} \times \frac{\text{Wt. of disk}}{\text{Wt. of P.S. solute}} \times \frac{1000}{\text{Vol. of disk}}$$

Polystyrene used in the preparation of the matrix samples was obtained from the Monomer-Polymer Laboratory, Philadelphia, U.S.A. (Lot #700, 215-8) and had a nominal molecular weight of 230,000 (M_w). The solutes were procured from various manufacturers, mostly the Aldrich Chemical Co., and were purified appropriately wherever necessary.

It should be particularly mentioned that the solutes were of low concentration in the matrices such that they were molecularly dispersed (3) and, hence, any strong internal electric field would be largely eliminated. Such a low concentration would not affect the relaxation process appreciably, for Borisova and Chirkove (5) showed that the energy barriers for relaxation of small molecules

in polystyrene matrices are independent of concentration below 5-7 mol per cent.

Compressed disks were prepared by pressing the finely powdered solid samples in the same stainless steel die at room temperature but under much higher pressure (10^{-15} tons psi). In a few cases solid disks were prepared with samples which were liquid at room temperature. The sample was first frozen into a solid by dipping a mortar containing the liquid into liquid nitrogen and the solid mass was finely powdered and then pressed in the previously cooled die. The disk was quickly pressed out before it started melting and preserved in a freezer for measurements.

Solutions for IR studies were prepared by dissolving the solutes (~ 0.5 g) in pure carbon tetrachloride (~ 4.5 g) in order to have 10% (by weight) solutions unless otherwise specified. CCl_4 was also used as the solvent in the preparation of solutions for n.m.r. measurements. Standard solutions for each compound were first prepared from which other solutions of lower concentrations were obtained by the dilution method.

ANALYSIS OF RESULTS

For each temperature of measurement, the experimental data of dielectric loss factor as a function of frequency was subjected to analysis by a series of computer programs written in the APL language. The analysis was done according to the Fuoss-Kirkwood Eqn. I-12 which has been employed (3), when a continuous range of relaxation times due to much broader Debye curves exists. In case of solute in a polystyrene matrix, the loss due to the solute itself, $\epsilon''_{\text{solute}} = \epsilon''_{\text{matrix}} - \epsilon''_{\text{P.S.}}$, was calculated by subtracting the values for polystyrene, obtained through similar measurements, from those observed for the matrix. The computer program by iteration found the value of ϵ''_{max} which provided the best linear fit to plot of $\cos^{-1}(\epsilon''_{\text{max}}/\epsilon'')$ against $\log(f_{\text{obs}})$. The slope of the straight line gave the value of the distribution parameter (β), and the frequency of maximum absorption (f_{max}) was obtained from the slope and the intercept of the line on the \cos^{-1} axis. The ϵ_{∞} values could not be obtained from the Fuoss-Kirkwood equation since the equation does not consider the real

part of the complex permittivity, nor does it deal with the limiting values (ϵ_0 and ϵ_∞) at low and high frequencies respectively, except that the total dispersion is given by the expression:

$$\Delta\epsilon' = \epsilon_0 - \epsilon_\infty = 2\epsilon''_{\max}/\beta \quad \text{II-9}$$

The analysis was therefore supplemented with the Cole-Cole Equation I-14 to obtain ϵ_∞ in conjunction with the equation (6):

$$\beta = \frac{1 - \alpha}{\sqrt{2} \cos^{-1} \frac{\mu(1-\alpha)}{4}}$$

where α is the Cole-Cole distribution parameter. By use of the values of ϵ' at various frequencies several estimates of ϵ_∞ were obtained and the average was calculated along with a value for ϵ' at the frequency of maximum loss.

The results of the foregoing analyses were utilized to obtain the effective dipole moments (μ) involved in the relaxation process from both the Debye (7)

Equation (II-11) and the Onsager (8) Equation (II-12):

$$\mu^2 = \frac{2700kT(\epsilon_0 - \epsilon_\infty)}{4\pi Nc(\epsilon'_m + 2)^2} \quad \text{II-11}$$

$$\mu^2 = \frac{900kT(2\epsilon_0 + \epsilon_\infty)(\epsilon_0 - \epsilon_\infty)}{4\pi Nc\epsilon_0(\epsilon_\infty + 2)^2} \quad \text{II-12}$$

where the value of $\epsilon_0 - \epsilon_\infty$ is given by Equation II-9, ϵ'_m is the value of ϵ' at f_{\max} , ϵ_0 is the static dielectric constant derived from ϵ_∞ and Equation II-9, c is the concentration in mol/litre, T is the temperature in K, N is the Avogadro's number, and k is the Boltzmann constant.

These two equations yield μ in units of e.s.u. - cm which were converted into the more common Debye units (1 D = 10^{-18} e.s.u. - cm). From the observed μ -values at different temperatures extrapolated values for different compounds around room temperature (300 K) were obtained

for comparison with the corresponding literature values. It should be mentioned that the dipole moments at various experimental temperatures should appropriately be regarded as only the effective or apparent dipole moment.

Reorientation of dipoles has been considered as a rate phenomenon (9), and consequently the Eyring rate equation was utilized in order to evaluate the energy barriers which must be surmounted for dipolar reorientation. In dielectric relaxation studies (3,4,6) this has been a commonly used procedure despite a few of its limitations (10). The Eyring rate expression,

$$\tau = \frac{1}{\text{rate constant}} = \frac{h}{kT} \exp\left(\frac{\Delta G_E}{RT}\right) \quad \text{II-13}$$

can be rearranged to the following linear form:

$$\ln(T\tau) = \frac{\Delta H_E}{RT} - \frac{\Delta S_E}{R} - \ln(h/k) \quad \text{II-14}$$

where the terms have got their usual significance. According to Equation II-14, the plot of $\log(T\tau)$ against $1/T$ gave

a straight line of which the slope and the intercept yielded the enthalpy of activation and the entropy of activation respectively through a computer programme. The programme also provided the relaxation times (τ) and the free energies of activation (ΔG_E) at different temperatures.

Standard statistical techniques (11) were employed in fitting the analyses of the experimental data with various computer programmes which provided different confidence interval widths for important parameters, viz. $\log(f_{\max})$, β , and enthalpies and entropies of activation. For the present purpose, however, 95% confidence interval was chosen as a good representation of experimental error. This consideration was found to yield an error of $\pm 10\%$ in ΔH_E in the worst case while that in ΔS_E might be as high as $\pm 50\%$. The values of enthalpies and entropies of activation have been quoted in round figures for comparative purposes only.

The Fuoss-Kirkwood parameters, $\log(f_{\max})$, ϵ''_{\max} and β , relaxation times (τ), the limiting high frequency dielectric constants (ϵ_{∞}) and effective dipole moments (μ) obtained from the computer analyses are given in tables in relevant chapters. Results of Eyring analyses have also

been presented in these chapters.

Analyses of results from IR and n.m.r. studies have been discussed in the respective chapters.

REFERENCES

1. C. P. Smyth, "Dielectric Behaviour and Structure", McGraw Hill Book Co., New York, 1955, p. 203.
2. F. E. Terman, "Radio Engineer's Handbook", (1st ed.), McGraw-Hill Publishing Co. Ltd., London, 1950, p. 112.
3. M. Davies and J. Swain, Trans. Faraday Soc., 1971, 67, 1637.
4. S. P. Tay and S. Walker, J. Chem. Phys., 1975, 63, 1634.
5. T. I. Borisova and V. N. Chirkov, Russ. J. Phys. Chem., 1973, 47, 949.
6. N. E. Hill, W. E. Vaughan, A. H. Price and M. Davies, "Dielectric Properties and Molecular Structure", Van Nostrand-Reinhold Co., London, 1969, p. 292.
7. Ref. 6, p. 235.
8. C. J. F. Bottcher, "Theory of Electric Polarization", Elsevier Publishing Co., Amsterdam, Netherlands, 1952, p. 323.
9. S. Glasston, K. J. Laidler and H. Eyring, "The Theory of Rate Processes", McGraw-Hill, New York, 1941, Ch. IX.
10. M. Davies and C. Clemett, J. Phys. and Chem., Solids. 1961, 18, 80.
11. B. Ostle, "Statistics in Research", (2nd ed.), Iowa State University Press, Ames, Iowa, U.S.A., 1963.

CHAPTER III: INFRARED STUDIES ON SOME
 PHENOLS AND THEIR H-BONDED
 COMPLEXES, AND ON SOME OTHER
 RELATED HYDROXY COMPOUNDS

INTRODUCTION

This chapter of the thesis will be devoted to the infrared spectroscopic studies of H bonding in a number of hydroxy compounds, principally phenols, and their complexes with a few common organic bases. A majority of such studies in the literature has been concerned with the stretching frequency (ν_{A-H}) of the A-H functional group and the change (decrease) observed for H bonded system A-H---B. Prominent spectral changes provide qualitative evidence for H bond formation and the quantitative indices of the H bond energy and of other physical properties. The present ir investigation was attempted in order to obtain some first hand information (mostly qualitative) on the H bonding systems of our interest; such information was expected to supplement the results of dielectric relaxation studies on some of these and other related systems (Chapters V and VI).

Infrared studies on H bonding in phenols are numerous in the literature (1-3) which, for our convenience, can be classified into three categories. These are on:

a) intermolecular H bonding self-associated phenols;

b) intramolecular H bonding in some ortho-substituted phenols; and

c) intermolecular H bonding of phenols with proton acceptor (base) molecules.

In the first category comes phenol itself for which a monomer-dimer-polymer model has been proposed (4) in order to explain three absorption bands around 3612 ± 1 , 3487 ± 5 , and $3346 \pm 5 \text{ cm}^{-1}$, respectively. Association behaviour of various alkyl-substituted phenols has been studied extensively (5-12); important findings of these studies can be outlined as follows:

i) In ortho-substituted phenols the various alkyl groups other than t-butyl have little effect on the H bonding, while in di-ortho-substituted phenols there is a steady increase in the hindering effect of the alkyl group with increasing branching; most effective steric hindrance is observed in 2,6-di-tert-alkylphenols (6-11).

ii) Phenols containing a single ortho alkyl-substituent (principally tert-alkyl) exist as cis and trans isomers in unequal amounts, the trans isomer being more abundant (6,8-11). The cis isomer decreases as the size of the t-alkyl substituent in the o-position is increased (10), but is

increased by substitution of a methyl (or other alkyl) group at the 6-position (6,10).

iii) In all phenols the hydroxyl group is co-planar with the aromatic ring (5,8). Even in the most hindered molecule, 2,6-di-t-butylphenol, the H atom of the OH group is believed to lie in the t-butyl 'basket', in the plane of the aromatic ring (13).

iv) The frequency and intensity of the fundamental O-H stretching band in 2-alkyl and 2,6-dialkyl phenols are determined by internal steric and environmental factors in addition to the normal inductive and resonance effects (8-10).

Intramolecular H bonds in ortho-substituted phenols are single bridge H bonds similar to those in the dimeric association and accordingly, relatively weak as compared to those which are resonance stabilized (14). Of the various phenolic systems involving intramolecular H bond, o-halogenophenols are the ones which have been investigated in great detail (15-19). Some of the important observations in these studies are the following:

i) Like o-alkylphenols, o-halogenophenols

do also exist as cis and trans isomers - which results in the doubling of their O-H stretching bands. In both the isomers the OH group is coplanar with the aromatic ring, but, unlike in o-alkylphenols, the absorption band corresponding to cis-component gets shifted to lower wave numbers due to H bond with the halogen in the ortho position.. In 2,6-di-halogenophenols only one O-H band is observed which corresponds to the cis isomer.

ii) The frequency shifts ($\Delta\nu_{OH}$) of the bonded OH group in o-halogenophenols are in the order of $F < Cl < Br < I$ (17), while the order of H bond strengths is $Cl > Br > F > I$ (17,18).

iii) The energy of intramolecular halogen hydroxyl interaction is considered to be less than that of intermolecular H bonds. An estimate of enthalpies of such interaction in 2-halogenophenols dissolved in CCl_4 yielded the values in k cal/mol: $Cl = 1.44$, $Br = 1.21$, and $I = 1.08$ (18).

Study of H bonding in H-bonded complexes between phenols (or other hydroxy compounds) and various bases has been another area where ir spectroscopy has been employed extensively (1,2,20). Detailed studies on complexes of phenols with a large variety of bases have been reported

in the literature (1-3,21-35). Similar studies on complexes of o-substituted phenols seem to be rather scarce. Wren and Lenthen (12) have, however, shown that even in the hindered systems like 2,6-di-t-alkyl-4-methylphenols there exists a slight but measurable tendency to form H bonds with bases.

One of the most important quantitative applications of ir spectroscopy has been the estimation of H bond energy ($-\Delta H$) for a particular $A-H \cdots B$ bond using the frequency shift ($\Delta\nu_{AH}$). Various empirical equations derived to correlate these two quantities ($-\Delta H$ and $\Delta\nu$) have been reviewed by Joesten and Schaad (2. Ch. 4). The general form of various equations for different reference acids is (2 Ch. 4):

$$-\Delta H(\text{kcal/mol}) = m\Delta\nu_{OH}(\text{cm}^{-1}) + b \quad \text{III-1}$$

where m and b are empirical parameters characteristic of each acid. The same general equation also applied to phenol adducts of different bases. Drago and Wayland (32,33) developed another empirical equation which is useful for predicting enthalpies for H bonds in the H bonded complexes. This equation is:

$$-\Delta H (\text{kcal/mol}) = E_A E_B + C_A C_B \quad \text{III-2}$$

where, E and C parameters assigned to each acid (A) and each base (B) estimate electrostatic (E) and covalent (C) contributions to the H bonding; these parameters have been obtained by Drago and co-workers (34,35).

In view of the above introductory discussion and with our objective in mind, the following problems will be of main concern in the present investigation.

i) Attempts will be made to reveal the nature and the relative strengths of H bonds in the self associated species of o-alkylphenols. As well they will be examined carefully in their adduct formation of highly hindered phenols.

ii) The nature and extent of intermolecular interactions in self-association and complex formation of intramolecularly H bonded phenols, viz., o-halogeno and 2,6-dihalogenophenols, will be investigated.

iii) Infrared spectra of some systems other than phenols will be examined in order to obtain a first-hand information on the nature and strength of H bonds in these systems.

iv) Finally, an assessment of H bond enthalpies

($-\Delta H$) for several systems will be attempted using empirical equations from the literature (2. Ch. 4).

EXPERIMENTAL

Infrared spectra of various compounds were taken mostly in carbontetrachloride solution containing 10% (by wt.) of the solute. Three component solutions (for studying H bonded complexes) were prepared by adding the base compounds (proton acceptor) to the 10% solutions in excess of what is required to make equimolecular solutions with respect to both the compounds. Triethylamine was found to react with CCl_4 forming brown precipitate. In order to avoid this problem three component systems containing triethylamine as proton acceptor were prepared by adding the same directly to the proton donor compounds and then the solvent (CCl_4) was added to the systems. Spectra were recorded with the double beam spectrometer in the region of $2200\text{-}4000\text{ cm}^{-1}$ by the use of two NaCl ir cells (equal path length of 0.1 mm) one containing the experimental solution while the other (reference) contained the pure solvent; absorptions due to the solvent were thus eliminated.

In a few cases spectra were recorded with the samples dispersed in polystyrene matrices in which most of

our dielectric relaxation measurements were carried out. Thin fillets were cut from the polystyrene discs prepared for dielectric measurements and their spectra were taken with a blank reference.

RESULTS

Infrared studies were carried out on a number of alkyl-substituted phenols as well as on their adducts with methyl cyanide (MC); 1,4-dioxan (DO), pyridine (Py) and triethylanine (TEA). 2-Phenylphenol was also included in this study. Absorption frequencies for free (O-H) and H bonded O-H stretching vibrations in these systems are given in Table III-4. Similar results with halogen-substituted phenols and their H bonded complexes are given in Table III-5. Besides phenols, some other hydroxy and carboxylic compounds were also studied; O-H frequencies for these compounds are tabulated in Table III-6.

DISCUSSION

Alkyl-substituted Phenols and 2-Phenylphenol

In Table III-1 $\nu_{\text{O-H}}$ represents the absorption frequency due to free O-H while $\nu_1_{\text{O-H}}$ and $\nu_2_{\text{O-H}}$ represent the H-bonded O-H frequencies in different H-bonding systems under investigation. Assignments of these absorption

bands for different compounds have been elaborately discussed in the literature (1,2,4-12). The last column of the Table III-1 shows the frequency shifts ($\Delta\nu_{1 \text{ O-H}} = \nu_{\text{O-H}} - \nu_{1 \text{ O-H}}$) caused by H bonds formed in the donor-acceptor systems.

Three major peaks for phenol can be assigned to the O-H vibrations in monomer ($\nu_{\text{O-H}}$), dimer ($\nu_{\text{O-H}}$) and polymer ($\nu_{3 \text{ O-H}}$) (4,7). Other o-alkylphenols and 4-isopropylphenol do exhibit almost similar absorption behaviour in the O-H region; three major peaks for each of these compounds can thus be assigned according to the same monomer-dimer-polymer model. It is to be noted that for 2-t-butylphenol two monomer-peaks were observed corresponding to its cis and trans isomers (6-10). The higher frequency peak ($\sim 3650 \text{ cm}^{-1}$) has been assigned to the cis component while the lower frequency peak ($\sim 3610 \text{ cm}^{-1}$) is thought to be due to the more abundant trans isomer, the estimated percentage of the latter being about 90% (6,10,11) in an inert solvent. With the decreasing size of the o-alkyl groups the relative amounts of the cis isomers should be increased. On the contrary, our experiment apparently showed only one monomer peak for each o-alkylphenol other than 2-t-butylphenol. This single peak ($\nu_{\text{O-H}}$) appeared to correspond to the trans isomer. Coexistence of both the

cis and trans isomers in such compounds has, however, been evidenced by Ingold and Williams (10) in the form of two unresolved bands. These bands were not resolved since they appeared to be only 10 cm^{-1} apart. The half band widths ($\Delta\nu_{\frac{1}{2}}$) of the unresolved bands in these non-tertiary o-alkylphenols were, however, greater as compared to the same for phenol or for corresponding 2,6-dialkylphenol. Our results also appear to demonstrate such behaviour (Table III-1).

TABLE III-1: Comparative $\Delta\nu_{\frac{1}{2}}$ OH values for phenol and o-alkylphenols

<u>Compound</u>	<u>$\Delta\nu_{\frac{1}{2}}$ O-H (cm^{-1})</u>
Phenol	27
o-Cresol	32
2-Ethylphenol	35
2-Isopropylphenol	40
2,6-di-t-isopropylphenol	24

The behaviour with regard to self-association of all the o-alkylphenols was almost the same except the extent of association appeared to decrease as compared with that for phenol; this decrease was most significant in the case of 2-t-butylphenol (Figure III-1).

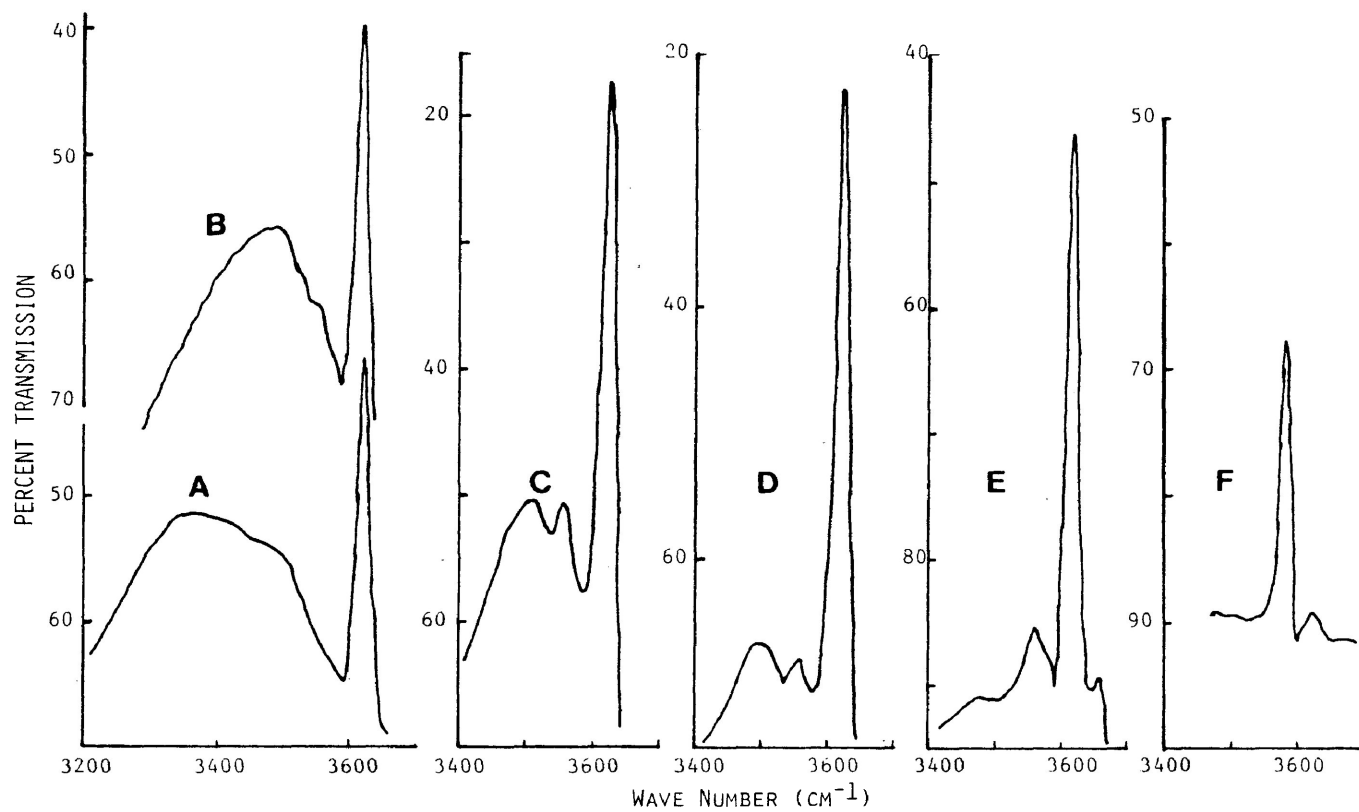
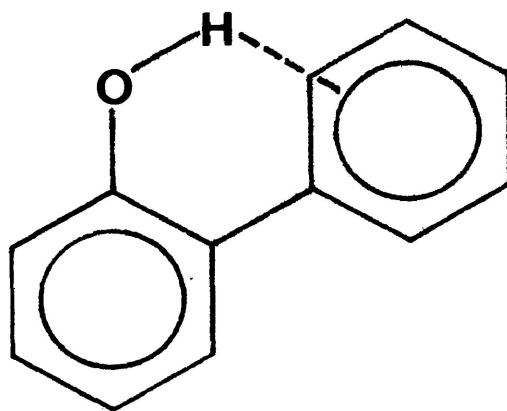


FIGURE III.1 INFRARED SPECTRA OF PHENOL (A), O-CRESOL (B), 2-ETHYLPHENOL (C), 2-ISOPROPYPHENOL (D), 2-T-BUTYLPHENOL (E) AND 2-PHENYLPHENOL (F).

The observed absorption bands for 2-phenylphenol, however, presented a different situation of H bonding. Unlike the absorption band in *o*-*t*-butylphenol, the band corresponding to the *cis* isomer of this compound appeared at a much lower frequency (3575 cm^{-1}) as compared to that for the *trans* component (3615 cm^{-1}). The reason for this apparently unusual behaviour could be that in the *cis* component the π -electron cloud of the *o*-phenyl group interacts with the O-H proton forming the intramolecular bridge as shown below:

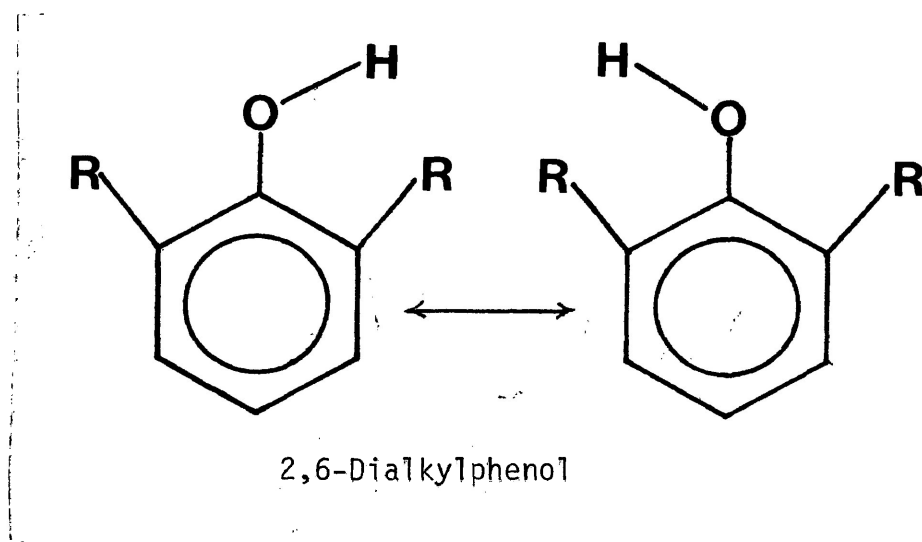


2-Phenylphenol

The energy of this intramolecular interaction would stabilize the *cis* isomer over the *trans* and consequently the major component should be the *cis* as observed in our experiment.

For each of the hindered phenols, namely 2,6-di-isopropylphenol, 2,6-di-*t*-butylphenol, 2,4,6-trimethyl-

phenol and 2,4,6-tri-t-butylphenol, only one absorption band was observed in the O-H region which corresponded to the O-H band for the cis components of o-alkylphenols. The reason is obvious; both the coplanar positions of the O-H group in these compounds are exactly equivalent (as shown below) and correspond to the cis position in monosubstituted o-alkylphenols.



In the experimental concentration range (10% wt) none of these compounds showed any H-bonded O-H absorption band. This appears to negate the possibility of any appreciable intermolecular association in the said concentration range. Infrared spectra of these compounds at higher concentrations, however, presented an interesting situation (Table III-4 and Figure III-2). In the case of 2,4,6-trimethylphenol two additional absorption bands gradually showed up with the increase of concentration. These bands could possibly be due to the H-bonded dimer

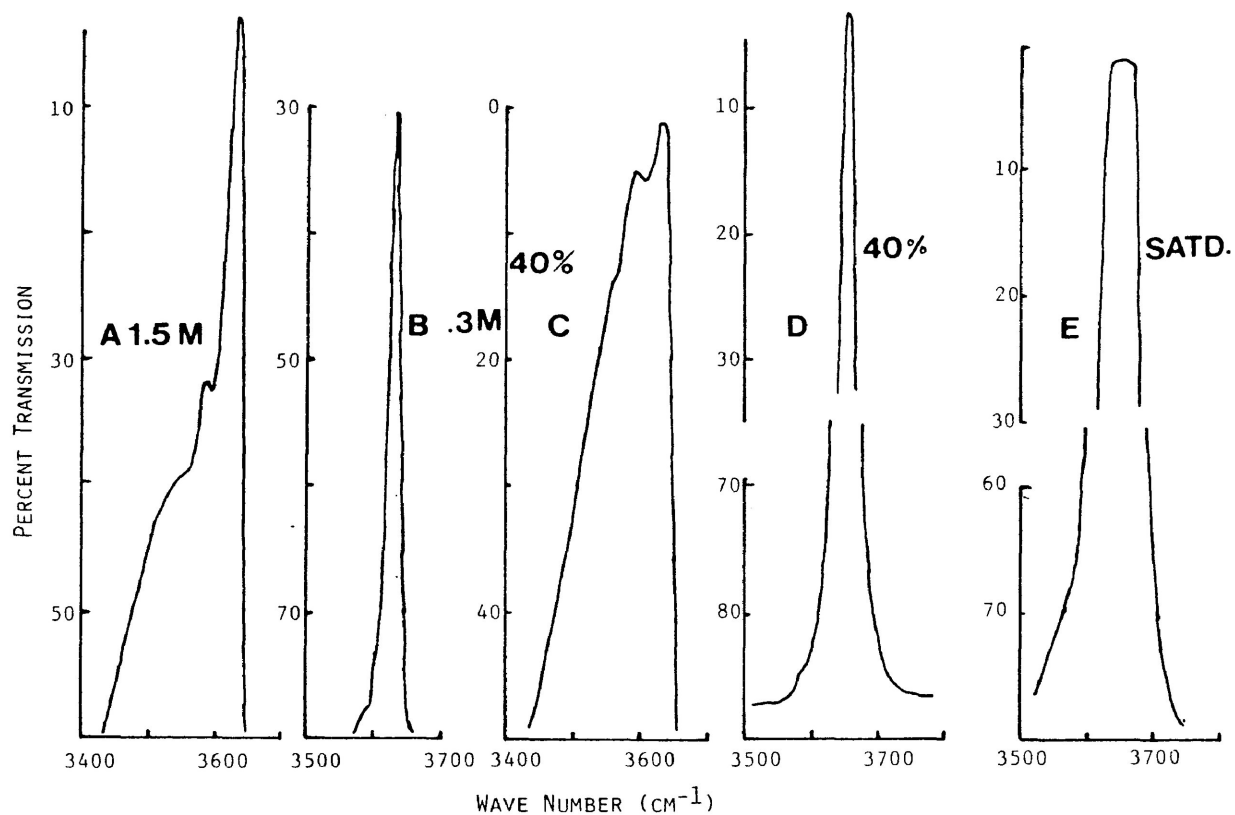


FIGURE III.2. INFRARED SPECTRA OF 2-4-6-TRIMETHYLPHENOL (A,B), 2,6-DIISOPROPYLPHENOL (C), 2,4,6-TRI-T-BUTYLPHENOL (D) AND 2,6-DI-T-BUTYLPHENOL (E).

(3585 cm^{-1}) and polymer (3540 cm^{-1}). Such additional absorption bands were also detectable in the spectrum of 40% wt of 2,6-di-isopropylphenol. Similar solution of 2,6-di-t-butylphenol and 2,4,6-tri-t-butylphenol, did not, however, show any additional peak. In view of these results it could be suggested that the intermolecular interaction of the O-H proton in 2,6-dialkyl-substituted phenols is effectively prevented by bulky t-butyl groups while smaller alkyl groups cannot totally prevent such interaction particularly when the solution concentration is very high.

Halogenophenols

Most of our infrared data on halogenophenols are in good agreement with those available in the literature (15-18,37). Each of the three o-halogenophenols (o-chloro, o-bromo- and o-iodophenol) exhibited two absorption peaks in the O-H region (Figure III.3). The very weak peak at higher frequency (3610 - 3615 cm^{-1}) corresponded to the free O-H band and, consequently, has been attributed to the trans orientation while the sharp and very strong peak at lower frequency represented the cis orientation of the compound in which the O-H hydrogen is intramolecularly H-bonded to the halogen in the ortho position. The relative

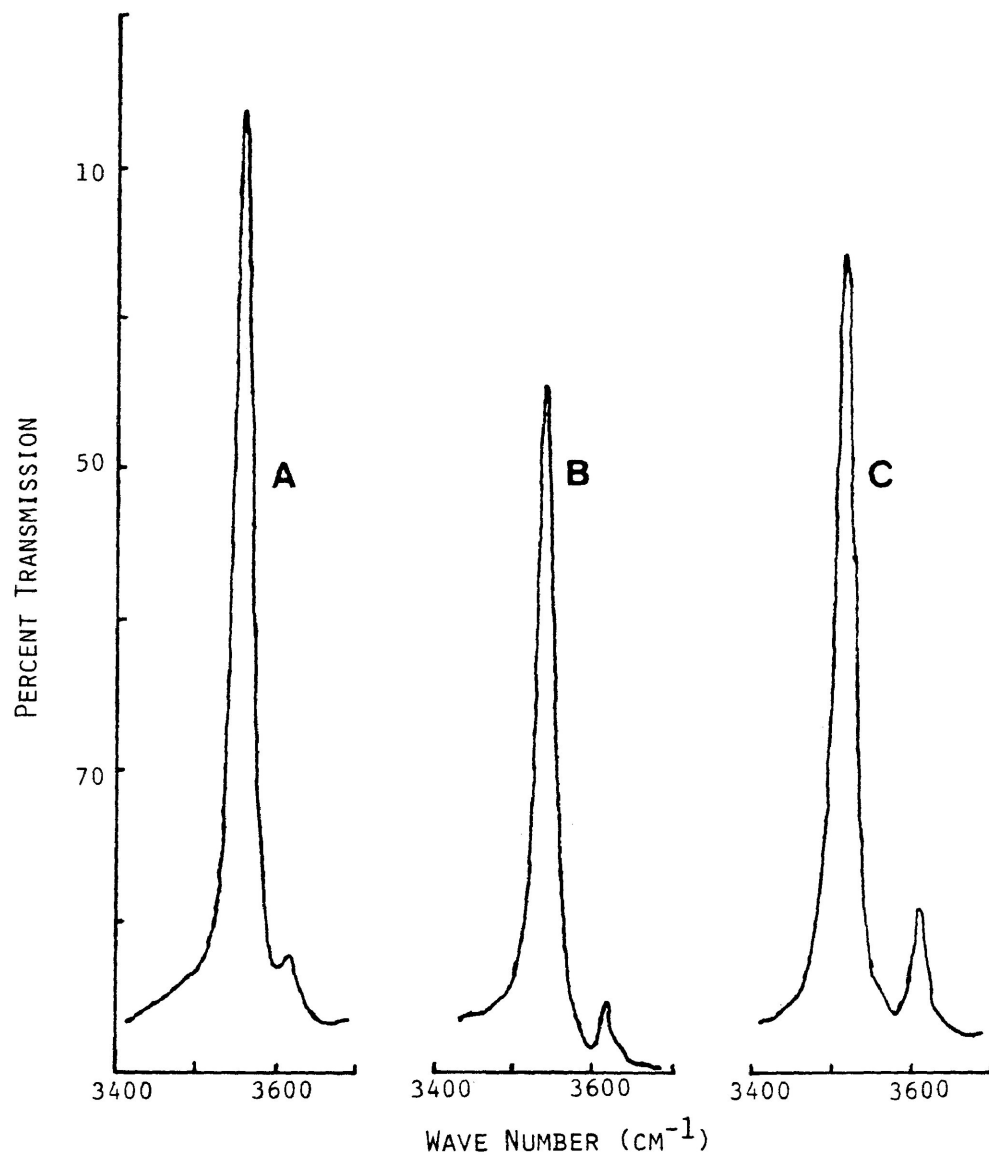


FIGURE III.3. INFRARED SPECTRA OF O-CHLOROPHENOL (A), O-BROMOPHENOL (B) AND O-IODOPHENOL (C).

intensity of the two peaks clearly demonstrate that the cis configuration greatly predominates over the trans; this is due to the fact that the energy of the intramolecular H bond stabilizes the former configuration (cis) by 1-3 k cal/mole (15-18, 38-40).

The frequency shift, $\Delta\nu_{\text{O-H}}$ in halogenophenols, was found to increase in the order Cl<Br<I; the relative intensity of the trans-peak also increased in the same order. According to Badger's rule (41) progressive shift to lower frequency is an indication of increasing strength of H bond. On the contrary, there is convincing experimental evidence (16-18) supporting almost the opposite order: Cl>Br>F>I for H bond strength in o-halogenophenols. The anomalous order has been explained in terms of several factors (16,17): (1) resonance interaction of the O-H group and halogens with the aromatic ring; (2) repulsive interaction between a lone-pair orbital of halogen with the O-H bonding orbital, and (3) interacting distance which depends upon the size of the halogen atom in the ortho position. It has been suggested that since the resonance ability of the halogens increases markedly from iodine through fluorine, the resonance interaction of the O-H group should decrease in the same order. This would tend to destabilize the trans O-H adjacent to the smaller

halogens. In passing from chlorine to bromine to iodine the effects of repulsive orbital interaction which tends to destabilize the intramolecular H bond is thought to be dominant. The repulsive interaction is, however, not manifested in the frequency shift, $\Delta\nu_1$ O-H', probably because the O-H group is held within interacting distance by molecular geometry and resonance: For this reason the order of H bond strength does not correspond to that of the frequency shift, $\Delta\nu_1$ O-H.

In phenols having halogen atoms in both the ortho positions the O-H hydrogen is intramolecularly H bonded to either halogen, giving rise only to cis configuration. Consequently, the compounds should exhibit only one O-H band (cis) as shown in the Figure III.4.

Infrared spectra of 2,4,6-trihalogenophenols at different concentrations (Figure III.5) presented some interesting features which are:

(1) As expected, each of the 2,4,6-trihalogenophenols at different concentrations exhibited only one O-H band corresponding to the respective cis configuration. However, the peaks at higher concentrations of the trichloro- and tribromo compounds were asymmetrical, the

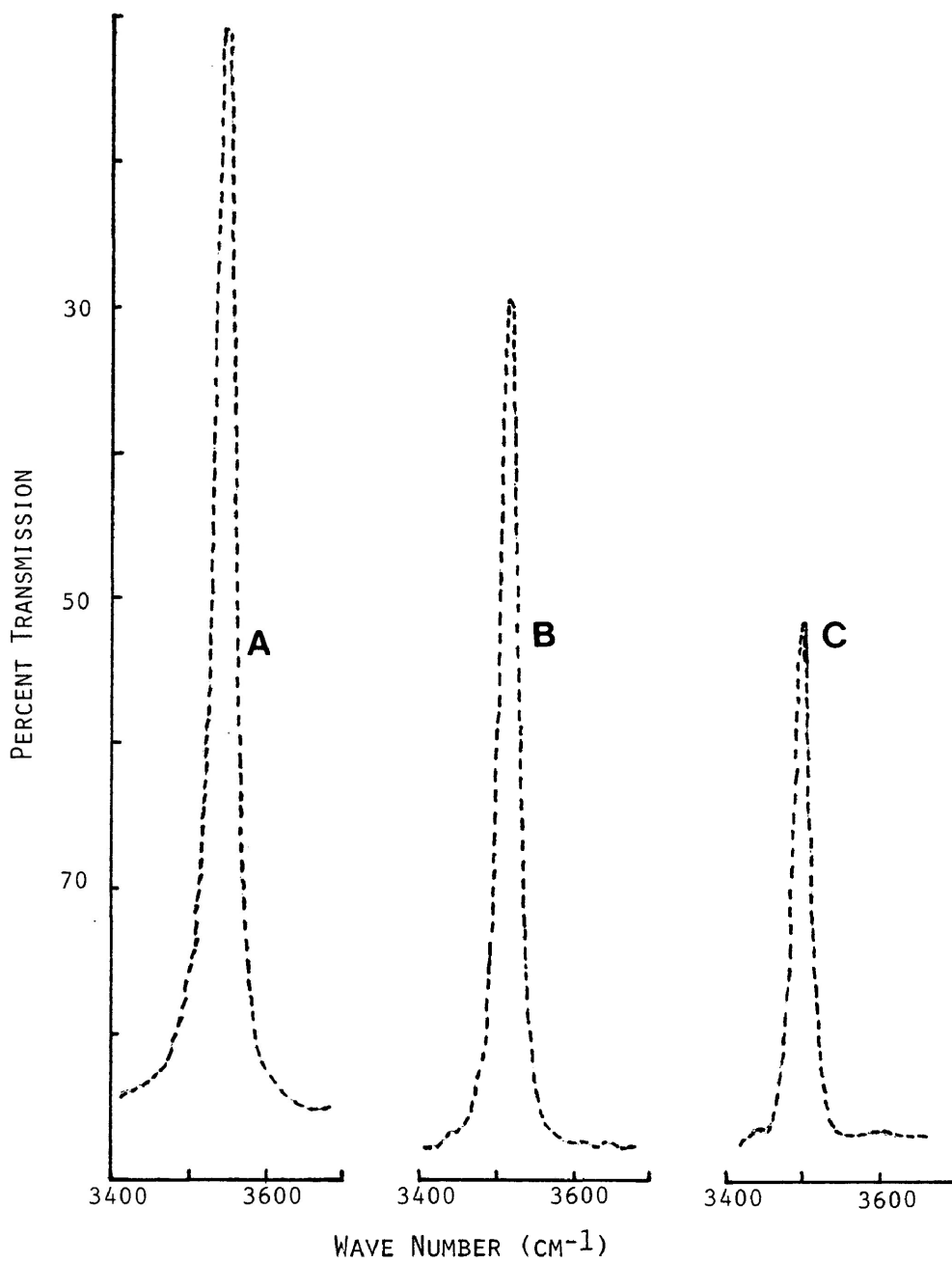


FIGURE III.4. INFRARED SPECTRA OF 2,6-DICHLOROPHENOL (A), 2,4,6-TRIBROMOPHENOL (B), AND 2,4,6-TRIIODOPHENOL (C).

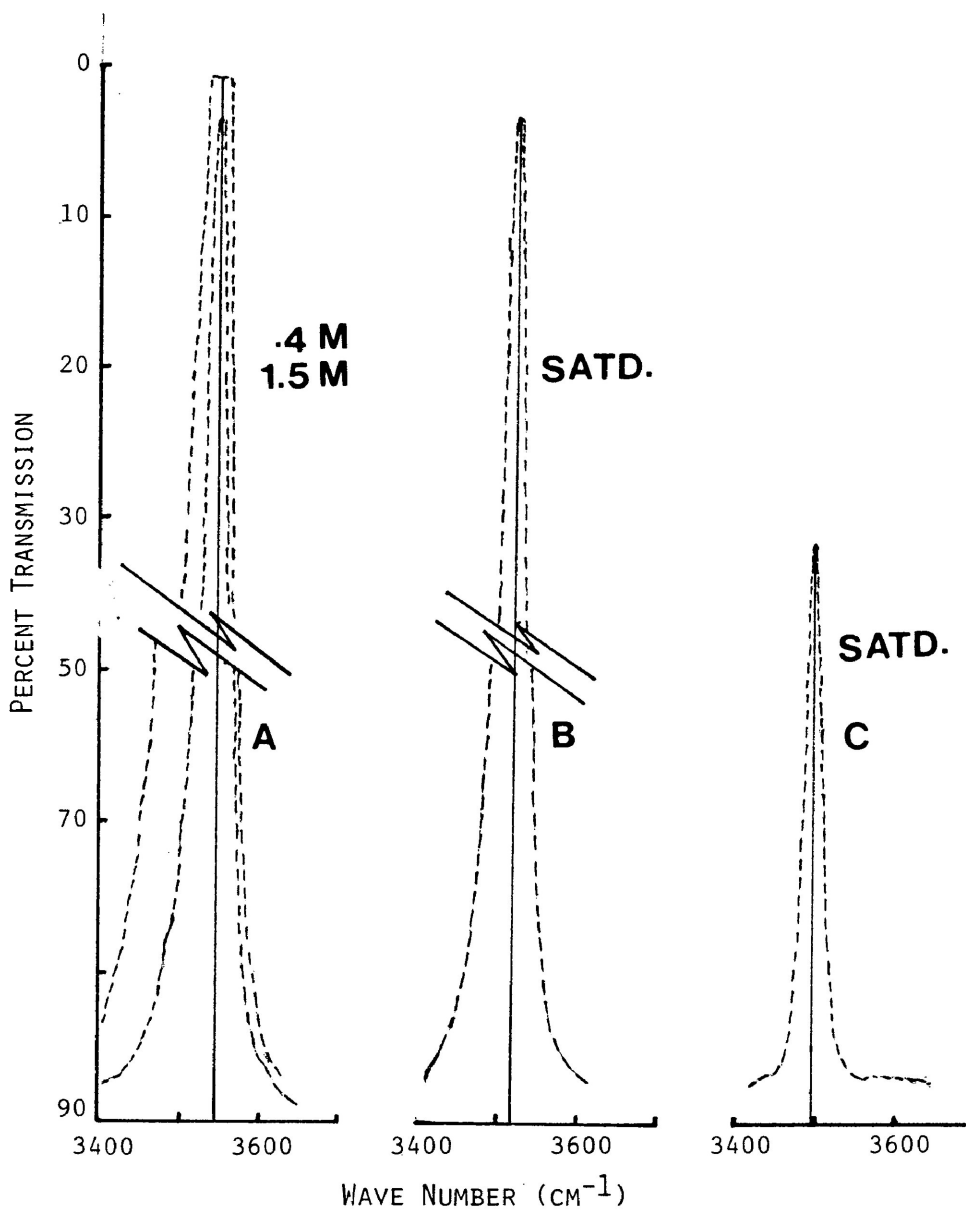


FIGURE III.5. INFRARED SPECTRA OF 2,4,6-TRICHLOROPHENOL (A), 2,4,6-TRIBROMOPHENOL (B) AND 2,4,6-TRIODOPHENOL (C).

asymmetry being more pronounced as the concentration of the solution increased.

(2) The asymmetry in the O-H peak appeared to be less pronounced in the case of the bromo-compound than in the chloro- compound.

(3) The O-H peak obtained with the saturated 2,4,6-triiodophenol showed no sign of asymmetry.

The asymmetry in the O-H peak could be attributed to the occurrence of intermolecular H bonding in addition to any intramolecular H bonding in the compounds in question, particularly at high concentrations. Dielectric relaxation studies of these compounds in this laboratory (42) have provided evidence of such H-bonding.

Hydrogen Bonded Complexes of Phenols

Each of the phenolic compounds under investigation was found to form strong H bonds, with the organic bases added to its solution in CCl_4 . An additional broad and strong O-H peak showed up in most of the cases while the other O-H peak or peaks (free or H-bonded) either disappeared or greatly decreased in intensity. Numerical data from the spectra of these three component systems (phenol-base- CCl_4)

are presented in Tables III-4 and III-5. Representative spectra are shown in Fig. III-6. A careful examination of these data and spectra would provide the following general information:

(i) The observed frequency shifts ($\Delta\nu_2$ O-H for 2-phenylphenol and halogenophenols and $\Delta\nu_1$ O-H for others) caused by the adduct formation were largely dependent on the strength of the base; the stronger the base the larger was the frequency shift. The base parameters (35) has clearly established the following decreasing order of basicity:

triethylamine > pyridine > 1,4-dioxane > methyl cyanide

According to the Badger's rule (41), the H bond energy involved in the adduct formation of the phenols with this bases would decrease in the same order.

(ii) In the alkyl-substituted phenols, the size of the substituent had little effect on the observed frequency shift ($\Delta\nu_1$ H-O). In the hindered phenols (2,6-dialkyl-substituted) the $\Delta\nu_1$ O-H was significantly decreased and in the extreme case of 2,6-di-t-butylphenol the decrease was dramatic. With methyl cyanide (the weakest base of

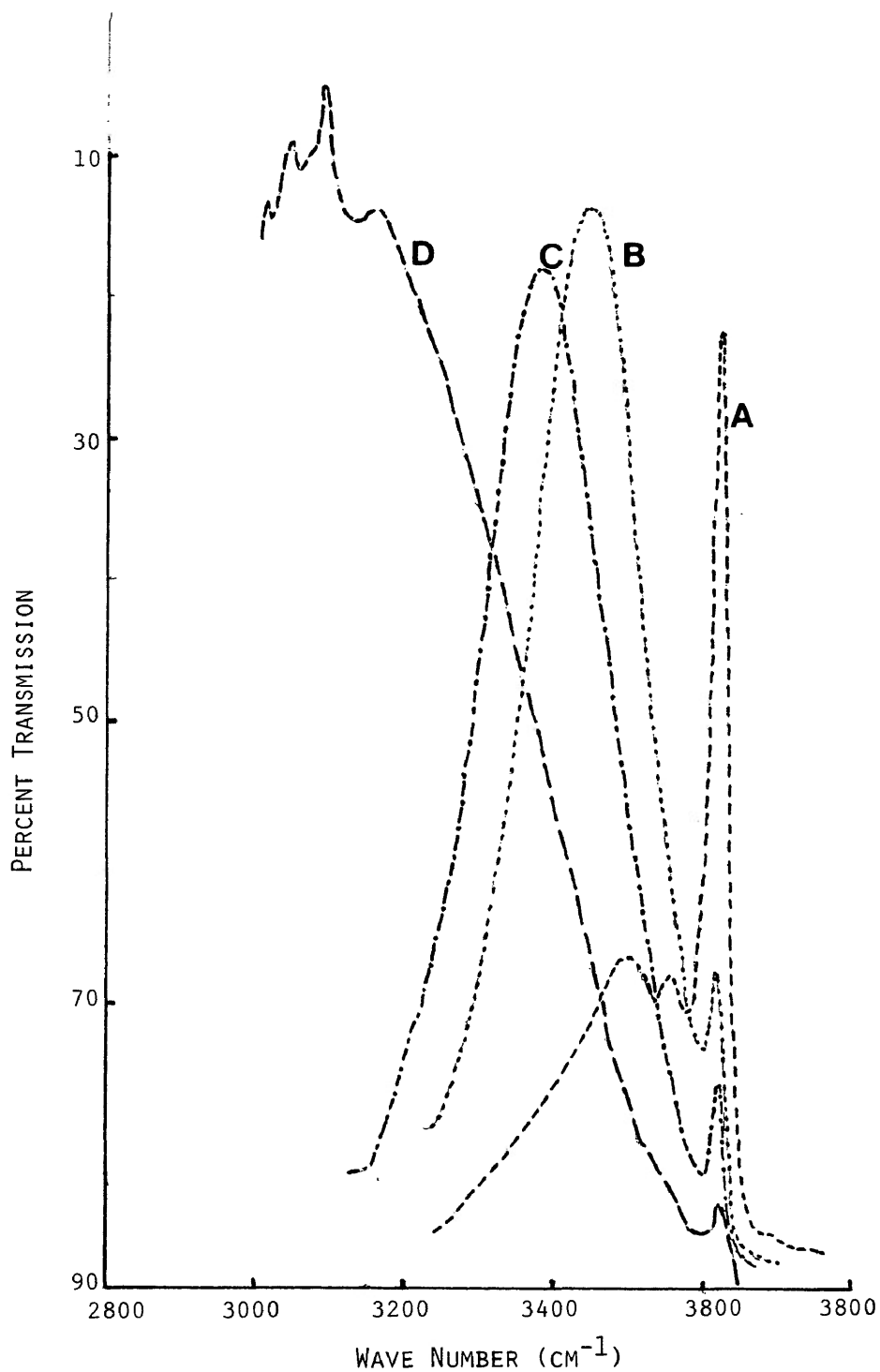


FIGURE III.6. INFRARED SPECTRA OF 2-ISOPROPYLPHENOL (A) AND ITS COMPLEXES WITH METHYL CYANIDE (B), 1,4-DIOXANE (C) AND PYRIDINE (D).

the four) this compound did not exhibit any additional peak; however, its presence could barely be detected in the slight broadening and shift of the single O-H (supposedly free) peak. From the self-association behaviour of alkylphenols it was earlier suggested that the steric hindrance to H bonding becomes significantly strong when the phenol is substituted both at 2- and 6-positions and more so when the substituted alkyl groups are bulky. Obviously the H bond energy in the adducts of these hindered phenols would be significantly smaller as is represented by the observed decrease in the frequency shifts.

(iii) The frequency shifts ($\Delta\nu_2$ O-H) observed with the halogenophenol-base complexes were, however, somewhat larger as compared to those observed with unhindered phenol-complexes. The observed frequency shifts with complexes of 2,6-dichloro- and 2,4,6-tribromophenols were still larger. It is highly unlikely that halogen-substitution would increase the acidity of the phenolic proton significantly which might enhance the H bond energy in their adducts. Moreover, on consideration of the steric factor of two ortho halogens, the possibility of higher H bond energy in these adducts appear to be far remote. Increased frequency shifts in these cases could possibly be explained in terms of the co-existence of both the intramolecular and intramolecular

H bond in the H-bonded complexes in question. The O-H bond is to some extent weakened by the intramolecular H bond with the ortho halogen; the same bond is further weakened by the adduct formation with the base molecule through intermolecular H bonding. In o-halogenophenols the base molecule forms H bonding with both the cis and trans O-H, and the peak in the "cis-adduct" possibly appears at a relatively lower frequency as compared to that due to the "trans-adduct". The observed peak in these cases perhaps represents two closely-spaced and thereby overlapping peaks, one due to each type of adduct formation. In phenols having halogens in both the ortho-positions, the O-H can have only cis orientation, and therefore the additional peak due to the adducts appear at a still lower frequency.

The numerical values of the base parameters for the base molecules used as proton acceptors are given in Table III-2:

TABLE III-2: Base Parameter of the Organic Bases Used As Proton Acceptors (Ref. 35)

Base	C_B	E_B
Methyl cyanide	1.34	0.886
1,4-Dioxane	2.38	1.09
Pyridine	6.40	1.17
Triethyl Amine	11.09	0.991

The values of acid parameters C_A and E_A for phenol are 0.442 and 4.33 respectively. Values of these parameters when inserted in Eqn. III-2 yield an estimate of the H bond energy ($-\Delta H$) in the adduct formation. An empirical equation (31) of the type of Eqn. III-1, viz.,

$$-\Delta H(\pm 0.2, \text{ kcal/mol}) = 0.0105\Delta\nu \pm 3.0 \quad \text{III-3}$$

was used in conjunction with our ir data to obtain experimental values of $-\Delta H$. A similar equation (31) viz.

$$-\Delta H(\pm 0.2, \text{ kcal/mol}) = 0.0103\Delta\nu + 3.1 \quad \text{III-4}$$

was used to estimate the H bond energies in various alkyl-substituted phenol-base complexes. Results of these estimates are presented in Table III-3.

It should be mentioned here that the results in Table III-5 represent only the approximate estimate. Several empirical equations appearing in the literature (2) have been found to give widely scattered results. Particularly in o-substituted phenols such estimates might be complicated owing to an unpredictable steric factor and the possibility of intramolecular H bonding (31). We omitted the phenols which clearly exhibited intramolecular H bonding.

Other Hydroxy Compounds

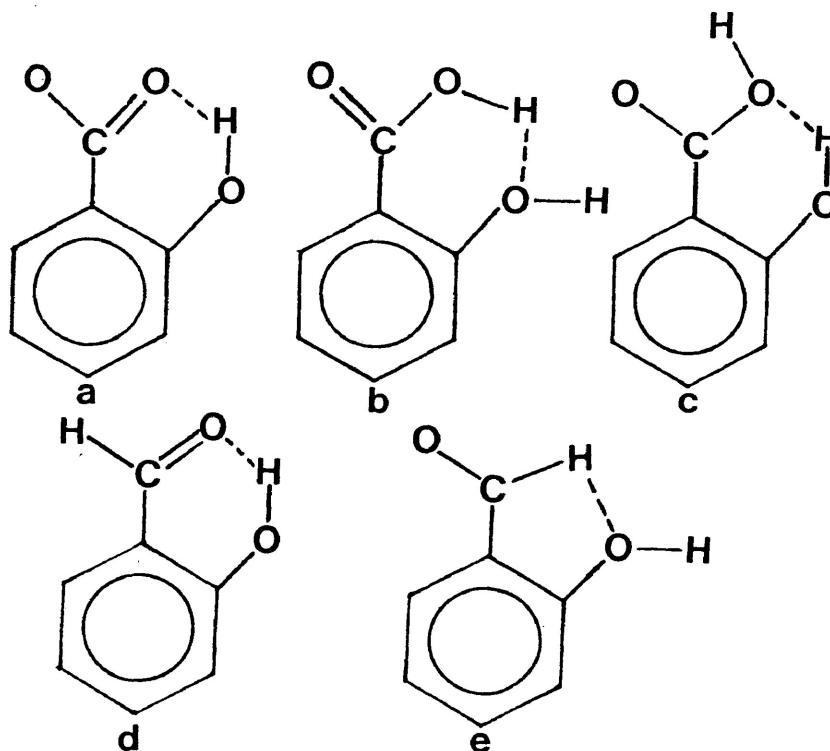
Infrared spectral data for some typical hydroxy

TABLE III-3 ESTIMATED VALUES OF H-BOND ENERGIES ($-\Delta H$) IN THE H-BONDED COMPLEXES OF ALKYL-PHENOLS WITH ORGANIC BASES

Phenolic compound	ΔH values (kcal/mol)			Triethylamine	Source of Estimate
	Methyl-cyanide	1,4-dioxane	Pyridine		
Phenol	4.4	5.8	7.9	9.2	Eqn. III-2
	4.9(4.65)	5.5	7.8(8.0)	-(9.1)	Eqn. III-3
o-Cresol	5.0	5.6	7.8	-	Eqn. III-4 and i.r. data
	4.9	5.5	7.7	8.6	"
2-Ethylphenol	4.9	5.5	7.8	8.8	"
2-Isopropylphenol	4.7	5.5	7.7	8.7	"
2-t-Butylphenol	4.4	4.7	7.3	8.0	"
2,4,6-Trimethylphenol	4.3	4.7	7.2	7.9	"
2,6-Diisopropylphenol	-	3.7	5.5	"	"
2,6-Di-t-butylphenol	5.0	5.6	7.9	8.8	"
4-Isopropylphenol					

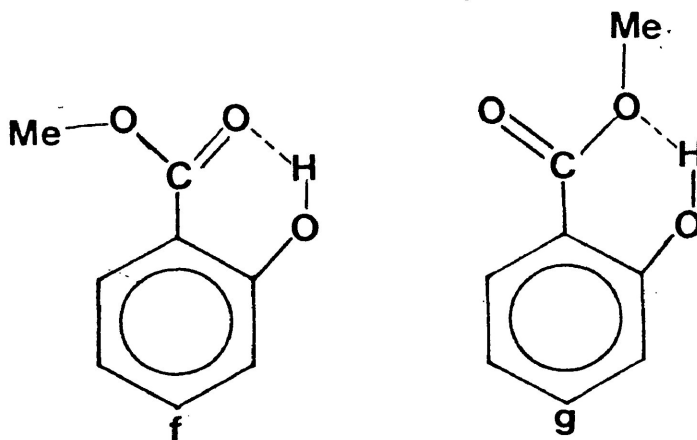
compounds of our interest presented in Table III-6 clearly exhibit the occurrence of H bonding in these compounds. Apparently, none of these compounds showed any absorption band due to free O-H (above 3600 cm^{-1}) and each of them showed at least one peak due to H bonded O-H. The possible nature of H bonding in these compounds under consideration is discussed below:

Salicylaldehyde and its derivative compounds are well known examples of compounds exhibiting intramolecular H bonding. Possible isomeric structures for salicylaldehyde, salicylic acid, and methylsalicylate are shown below:



a,b,c: Salicylic acid

d,e : Salicylaldehyde



f,g: Methylsalicylate

Each of these compounds showed two O-H peaks (Fig. III-7), one around 3200 cm^{-1} (strong) and another (weak) at a higher frequency widely different from one another. For salicylic acid Mori et al observed two bands at 3530 cm^{-1} and 3200 cm^{-1} which were attributed to structure 'a' (44). The peak at 3200 cm^{-1} was obviously due to intramolecularly H bonded O-H while the higher frequency peak at 3530 represented the free O-H of the carboxyl group. Our results showing these peaks at 3210 cm^{-1} and 3520 cm^{-1} are in excellent agreement with these results. The H-bonded phenolic O-H in structures 'd' and 'f' correspond to that in structure 'a'. Consequently the absorption bands at 3195 and 3200 respectively for salicylaldehyde and methylsalicylate could be assigned to the H-bonded phenolic O-H. The weak peaks in these two compounds (3310 cm^{-1} and 3450 cm^{-1}) could possibly be due to H bonding in structures 'e' and 'g' respectively.

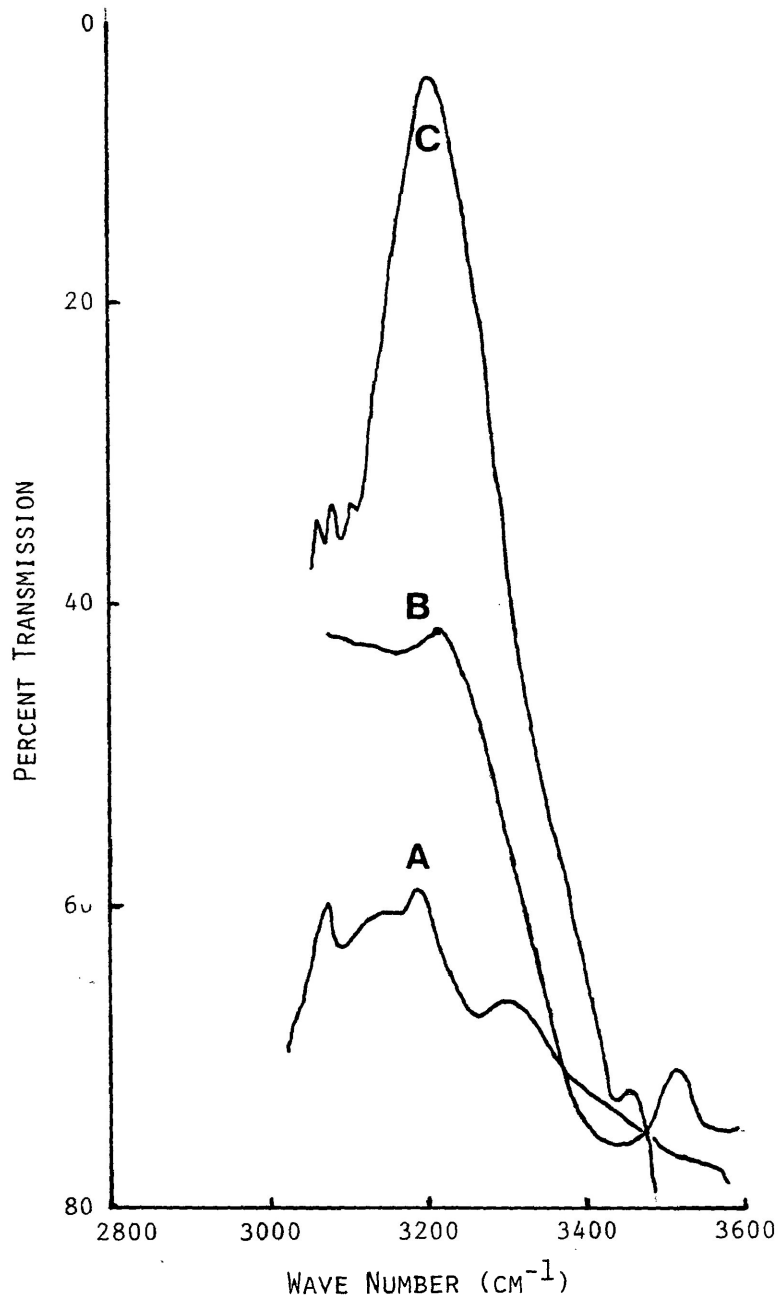
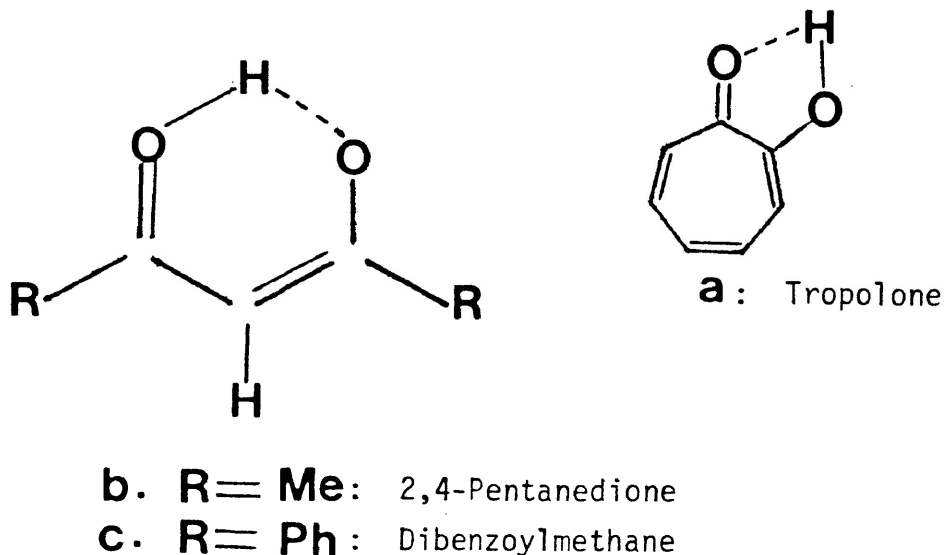


FIGURE III.7. INFRARED SPECTRA OF SALICYLAL-
DEHYDE (A), SALICYLIC ACID (B),
AND METHYLSALICYLATE (C).

The compounds 2,4-pentanedione and dibenzoyl-methane do exist mostly in the enol form (>80%) (45). The intramolecularly H-bonded enol structure is resonance stabilized (as shown below 'a') and consequently the H bond is strong.



The H bonded chelate structure of tropolone is also resonance stabilized 'b'. The positions of the observed single peaks around 3200 cm^{-1} (Fig. III-8) clearly indicated the strength of the intramolecular H bonds in these compounds. Like these compounds, triphenylmethanol also exhibited only one O-H peak but the peak position was at much higher frequency (3480 cm^{-1}) indicating the occurrence of weak H bonding. Most reasonably, the bond is formed owing to the weak interaction of the O-H proton with the π -electron cloud of the benzene rings. Owing to steric crowding

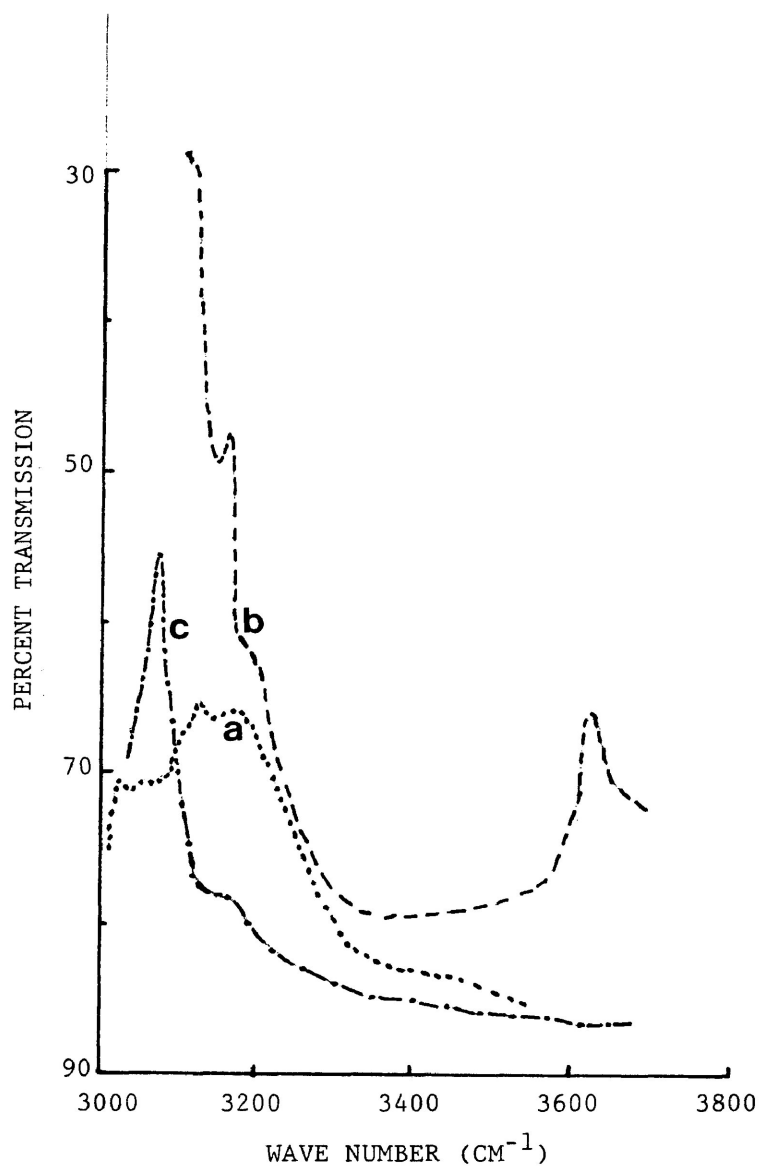


FIGURE III.8. INFRARED SPECTRA OF TROPOLONE (a),
2,4,-PENTANEDIONE (b) AND DIBENZOYL-
METHANE (c).

the possibility of any intermolecular interaction appears to be very remote.

Infrared spectra of three naphthol molecules (Fig. III-9) studied in polystyrene matrices showed only one O-H peak ($\sim 3300 \text{ cm}^{-1}$) for each except 6-bromo-2-naphthol exhibited an additional peak at 3590 cm^{-1} . It appears highly improbable that any intramolecular interaction could give rise to the common peak around 3300 cm^{-1} . The only possibility could be the formation of intermolecular H bonding (O-H-O or O-H--- π -electron bridging) in all three cases. Substitution of Br in 6-position perhaps reduced the H-bonding capability of 2-naphthol significantly which allowed the monomer O-H peak to show up at 3590 cm^{-1} . The total absence of such a peak in 1-naphthol and 2-naphthol, however, remains unclear.

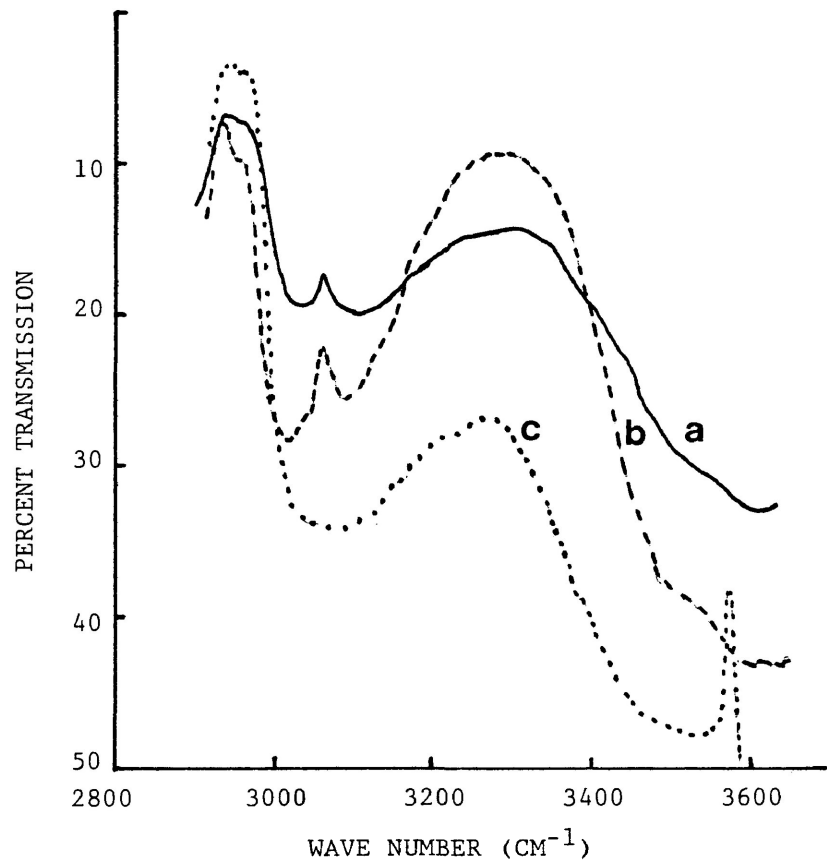


FIGURE III.9. INFRARED SPECTRA OF 1-NAPHTHOL (a), 2-NAPHTHOL (b) AND 6-BROMO-2-NAPHTOL (c).

REFERENCES

1. G. C. Pimentel and A. L. McClellan, "The Hydrogen Bond", W. H. Freeman and Co., San Francisco, 1960.
2. M. D. Joesten and L. J. Schaad, "Hydrogen Bonding", Marcel Dekker, Inc. New York, 1974.
3. A. S. N. Murthy and C. N. R. Rao, "Hydrogen Bonding", Technical Report, Department of Chemistry, I.I.T., Kanpar, India, 1964.
4. H. F. Shurvell, K. Chitambo, A. Dunham and L. Chappell, Can. J. Chem., 1976, 21, 53.
5. L. Y. Bellamy and R. L. Williams, Proc. Roy. Soc. (London), 1960, A254, 119.
6. R. F. Goddu, J. Am. Chem. Soc., 1960, 82, 4533.
7. N. A. Puttnam, J. Chem. Soc. 1960, 486.
8. N. A. Puttnam, J. Chem. Soc. 1960, 5100.
9. K. U. Ingold, Can. J. Chem. 1962, 40, 111.
10. K. U. Ingold and D. R. Taylor, Can. J. Chem. 1961, 39, 471.
11. K. U. Ingold and D. R. Taylor, Can. J. Chem. 1961, 39, 481.
12. J. Juffernbruch and H. H. Perkampus, Spectrochim. Acta. 1980, 36A, 477.
13. K. U. Ingold, Can. J. Chem. 1960, 38, 1092.
14. L. J. Bellamy, "Infrared Spectra of Complex Molecules". Methuen and Co. Ltd., London, 1954, p. 89.
15. G. Rossmly, W. Luttkke and R. Mecke, J. Chem. Phys. 1953, 21, 1606.
16. A. W. Baker, J. Amer. Chem. Soc. 1958, 80, 3598.

17. A. W. Baker and W. W. Kaeding, J. Amer. Chem. Soc. 1959, 81, 5904.
18. A. W. Baker and A. T. Salgin, Can. J. Chem. 1964, 43, 650, and refs. cited therein.
19. A. W. Baker and A. T. Sulgin, 1958, 80, 5358.
20. P. Schuster G. Zundel and C. Sandorfy, Ed. "The Hydrogen Bond. II Structure and Spectroscopy", North Holland Publishing Co., Amsterdam, 1976.
21. H. Dunken and H. Fritzsche, Z. Chem. 1961, 1, 127.
22. H. Dunken and H. Fritzsche, Z. Chem. 1961, 1, 249.
23. H. Dunken and H. Fritzsche, Z. Chem. 1962, 2, 345.
24. G. Aksnes, Acta Chem. Scand. 1960, 14, 1485.
25. D. R. van Damme and T. Zeegers-Huyskens, J. Phys. Chem. 1980, 84, 282.
26. T. Gramstad and W. J. Fuglevik, Acta. Chem. Scand. 1962, 16, 1369.
27. T. Gramstad, Acta Chem. Scand. 1962, 16, 807.
28. M. S. Nozari and R. S. Drago, J. Amer. Chem. Soc. 1970, 92, 7086.
29. G. C. Pimentel and A. L. McClellan, Ann. Rev. Phys. Chem., 1971, 22, 347.
30. A. S. N. Murthy and C. N. R. Rao, Appl. Spectrosc. Rev. 1968, 2, 69.
31. R. S. Drago and T. D. Epley, J. Amer. Chem. Soc., 1969, 91, 2883.
32. R. S. Drago, J. Chem. En., 1974, 51, 300.
33. R. S. Drago and B. B. Wayland, J. Amer. Chem. Soc., 1965, 87, 3571.
34. F. L. Slejko, R. S. Drago, and D. G. Brown, J. Amer. Chem. Soc. 1972, 92, 9210.

35. R. S. Drago, G. C. Vogel and T. E. Needham, J. Amer. Chem. Soc. 1971, 93, 6014.
36. M. D. Joesten and R. S. Drago. J. Amer. Chem. Soc. 1962, 84, 3817.
37. J. Kraft, S. Walker and D. Magee, J. Phys. Chem. 1975, 79, 881.
38. L. Pauling, J. Amer. Chem. Soc. 1936, 58, 94.
39. L. R. Zumwalt and R. M. Badger, J. Amer. Chem. Soc. 1940, 62, 305.
40. M. Davies, Trans Faraday Soc. 1940, 36, 333.
41. R. M. Badger and S. H. Bauer, J. Chem. Phys., 1937, 5, 839.
42. M. A. Mazid, M. A. Enayetullah and S. Walker, J. Chem. Soc. Faraday Trans. II, 1981.
43. T. D. Epley and R. S. Drago, J. Amer. Chem. Soc., 1967, 89, 5770.
44. N. Mori, Y. Asano, T. Irie and Y. Suzuki, Bull. Chem. Soc. Jap., 1969, 42, 482.
45. G. Allen and R. A. Dwek, J. Chem. Soc. (B)., 1966, 161.

TABLE III-4 * INFRARED ABSORPTION FREQUENCIES FOR O-H STRETCHING IN PHENOL ALKYLPHENOLS AND IN THEIR H-BONDED COMPLEXES IN CCl₄ SOLUTION

PROTON DONOR	PROTON ACCEPTOR	$\nu_{\text{O-H}} \text{ (cm}^{-1}\text{)}$	$\nu_1 \text{ O-H (cm}^{-1}\text{)}$	$\nu_2 \text{ O-H (cm}^{-1}\text{)}$	$\Delta\nu_1 \text{ O-H (cm}^{-1}\text{)}$
Phenol	none	3615(3612) ⁴ ; Sh.S.	3485(3487) ⁴ ; SR to ν_2	3345(3346) ⁴ ; S. VB.	--
	MC	3615; VW	3435; B.VS.	--	180(178) ³⁶
	DO	3615; VW	3375(3369) ⁵ B.VS.	--	240
	Py	--	3155; VB.S. (SR to C-H peak)	--	460(465) ³⁶
o-Cresol	none	3620(3615) ¹⁰ ; Sh.VS.	3540; SR. to ν_2	3470; VB.S.	--
	MC	3620; VW	3440; B.S.	--	180
	DO	3620; VW	3380; B.VS.	--	240
	Py	--	3160; VB.C. (SR. to C-H peak)	--	460
2-Ethylphenol	none	3620(3614) ¹⁰ ; Sh.VS.	3555; SR to ν_2	3490; VB.S.	--
	MC	3620; VW	3445; B.S.	--	175
	DO	3620; VW	3385; B.VS.	--	235
	Py	3620; VW	3165; B.VS. (SR to C-H peak)	--	455
	TEA	3620; VW	3070; B.VS. (SR. to C-H peak)	--	550
Isopropylphenol	none	3620(3615) ⁵ ; Sh.VS.	3560; B.S.	3505; VB.S.	--
	MC	3620; W	3450; B.VS.	--	170
	DO	3620; W	3385; VB.VS.	--	235
	Py	3620; VW	3165; VB.VS. (SR. to C-H peak)	--	455
	TEA	3620; VW	3070; VB.VS. (SR. to C-H peak)	--	550

continued...

TABLE III-4 * INFRARED ABSORPTION FREQUENCIES FOR O-H STRETCHING IN PHENOL ALKYLPHENOLS AND IN THEIR H-BONDED COMPLEXES IN CCl₄ SOLUTION

PROTON DONOR	PROTON ACCEPTOR	$\nu_{\text{O-H}}$ (cm ⁻¹)	$\nu_{\text{I O-H}}$ (cm ⁻¹)	$\nu_{\text{2 O-H}}$ (cm ⁻¹)	$\Delta\nu_{\text{1 O-H}}$ (cm ⁻¹)
2-t-Butylphenol	none	3650(3643) ⁶ ; Sh., VW	3560; W	3475; VW	--
	MC	3615; VW	3450; B.S.	--	160
	DO	3615; VW	3385; B.S.	--	230
	Py	--	3165 VB.S. (SR to C-H peak)	--	450
	TEA	--	3075; VB.S. (SR. to C-H peak)	--	540
2-Phenylphenol	none	3615(3604) ⁸ ; W.	3570(3562) ⁸ ; Sh.S.	--	--
	MC	--	3570; VW.	3435; B.S.	180 ($\Delta\nu_{\text{2 O-H}}$)
	DO	--	3570; VW.	3375; B.S.	240 ($\Delta\nu_{\text{2 O-H}}$)
	Py	--	3570; VW.	3155; B.S.	460 ($\Delta\nu_{\text{2 O-H}}$)
2,4,6-Trimethylphenol	none	3625(3624) ¹⁰ ; Sh.S.	--	--	--
	MC	3625; W	3500; B.S.	--	125
	DO	3625; VW	3465; B.S.	--	160
	Py	3625; VW	3220; VB.S.	--	405
	TEA	3625; VW	3150; VB.S.	--	475
2,6-Diisopropylphenol	none	3625(3623) ¹⁰ ; Sh.S.	--	--	--
	MC	3625; W	3510; B.S.	--	115
	DO	3625; VW	3470; B.S.	--	155
	Py	3625; VW	3225; VB.S.	--	400
	TEA	3625; VW	3155; VB.S.	--	470
2,6-Di-t-butylphenol	none	3650(3648) ¹⁰ ; Sh., VS	--	--	--
	MC	3645*	--	--	--
	DO	3650; Sh.S.	3590 B.VW.	--	60
	Py	3650	3420	--	230

continued...

TABLE III-4 * INFRARED ABSORPTION FREQUENCIES FOR O-H STRETCHING IN PHENOL ALKYLPHENOLS AND IN THEIR H-BONDED COMPLEXES IN CCl₄ SOLUTION

PROTON DONOR	PROTON ACCEPTOR	ν_{O-H} (cm ⁻¹)	ν_1 O-H (cm ⁻¹)	ν_2 O-H (cm ⁻¹)	$\Delta\nu_1$ O-H (cm ⁻¹)
4-Isopropylphenol	none	3625(3628) ⁷ ; Sh.S.	3490; W (SR to ν_2 O-H)	3355; VB.S.	--
	MC	3625; VW	3440; B.VS.	--	185
	DO	3625; VW	3385; B.VS.	--	240
	Py	3625; VW	3155; VB.VS.	--	470
	TEA	3625; VW	(SR to C-H peak) 3070; VB.VS. (SR to C-H peak)	--	555
2,4,6-Tri-t-butylphenol	none	3650(3642) ⁶ ; Sh.VS.	--	--	--
	MC	3650; Sh.VS.	--	--	--
	DO	3650; Sh.S.	3585; VW	--	65
	Py	3650; Sh.S.	3410; VW	--	240
	TEA	3650; Sh.S.	3345; VW	--	305
2,4,6-Trimethylphenol	0.3M none	3625(3624) ¹⁰ ; Sh.VS.	--	--	--
	0.6M none	3625; Sh.VS.	--	3540; VW	--
	0.9M none	3625; Sh. VS.	3585; W (SR to ν_{O-H})	3540; W (SR to ν_1 O-H)	--
1.5M (saturated)	none	3625; Sh. VS.	3585; S. (SR to ν_{O-H})	3540; S (SR to ν_1 H-O)	--
2,6-Diisopropylphenol	40%	3625; Sh. VS.	3590; S. (SR to ν_{O-H})	3555; S (SR to ν_1 O-H)	--
2,6-Di-t-butylphenol	40%	3650; Sh.VS.	--	--	--
2,4,6-Tri-t-butylphenol	40%	3650; Sh.VS.	--	--	--

* Abbreviations used in the Table are: MC - methylcyanide; DO - 1,4-dioxan; Py - pyridine; TEA - triethylanine; B - broad; Sh - sharp; S - strong; SR - shoulder; V - very; and W - weak. The bracketed frequencies represent the literature values, the reference number being given as the subscript of the bracket.

TABLE III-5* INFRARED ABSORPTION FREQUENCIES FOR O-H STRETCHING IN HALOGENOPHENOLS AND THEIR H-BONDED COMPLEXES IN CCl₄ SOLUTION

PROTON DONOR	PROTON ACCEPTOR	$\nu_{\text{O-H}}$ (cm ⁻¹)	ν_1 O-H (cm ⁻¹)	ν_2 O-H (cm ⁻¹)	$\Delta\nu_1$ O-H (cm ⁻¹)	$\Delta\nu_2$ O-H (cm ⁻¹)	**
o-Chlorophenol	none	3610(3603) ¹⁵ ; VW	3550(3545) ¹⁵ ; Sh.S	-	60	-	-
	none	3615(3605) ¹⁵ ; VW	3540(3530); Sh.S	-	75	-	-
	MC	-	3540; W	3390pB.S.	-	225	-
o-Bromophenol	DO	-	3540; W	3345; B.S.	-	270	-
	Py	-	3540; VW	3155; B.S. (SR. to C-H peak)	-	455	-
	none	3610(3601)	3515(3509); Sh.VS.	-	95	-	184
o-Iodophenol	MC	-	3515; W	3380; B.S.	-	235	-
	DO	-	3515; W	3315; B.S.	-	300	-
	Py	-	3515; W	3155; B.S. (SR. to C-H peak)	-	460	-
2,6-Dichlorophenol	none	-	3545; Sh.VS.	-	65	-	-
	MC	-	3545; Sh.W	3375; B.S.	-	235	-
	DO	-	3545; Sh.W	3290; B.S.	-	320	-
Py	-	3445; Sh.W	3150; VB.S (SR to C-H peak)	-	460	-	-

continued...

TABLE III-5 * INFRARED ABSORPTION FREQUENCIES FOR O-H STRETCHING IN HALOGENOPHENOLS AND THEIR H-BONDED COMPLEXES IN CCl₄ SOLUTION

PROTON DONOR	PROTON ACCEPTOR	$\nu_{\text{O-H}}$ (cm ⁻¹)	ν_1 O-H (cm ⁻¹)	ν_2 O-H (cm ⁻¹)	$\Delta\nu_1$ O-H (cm ⁻¹)	$\Delta\nu_2$ O-H (cm ⁻¹)
2,4,6-Tribromophenol**	none	-	3525 (3526) ³⁷ ; Sh.S	-	90	-
	MC	-	3525; Sh.W.	3370; B.S.	-	245
	DO	-	3525; Sh.W.	3290; B.S.	-	325
	Py	-	2525; Sh.VW	3150; VB.S	-	465
2,4,6-Trichlorophenol 0.3 M - 1.5 M (saturated)	none		\sim 3542) ³⁷		-	
2,4,6-Tribromophenol 0.15 M - 0.6 M (saturated)	none		\sim 3525 (3526) ³⁷		-	
2,4,6-Triiodophenol 0.11 M (saturated)	none	-	3495	-	-	-

* The abbreviations have the same meaning as in Table III-1

** $\Delta\nu_2$ O-H values were calculated as $\nu_{\text{O-H}} - \nu_2$ O-H, using $\nu_{\text{O-H}}$ values of the respective o-halogenophenols.

TABLE III-6* INFRARED ABSORPTION FREQUENCIES FOR O-H STRETCHING IN SOME TYPICAL HYDROXY COMPOUNDS

COMPOUND	MEDIUM**	ν_{O-H} (cm^{-1})	ν_1 O-H (cm^{-1})	ν_2 O-H (cm^{-1})
Salicylaldehyde	CCl ₄	--	3310; B.W.	3195; B.S.
Salicylic acid	PS	--	3520; B.W.	3210; B.S.
Methylsalicylate	CCl ₄	--	3450; VW (SR to ν_2 O-H)	3200; B.S.
Tropolone	CCl ₄	--	3175; B.S. (SR to C-H peak)	--
2,4-Pentanedione	PS	--	3180; B.VS (SR to C-H peak)	--
Dibenzoylmethane	CCl ₄	--	3200; S. (SR to C-H peak)	
Triphenylmethanol	Nujol mull	--	3180; W (SR to C-H peak)	
1-Naphthol	PS	--	3480; B.S.	
2-Naphthol	PS	--	3300; VB.S	
6-Bromo-2-Naphthol	PS	3590	3290; VB.S.	

*The abbreviations have the same meanings as in Table III-1

** Since dielectric studies were made mostly in polystyrene (PS) matrices it was in our own interest to see the i.r. spectra in the same medium. Nujol mull was used as medium because of solubility problems in CCl₄

CHAPTER IV: PROTON N.M.R. STUDIES ON THE
 HYDROGEN BONDING EQUILIBRIA
 OF PHENOL AND SOME HINDERED
 PHENOLS

INTRODUCTION

The H-bond shift; i.e. the downfield shift of the proton resonance signal caused by H bond formation, is the key parameter in the study of H bonding through n.m.r. The mechanism of this downfield shift and various factors influencing this key parameter have been summarized in the introductory chapter of this thesis. This chapter will deal with our proton n.m.r. studies on the self-association behaviour (through H bonding) of several o-alkyl and 2,6-dialkylphenols in CCl_4 solution.

In solutions of self-associating solutes in "inert" solvents the proton resonance signal is normally shifted in the same upfield direction by the increase of temperature and dilution (1-7). This shift is caused partly by various medium effects (8) and partly by the change in relative proportions in the H-bonded species (5,9-12). The use of internal reference and of isotropic solvents (e.g. CCl_4) eliminates the consideration of unknown medium effects, except the polar effects (13) which are usually small. Consequently, in these solvents the dilution shifts at constant temperature and pressure should have a definite correlation with the relative proportion of the H-bonded species. Utilizing this fact, several mathematical methods (8) have been developed in order to investigate the association equilibria through

H bonding. Of these methods the method of Saunders and Hyne (14-16) is the most general and widely accepted one, the very basic assumption of which is: the monomer and only one other polymer are in a dominant equilibrium. This method was utilized in the present n.m.r. study in order to determine the association characteristics of the molecules of our interest.

Proton n.m.r. studies of association equilibria in OH systems (alcohols and phenols) are quite abundant in the literature (7,14-22). Saunders and Hyne (16,17) determined the association constants for monomer-trimer equilibria for phenol and t-butanol and monomer-tetramer equilibria for methanol and ethanol. These authors suggested cyclic structures for polymers of alcohols and pure phenol and indicated that at low concentrations monomer-dimer equilibria become dominant over monomer-trimer and monomer-tetramer equilibria. Monomer-dimer equilibria in different OH systems at low concentrations have been widely supported by different workers (5,19,20). The n.m.r. data of Feeny and Walker (20) on 2-methoxyethanol fitted the monomer-dimer model at low and intermediate concentrations, but departed at higher concentrations toward the theoretical curve for trimer. Dale and Gramstad (22) investigated the self-association of phenol and a number of mono- and

polyfluorophenols in CCl_4 by measuring dilution shifts of OH proton and F resonance signals. Their data on phenol and 3- and 4-fluorophenols fitted well with monomer-trimer equilibria while the data for 2-fluoro and polyfluorophenols were consistent with monomer-dimer equilibria. Griffiths and Socrates (21) used Saunders-Hyne (SH) method to study H bonding equilibria in a series of monosubstituted phenols. Their experimental data, in general, gave the best fit with the theoretical data for monomer-trimer equilibria. Exceptions to this general behaviour were, however, observed with o-halogeno and o-nitrophenols which involved strong intramolecular H bonding and in some cases steric hindrance. It was suggested that these molecules were present mainly as monomers in their experimental concentration range and the small concentrations of associated species were the dimers.

As regards the association behaviour of phenols, the observations of Dale and Gramstad (22) and Griffiths and Socrates (21) appear to suggest that in the absence of any significant intramolecular H bonding and steric hindrance the monomer-trimer equilibria are dominant at higher concentration. The influence of intramolecular H bonding on the association equilibrium has been clearly demonstrated in the works of these authors. N.m.r. studies on the role of steric factor in the association equilibria, on the other hand, appear to be very

rare in the literature. The influence of this factor is, however, quite apparent in the results of Griffiths and Socrates (21). Results of these authors on o-cresol gave the best fit with the theoretical curve for monomer-trimer equilibrium. Somers and Gutowsky (7), assumed that the hindered and partially hindered phenols were unlikely to form associated species larger than dimers and determined the dimerization constants for several alkyl-substituted phenols with principally bulky alkyl (e.g. isopropyl or t-butyl) group(s) at 2- and 2,6-positions. The dimerization constant of o-cresol as determined by Griffith and Socrates (21) using the SH method was 0.335 l M^{-1} . As compared to this the values of the dimerization constants for isopropylphenol (17 ± 0.5), 2-t-butylphenol (1.0 ± 0.5) 2,6-diisopropylphenol (1.3 ± 0.5) etc. determined by Somers and Gutowsky (7) appear to be much higher and quite inconsistent.

One point to be noted here is that the latter authors used a simplified equation in the analysis of their n.m.r. data while the former used the well established SH method. In the present study the n.m.r. results on several partly hindered and hindered phenols will be analyzed using this method in order to determine the association constants for and the sizes of H-bonded aggregates of the molecules in question. This, it is hoped, will provide a clearer under-

standing of the complex H bonding equilibria and illustrate the influence of hindering alkyl groups in these equilibria for the molecules of our concern.

METHOD OF ANALYSIS

As mentioned earlier the method introduced by Saunders and Hyne (14-16) was used in the analysis of our n.m.r. results obtained as the shift of hydroxyl proton resonance with dilution by CCl_4 . The basic assumptions of the method are:

1. the dilution shift is due exclusively to H bonding.
2. the observed single O-H peak can be regarded as the time averaged signal of all the species present in the equilibrium system.
3. there exists only one H bonding equilibrium throughout the experimental concentration range.
4. the resonance frequency ν_m for an n-mer is constant throughout the concentration range.

According to the third assumption the O-H proton may find itself in two different magnetic environments corresponding to the monomer and only on polymer. Following the

equation derived by Gutowsky and Seika (23) the weighted average of the resonance frequencies (i.e. the observed frequency) can be expressed as:

$$\nu = (\nu_1 M_1 + n \nu_n K_n M_1^n) / C \quad \text{IV-1}$$

where: $C = M_1 + n K_n M_1^n \quad \text{IV-2}$

In these equations ν is the observed frequency; ν_1 is the resonance frequency of the monomer-OH proton; ν_n is the resonance frequency of the H-bonded polymer-OH proton; n is the number of monomers making one polymer; K_n is the equilibrium constant between the monomer and the polymer; M_1 is the monomer concentration, C is the total concentration.

If all frequencies are measured from ν_1 , then the slope of ν versus $\log C$ curve is proportional to ν_n at the inflection point and is given by (8):

$$\frac{d\nu}{(d \log C)_{ip}} = 2.303 (\nu_1 - \nu_n) \frac{n^{-\frac{1}{2}} - n^{\frac{1}{2}}}{n^{-\frac{1}{2}} + n^{\frac{1}{2}} + 2} \quad \text{IV-3}$$

Thus for each n , a value of ν_n can be obtained from equation IV-3 and the observed slope. If K_n is set equal to unity and the plots of ν versus $\log C$ are constructed for $n=2, 3, 4, \text{ etc.}$,

the displacement along $\log C$ axis of any calculated curve from the observed curve is equal to $(\log K_n)/(n-1)$. This property of Egn. IV-1 allows the evaluation of association constants, K_n and the n -value giving the best fit of the theoretical curve to the experimental curve indicate the size of the polymer species.

As the concentration decreases, the observed frequency approaches a limiting value corresponding to the complete dissociation to monomer. The extrapolation of this curve to infinite dilution will therefore yield the monomer frequency, ν_1 . Theoretical monomer concentrations for different total concentrations can be calculated by solving the n th order Egn. IV-2, first assuming $K_n=1$ for determining experimental K_n , and afterwards with experimental K_n to examine the curve-fitting.

It should be mentioned here that the SH method is inadequate to handle the equilibrium when $n > 4$ (8).

RESULTS AND DISCUSSION

The present nmr investigation was performed with the following phenolic compounds:

- IV.1 Phenol
- IV.2 0-Cresol
- IV.3 2-Ethylphenol
- IV.4 2-Isopropylphenol
- IV.5 2-t-Butylphenol
- IV.6 2,4,6-Trimethylphenol
- IV.7 2,6-Diisopropylphenol
- IV.8 2,6-Di-t-butylphenol

The resonance frequency of the O-H proton in each of these compounds was measured at 30°C in CCl₄ solutions and recorded as frequency, ν (Hz). Unlike the common practice, the downfield shift with TMS signal as zero reference has been expressed as a positive value of the frequency (Hz). The concentrations of the experimental solutions ranged, in most cases, from 0.1 M to 5.0 M; for 2,4,6-trimethylphenol the highest concentration was, however, limited to 1.0 M by solubility consideration. The observed chemical shifts (Hz) with respect to TMS are given in Tables IV.3 - IV.10. Theoretical values of this parameter for different monomer-polymer equilibria (i.e., for n=2,3 and 4) obtained by SH method are also

given in these tables.

The observed shifts in Hz for different compounds have been plotted against their molar concentrations in Figs. IV.1 and IV.2. Extrapolation of these plots to infinite dilution should provide the monomer frequencies (ν_1) for respective compounds. As shown in these figures the ν vs. C plots for most of the compounds do not give straight lines. Linear relationship could, however, be approximated at very low concentration region. Extrapolations were thus made only with very low concentration data in order to obtain the monomer frequencies (ν_1). The values of ν_n and K_n for $n=2,3$ and 4 were calculated following the procedure described in the method of analysis. These values for different compounds are presented in Table IV.2.

The ν_n values were calculated (using Eq. IV-3) from the slopes of $(\nu - \nu_1)$ vs. $\log C$ curves at their inflection points; such curves for a few compounds are shown in Fig. IV.3. Plots of ν (experimental) vs. $\log C$ for different compounds have been presented in Figs. IV.4 to IV.10 in which the fitting of the theoretical ν -values for $n=2,3$ and 4 have also been shown.

In a hydrogen bonding system the relative position of the O-H proton signal indicates a greater or lesser extent of H bonding. With some reservation, this is a

good approximation, although the influence of electronic screening, steric hindrance, and inductive effects should not be ignored completely. Table IV-1 presents the comparative values of the observed chemical shifts for different compounds at three different concentrations (5.0 M, 1.0 M and 0.1 M). This table does also contain the values of H-bond shifts for the same compounds at 1.0 M. Let us discuss the experimental chemical shifts at 1.0 M concentration. Very clearly, phenol exhibited maximum amount of H bonding. The extent of H bonding was greatly decreased by the substitution of an alkyl group in the o-position which was demonstrated by the decrease in the observed ν -values. With increasing size of the o-alkyl group the decrease of the observed shift was gradual which suggested that the steric hindrance could play a significant role in determining the extent of H bonding in o-alkylphenols. In the cases of phenol molecules having alkyl groups at both the o-positions the trend was, however, reversed; the experimental chemical shift was found to increase with the increasing size of the alkyl groups. This apparently anomalous behavior can easily be understood if we consider the values of the monomer frequencies (ν_1) for these compounds (Table IV-1). The reverse order, in fact, originated in these monomer frequencies

TABLE IV-1: COMPARATIVE VALUES OF OBSERVED CHEMICAL SHIFTS AND H BOND SHIFTS FOR DIFFERENT PHENOLS

COMPOUND	OBSERVED CHEMICAL SHIFT (Hz)		H BOND SHIFT (Hz)* at 1.0 M
	5.0 M	1.0 M	
Phenol	568.7	503.7	360.2
o-Cresol	486.7	426.1	350.5
2-Ethylphenol	470.2	406.1	349.8
2-Isopropylphenol	456.0	397.4	342.0
2-t-Butylphenol	377.9	363.4	355.6
2,4,6-Trimethylphenol	--	351.0	330.7
2,6-Diisopropylphenol	390.9	366.1	360.9
2,6-Di-t-butylphenol	--	398.04	398.63

*H bond shift calculated on ν_{obs} (at 1.0 M) - ν_1 ; except for the last compound the values are rounded off.

TABLE IV-2: RESULTS OF n.m.r. STUDIES ON H BONDING EQUILIBRIA OF PHENOLS OBTAINED BY SH METHOD

COMPOUNDS	ν-values (Hz)				Association Constants			
	ν ₁	ν ₂	ν ₃	ν ₄	K ₂ ℓ/mol	K ₃ ℓ ² /mol ²	K ₄ ℓ ³ /mol ³	
Phenol	325	730	584	534	0.71	5.26	53.09	
o-Cresol	341	597	505	473	0.35	1.29	6.03	
2-Ethylphenol	342	577	493	463	0.27	0.81	2.86	
2-Isopropylphenol	335	555	476	448	0.22	0.78	2.72	
2-t-Butylphenol	354	407	388	381	0.14	0.22	0.47	
2,4,6,-Trimethylphenol	328	437	398	384	0.20	0.33	0.80	
2,6-Diisopropylphenol	360	509	456	437	0.03	0.014	0.011	
2.6-Di-t-butylphenol	398.67	-	-	-	-	-	-	-

which are determined by different factors such as electronic screening and inductive effects, and various medium effects, and so on. .

The relative extent of H bonding in the compounds of our interest could more appropriately be represented in terms of 'H bond shift'. Values of this quantity (listed in Table IV-1 for 1.0 M solutions) for different compounds perhaps demonstrate the proper order of H bonding, higher the value of 'H-bond shift' greater is the extent of H bonding. Thus the maximum extent of H bonding was found to occur in phenol. In o-alkylphenol as well as in 2,6-dialkylphenols the observed H-bond shifts gradually decreased as the size of the alkyl groups increased. This clearly showed the influence of steric hindrance on the extent of H bonding although the electronic screening and inductive effects might also have some role in it. It is interesting to note here that the 'H bond-shift' for the most hindered molecule, 2,6-di-t-butylphenol, was negative although the numerical value was very small. The observed chemical shift for this compound remained almost constant over the concentration range of 0.1 M to 4.0 M indicating the total absence of H bonding. This is quite understandable in terms of massive steric hindrance by the bulky t-butyl groups which, as demonstrated by our ir results (Ch.III),

can effectively prevent any intermolecular H bonding. The observed negative 'H-bond shift', however, remains unexplained. Somers and Gutowsky (7) explained this phenomenon in terms of 'some shift-producing factor other than hydrogen bonding'. The authors did not, however, mention anything about what this shift-producing factor might be. One possible explanation could be given in terms of a very weak interaction of the phenolic proton with the π -electrons of neighboring aromatic ring which could cause a diamagnetic shift (upfield) due to shielding effect (24). Since the OH proton in the molecule in question is believed to lie in the t-butyl 'basket' (25) in the plane of the aromatic ring the proposed interaction must be very weak and its concentration dependence can be explained in terms of the relative distance of the interacting aromatic ring from the H in the t-butyl 'basket'.

The most elegant feature of the SH method is the fitting of the theoretical ν -values assuming different monomer-polymer equilibria (with $n=2,3$ and 4) in the ν versus $\log C$ plot obtained with the experimental ν -values. The best-fitting curve determines the most dominant equilibrium and thus the most abundant associated species in an H bonding system. Thus, for phenol

and o-cresol (Figs. IV.4 and IV.5, respectively) the best-fitting curves were for $n=3$. This clearly indicated that the monomer-trimer equilibrium was dominating in both of these compounds. These results clearly reaffirmed the results of Saunders and Hyne (15) on phenol and those of Griffiths and Socrates (21) on o-cresol. At higher concentration, the experimental curves for both of the compounds in question showed a tendency to shift toward the theoretical curves for $n=2$. This could most likely be due to the presence of some dimeric species in the solution. Although the SH method assumes only one equilibrium in the system, there is no way one could object to the presence of more than one associated species in the systems under consideration. Our infrared data (Ch. III) on these compounds very clearly showed the existence of at least two polymer species. Nevertheless, the SH method is quite capable of determining the most dominant equilibrium which, for phenol and o-cresol, was monomer-trimer type. Our experimental values of association constants ($K_3 \text{ l}^2 \text{ mol}^{-2}$) for phenol and o-cresol were, respectively, 5.26 and 1.29 as compared to the literature values of 4.78(15) and ~ 1.15 (21), respectively. The agreement is quite satisfactory. The monomer frequency (ν_1) for o-cresol, as observed by Griffiths

and Socrates (21), was 4.43 ppm (266 Hz) as compared to our value of 341 Hz. The difference is quite significant which could partly be due to the fact that our experimental temperature (30°C) was higher than that of these authors'. Their ν_1 -value was coincident with the experimental ν -value at their lowest concentration (0.1 M). This is not understandable; our results on o-cresol (Fig. 1) seem to negate such a possibility.

The Figs. IV.6-8 and IV.10 representing our nmr data for 2-ethylphenol, 2-isopropylphenol, 2-t-butylphenol and 2,6-diisopropylphenol, respectively, strongly suggest that the dominant equilibria in these systems were all between their respective monomers and dimers as opposed to the monomer-trimer equilibria observed for phenol and o-cresol. It is really interesting to note how dramatically the nature of the monomer-polymer equilibria of o-alkylphenols is changed by the bulkiness of the alkyl groups.

Figure IV.9 for 2,4,6-trimethylphenol appears to present a mixed situation. At lower concentration the experimental curve is closer to the theoretical curve for $n=2$ while the same curve at higher concentrations merges with the curves for $n=3$ and 4. This behavior of

the experimental curve seemed to suggest that, while monomer-dimer equilibrium might be operative in dilute solutions, larger polymer species (possibly trimer) become more abundant at higher concentrations. This could be a very likely situation if we consider the fact that methyl groups can exert a very weak steric hindrance and, consequently, cannot resist extensive H bonding, particularly at high concentration. This explanation is very much consistent with our ir results on the compound in question.

The K_n -values for different alkylphenols in Table V-2 also demonstrate the relative extent of H bonding in these compounds. Exactly the same order is observed in K_n -values as is shown by the H bond shifts at 1.0 M (Table IV-1). As our infrared results, these results do also suggest that the steric hindrance of the alkyl groups at 2- and 2,6-positions significantly reduces the extent of H bonding in alkylphenols. The steric hindrance increases with the size of the alkyl groups and is most effective when they occupy both 2- and 6-positions with respect to the phenolic O-H group. Thus, 2,6-di-t-butylphenol should be considered as the most hindered molecule in our list in which no H bonding was observed, and consequently, the data

could not be analyzed by SH method.

Our K_n -values for more hindered phenols appeared to be significantly lower than those obtained by Somers and Goutosky (7). The discrepancy could possibly be due to the fact that these authors used an oversimplified model for their analysis; the erratic nature of this model was humbly admitted by the authors (7).

REFERENCES

1. W. G. Schneider, H. J. Bernstein, and J. A. Pople, *J. Chem. Phys.*, 1958, 28, 601.
2. M. Van Thiel, E. D. Becker, and G. C. Pimentel, *J. Chem. Phys.* 1957, 27, 95.
3. W. C. Coburn and E. Grunwald, *J. Am. Chem. Soc.*, 1958, 80, 1318.
4. L. W. Reeves, *Trans. Faraday Soc.*, 1959, 55, 1684.
5. J. C. Davis, Jr., K. S. Pitzen, and C.N.R. Rao, *J. Phys. Chem.*, 1960, 64, 1744.
6. J. Feeney and L. H. Sutcliffe, *J. Chem. Soc.*, 1962, 1123.
7. B. G. Sourenn and H. S. Gutowsky, *J. Am. Chem. Soc.*, 1963, 85, 3065.
8. J.C. Davis, Jr., and K. K. Deb in *Advances in Magnetic Resonance, V-4*, Academic Press, New York, London, 1970, pp. 201-270.
9. M.E. Packard and J.T. Arnold, *Phys. Rev.*, 1951, 83, 210.
10. A.D. Cohen and C. Reid, *J. Chem. Phys.*, 1956, 25, 790.
11. J. F. Feeney and L. H. Sutcliffe, *Proc. Chem. Soc.*, 1961, p. 118.
12. S. H. Marcus and S. I. Miller, *J. Am. Chem. Soc.*, 1966, 88, 3719.
13. P. Diehl and R. Freeman, *Mol. Phys.*, 1961, 4, 39.
14. M. Saunders and J. B. Hyne, *J. Chem. Phys.*, 1958, 29, 253.
15. M. Saunders and J. B. Hyne, *J. Chem. Phys.*, 1958, 29, 1319.
16. M. Saunders and J. B. Hyne, *J. Chem. Phys.*, 1959, 31, 270.
17. C. M. Huggins, G. C. Pimentel and J. N. Shooleny, *J. Phys. Chem.*, 1956, 60, 1311.

18. E. A. Allan and L. W. Reeves, *J. Phys. Chem.*, 1962, 66, 613.
E.A. Allan and L. W. Reeves, *J. Phys. Chem.*, 1963, 67, 591.
19. E. D. Becker, *J. Chem. Phys.*, 1959, 31, 269.
20. J. Feeney and S. M. Walker, *J. Chem. Soc. A.*, 1966, p. 1148.
21. V. S. Griffiths and G. Socrates, *J. Mol. Spectry.*, 1966, 21, 302.
22. A. J. Dale and T. Gramstad, *Spectrochim. Acta.*, 1972, 28A, 639.
23. H. S. Gutowsky and A. Saika, *J. Chem. Phys.*, 1953, 21, 1688.
24. J. W. Emsley, J. Feeney and L. H. Sutcliffe, "High Resolution Nuclear Magnetic Resonance Spectroscopy", Vol. 1, Pergamon Press, New York, 1965.
25. K. V. Ingold, *Can. J. Chem.*, 1960, 38, 1092.

TABLE IV-3: OBSERVED CHEMICAL SHIFTS FOR PHENOL AT DIFFERENT CONCENTRATIONS AND THEIR THEORETICAL VALUES ASSUMING DIFFERENT MONOMER-POLYMER EQUILIBRIA

<u>Molar Concentration</u>	<u>Observed Chemical Shift, ν(hz)</u>	<u>Theoretical ν-values for different monomer-polymer equilibria</u>		
		<u>n = 2</u>	<u>n = 3</u>	<u>n = 4</u>
0.1	360.2	370.7	355.2	352.7
0.2	392.9	400.9	395.2	393.6
0.3	419.8	423.7	421.6	420.9
0.4	440.5	441.6	445.4	445.9
0.5	458.4	456.4	460.5	455.6
0.6	470.2	468.7	469.2	468.0
0.8	489.3	488.6	484.5	475.4
1.0	503.7	504.1	497.5	480.7
1.50	521.6	528.1	513.5	498.3
2.0	534.1	550.8	524.7	502.2
2.5	543.0	565.0	532.6	507.5
3.0	549.9	575.2	540.0	512.6
3.5	555.9	584.7	543.1	514.9
4.0	559.6	592.1	548.0	517.0
4.5	564.5	598.7	550.7	517.6
5.0	568.7	603.8	552.9	518.0

TABLE IV-4: OBSERVED CHEMICAL SHIFTS FOR o-CRESOL AT DIFFERENT CONCENTRATIONS AND THEIR THEORETICAL VALUES ASSUMING DIFFERENT MONOMER-POLYMER EQUILIBRIA

<u>Molar Concentration</u>	<u>Observed Chemical Shift, ν(hz)</u>	<u>Theoretical ν-values for different monomer-polymer equilibria</u>		
		<u>n = 2</u>	<u>n = 3</u>	<u>n = 4</u>
0.1	350.5	358.1	346.6	343.4
0.2	361.5	370.4	358.6	358.0
0.3	373.2	380.5	372.0	373.8
0.4	383.8	389.1	385.6	384.8
0.5	393.5	397.0	393.7	392.5
0.6	400.2	404.0	400.7	400.0
0.8	414.4	414.8	412.5	411.8
1.0	426.1	423.4	422.0	421.9
1.5	444.0	441.2	437.8	432.5
2.0	455.4	453.7	448.1	438.8
2.5	464.8	463.2	454.3	443.9
3.0	470.6	471.2	459.6	448.0
3.5	476.6	477.5	463.5	451.0
4.0	481.6	483.2	466.9	453.2
4.5	484.5	487.8	469.9	455.0
5.0	486.7	491.9	472.9	456.8

TABLE IV-5: OBSERVED CHEMICAL SHIFTS FOR 2-ETHYLPHENOL AT DIFFERENT CONCENTRATIONS AND THEIR THEORETICAL VALUES ASSUMING DIFFERENT MONOMER-POLYMER EQUILIBRIA

<u>Molar Concentration</u>	<u>Observed Chemical Shift, ν(hz)</u>	<u>Theoretical ν-values for different monomer-polymer equilibria</u>		
		<u>n = 2</u>	<u>n = 3</u>	<u>n = 4</u>
0.1	349.8	354.3	345.2	344.1
0.2	357.2	363.8	354.4	351.9
0.3	365.0	371.5	362.6	360.6
0.4	373.3	379.2	371.6	368.8
0.5	380.2	385.2	381.1	381.2
0.6	387.2	391.0	387.3	388.4
0.8	397.8	400.3	399.4	397.7
1.0	406.1	407.5	409.3	406.6
1.5	423.0	423.6	425.2	420.9
2.0	436.2	435.0	433.0	428.9
2.5	444.2	444.1	440.7	433.7
3.0	452.0	451.0	445.5	436.7
3.5	459.0	457.2	449.1	438.2
4.0	462.9	462.5	452.8	440.6
4.5	466.5	467.1	455.9	441.9
5.0	470.2	472.9	457.5	443.4

TABLE IV-6: OBSERVED CHEMICAL SHIFTS FOR 2-ISOPROPYLPHENOL AT DIFFERENT CONCENTRATIONS AT THEIR THEORETICAL VALUES ASSUMING DIFFERENT MONOMER-POLYMER EQUILIBRIA

<u>Molar Concentration</u>	<u>Observed Chemical Shift, ν(hz)</u>	<u>Theoretical ν-values for different monomer-polymer equilibria</u>		
		<u>n = 2</u>	<u>n = 3</u>	<u>n = 4</u>
0.1	342.9	344.6	338.4	336.7
0.2	351.4	351.8	346.0	342.8
0.3	359.0	359.2	353.8	351.3
0.4		364.0	362.7	363.1
0.5	372.0	369.8	370.4	371.5
0.6		374.2	376.6	377.9
0.8	389.6	382.5	387.8	388.4
1.0	397.4	390.0	395.8	395.4
1.2				
1.5	411.7	403.7	411.3	406.1
2.0	422.5	414.4	419.1	414.1
2.5	431.6	422.5	426.2	419.4
3.0	439.3	429.4	431.1	423.3
3.5	445.0	435.2	435.3	426.1
4.0	450.0	440.4	438.0	427.4
4.5	453.2	444.7	441.3	428.7
5.0	456.0	449.4	443.0	430.6

TABLE IV-7: OBSERVED CHEMICAL SHIFTS FOR 2-t-BUTYLPHENOL AT DIFFERENT CONCENTRATIONS AT THEIR THEORETICAL VALUES ASSUMING DIFFERENT MONOMER-POLYMER EQUILIBRIA

<u>Molar Concentration</u>	<u>Observed Chemical Shift, ν(hz)</u>	<u>Theoretical ν-values for different monomer-polymer equilibria</u>		
		<u>n = 2</u>	<u>n = 3</u>	<u>n = 4</u>
0.1	355.6	355.5	354.4	354.4
0.2	356.5	356.7	355.3	354.6
0.3	357.5	357.9	356.5	354.9
0.4	358.5	358.9	357.5	356.0
0.5	359.6	359.9	358.5	357.7
0.6	360.6	360.9	359.9	359.1
0.8	362.1	362.3	361.5	361.7
1.0	363.4	363.8	363.3	364.0
1.50	366.0	366.8	366.7	366.8
2.00	369.0	369.2	368.8	369.1
2.5	370.3	371.0	370.2	370.5
3.0	372.4	372.7	372.2	372.0
3.50	373.6	374.0	373.5	373.0
4.0	374.8	375.3	374.5	373.7
4.5	376.0	376.3	375.3	374.5
5.0	377.9	377.3	376.0	374.6

TABLE IV-8: OBSERVED CHEMICAL SHIFTS FOR 2,4,6-TRIMETHYLPHENOL AT DIFFERENT CONCENTRATIONS & THEIR THEORETICAL VALUES ASSUMING DIFFERENT MONOMER-POLYMER EQUILIBRIA

<u>Molar Concentration</u>	<u>Observed Chemical Shift, ν(hz)</u>	<u>Theoretical ν-values for different monomer-polymer equilibria</u>		
		<u>n = 2</u>	<u>n = 3</u>	<u>n = 4</u>
0.1	330.7	332.1	328.6	328.1
0.2	332.7	334.5	330.5	329.2
0.3	335.0	337.7	333.0	331.7
0.4	337.2	340.3	335.4	334.9
0.5	339.5	342.6	338.6	338.1
0.6	341.7	344.8	341.4	341.2
0.7	344.1	346.8	343.7	344.6
0.8	346.4	348.6	346.0	346.5
0.9	348.7	350.3	348.2	348.7
1.0	351.0	351.9	350.1	350.6

TABLE IV-9: OBSERVED CHEMICAL SHIFTS FOR 2,6-DIISOPROPYLPHENOL AT DIFFERENT CONCENTRATIONS & THEIR THEORETICAL VALUES ASSUMING DIFFERENT MONOMER-POLYMER EQUILIBRIA

<u>Molar Concentration</u>	<u>Observed Chemical Shift, ν(hz)</u>	<u>Theoretical ν-values for different monomer-polymer equilibria</u>		
		<u>n = 2</u>	<u>n = 3</u>	<u>n = 4</u>
0.1	360.9	360.8	360.0	360.0
0.2	361.5	361.7	360.2	360.0
0.3	362.2	362.6	360.4	360.1
0.4	362.7	363.4	360.6	360.2
0.5	363.3	364.2	361.0	360.4
0.6	363.9	365.0	361.4	360.7
0.8	364.9	366.6	362.4	361.6
1.0	366.1	368.0	363.6	362.9
1.5	368.5	371.4	367.2	367.6
2.0	371.9	374.6	371.1	372.9
2.5	374.7	377.4	375.1	378.1
3.0	377.7	380.1	378.8	382.7
3.5	381.8	382.5	382.3	386.6
4.0	384.4	384.8	385.5	390.0
4.5	387.8	387.0	388.4	393.0
5.0	390.9	389.0	391.1	395.6

TABLE IV-10: OBSERVED CHEMICAL SHIFTS FOR 2,6-DI-T-BUTYL-PHENOL AT DIFFERENT CONCENTRATIONS

<u>MOLAR CONCENTRATION</u>	<u>OBSERVED CHEMICAL SHIFT ν(Hz)</u>
0.1	398.6
0.2	398.6
0.4	398.5
0.6	398.4
0.8	398.2
1.0	398.0
1.5	397.5
2.0	397.2
2.5	396.8
3.0	396.4
3.5	395.6
4.0	395.1

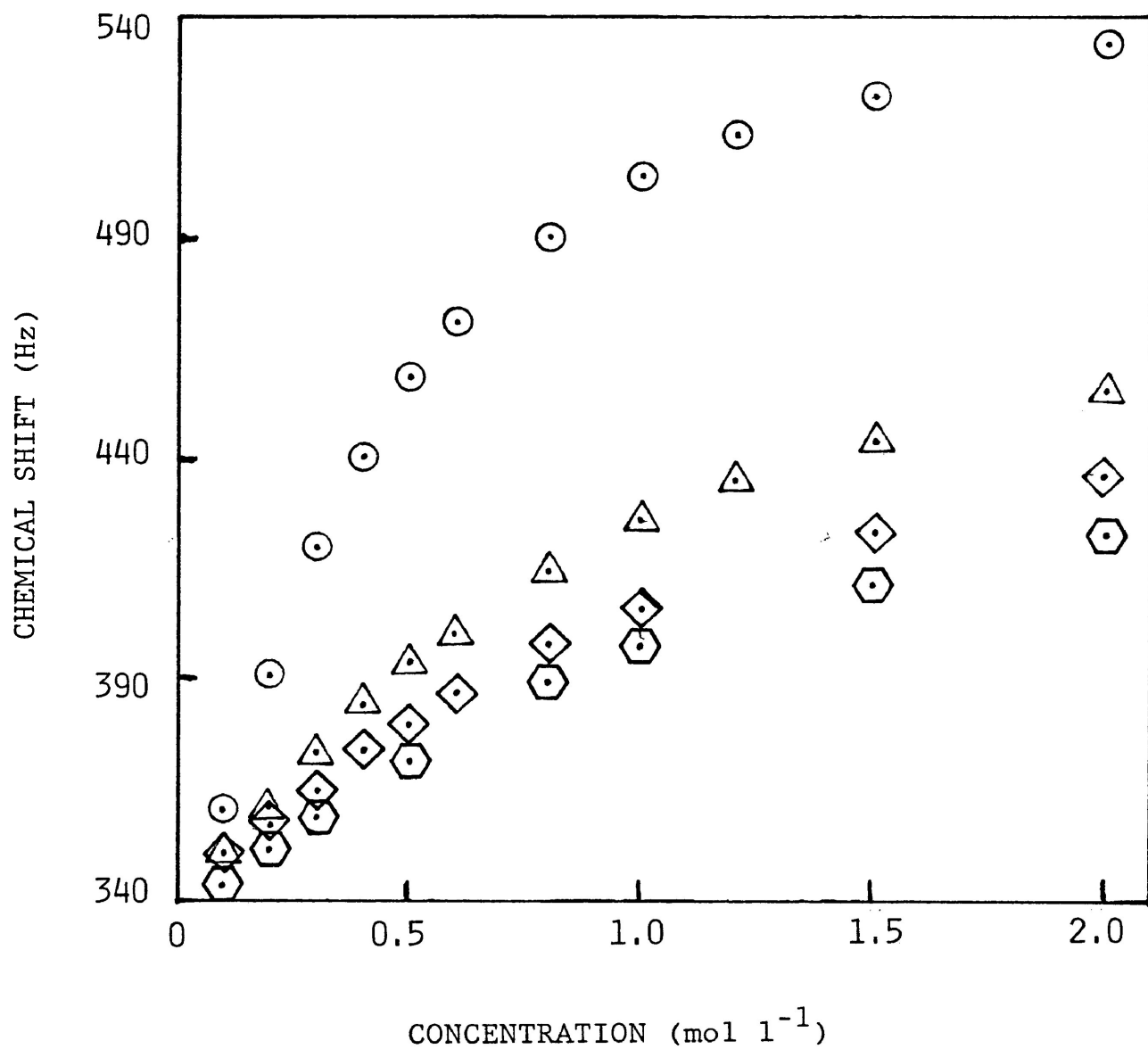


FIGURE IV.1. Plots of observed chemical shift (Hz) versus molar concentration for phenol (⊙). o-cresol (Δ), 2-ethylphenol (◊) and 2-isopropylphenol (⊞).

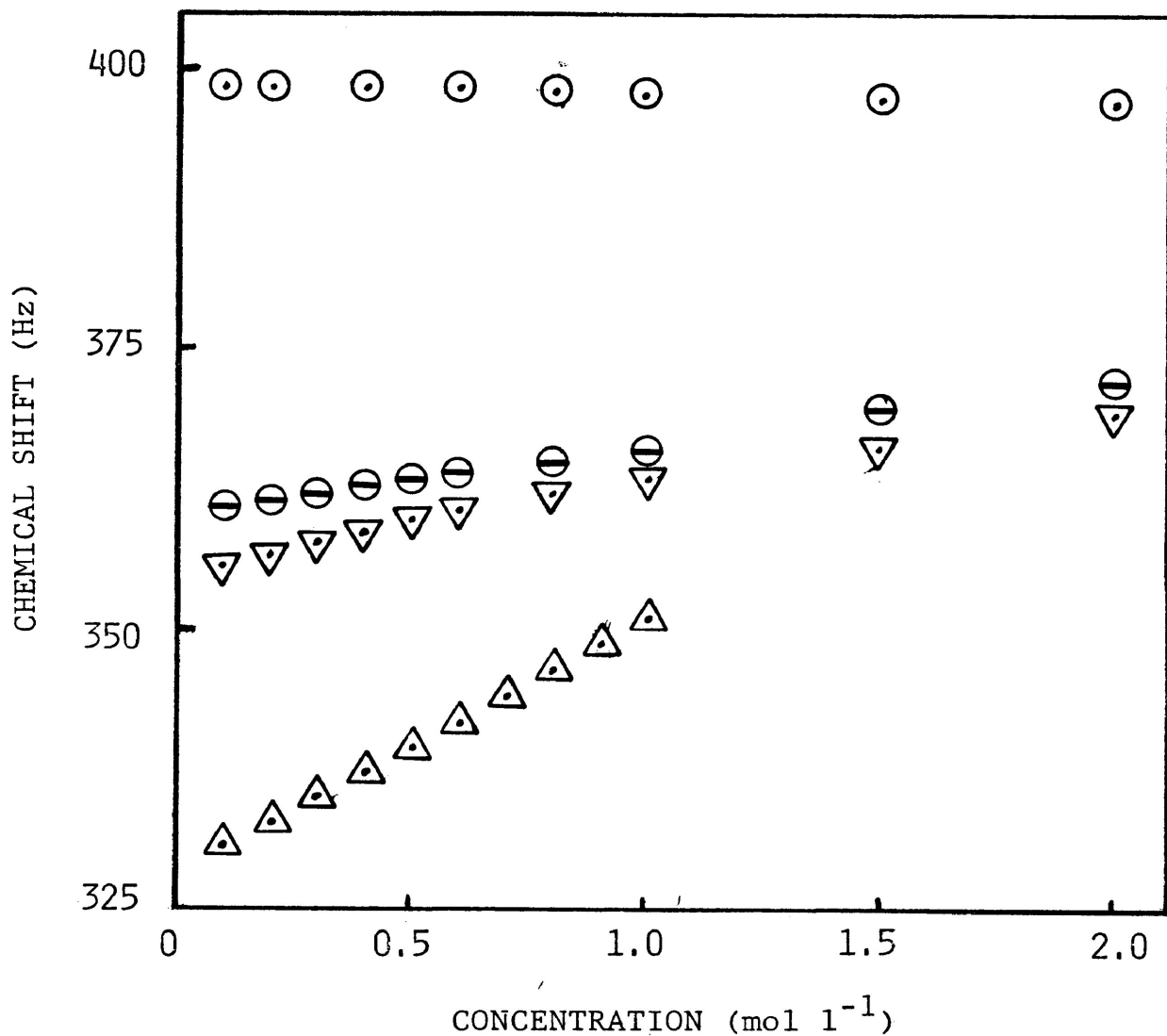


FIGURE IV.2. Plots of observed chemical shift (Hz) versus molar concentration for 2-t-butylphenol (⊙), 2,4,6-trimethylphenol (Δ), 2,6-diisopropylphenol (▽), and 2,6-di-t-butylphenol (⊖).

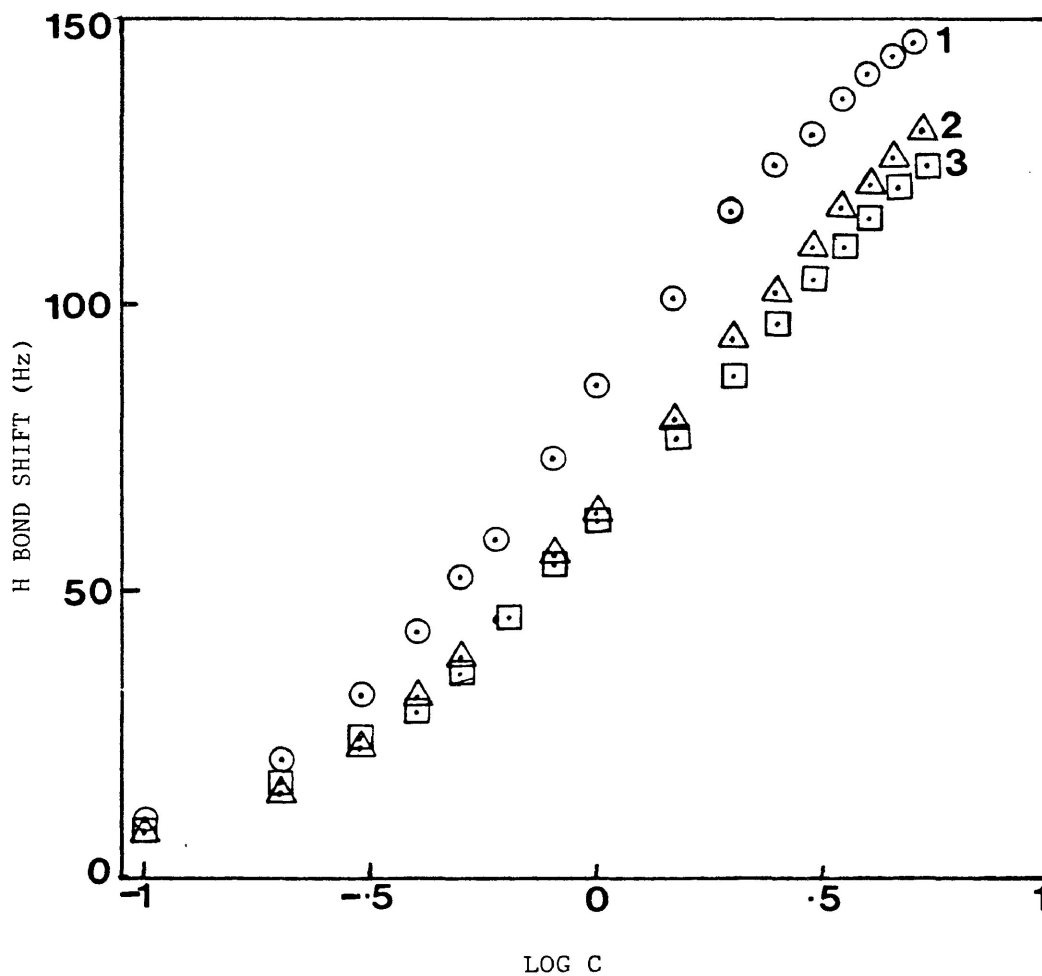


FIGURE IV.3. PLOTS OF OBSERVED H BOND SHIFT, $\nu - \nu_1$ (HZ) VERSUS LOG C FOR o-CRESOL (1), 2-ETHYLPHENOL (2) AND 2-ISOPROPYLPHENOL (3).

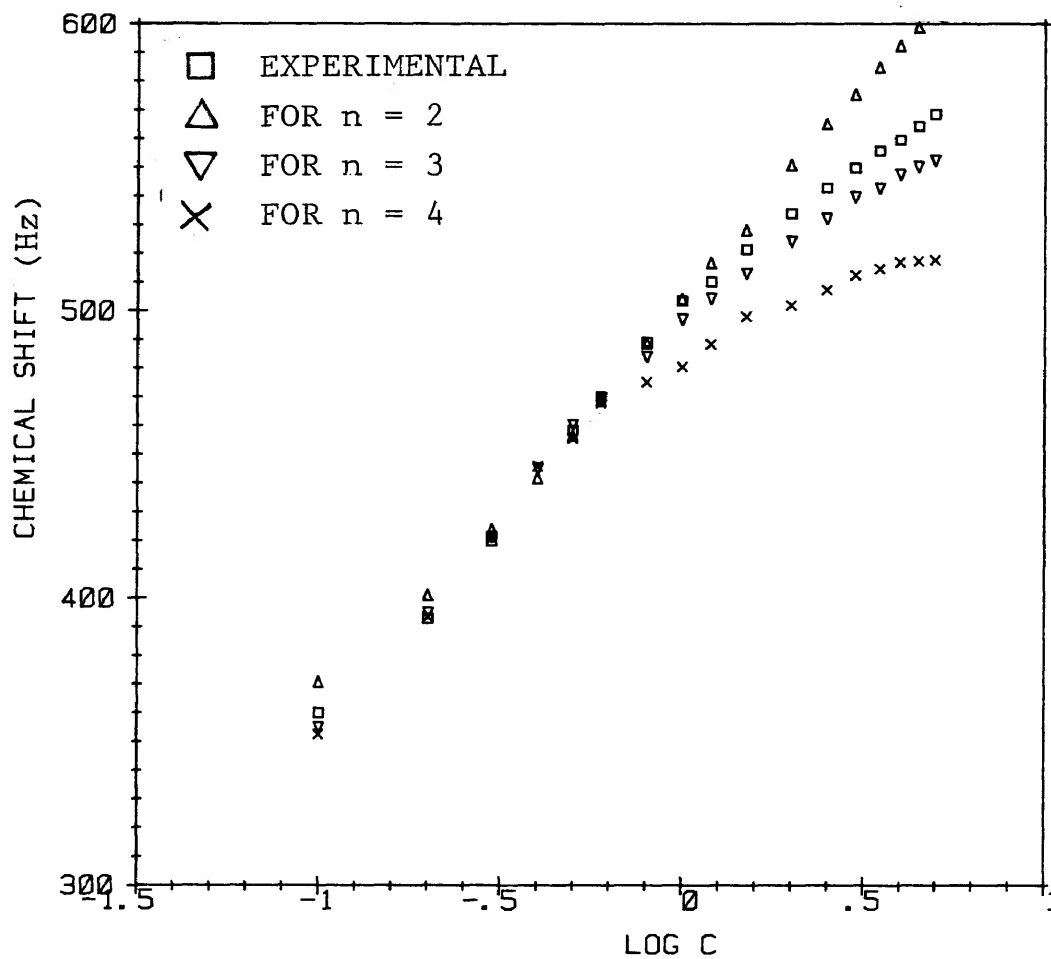


FIGURE IV.4. Plots of experimental and theoretical (for n = 2,3 and 4) chemical shifts versus log C for phenol.

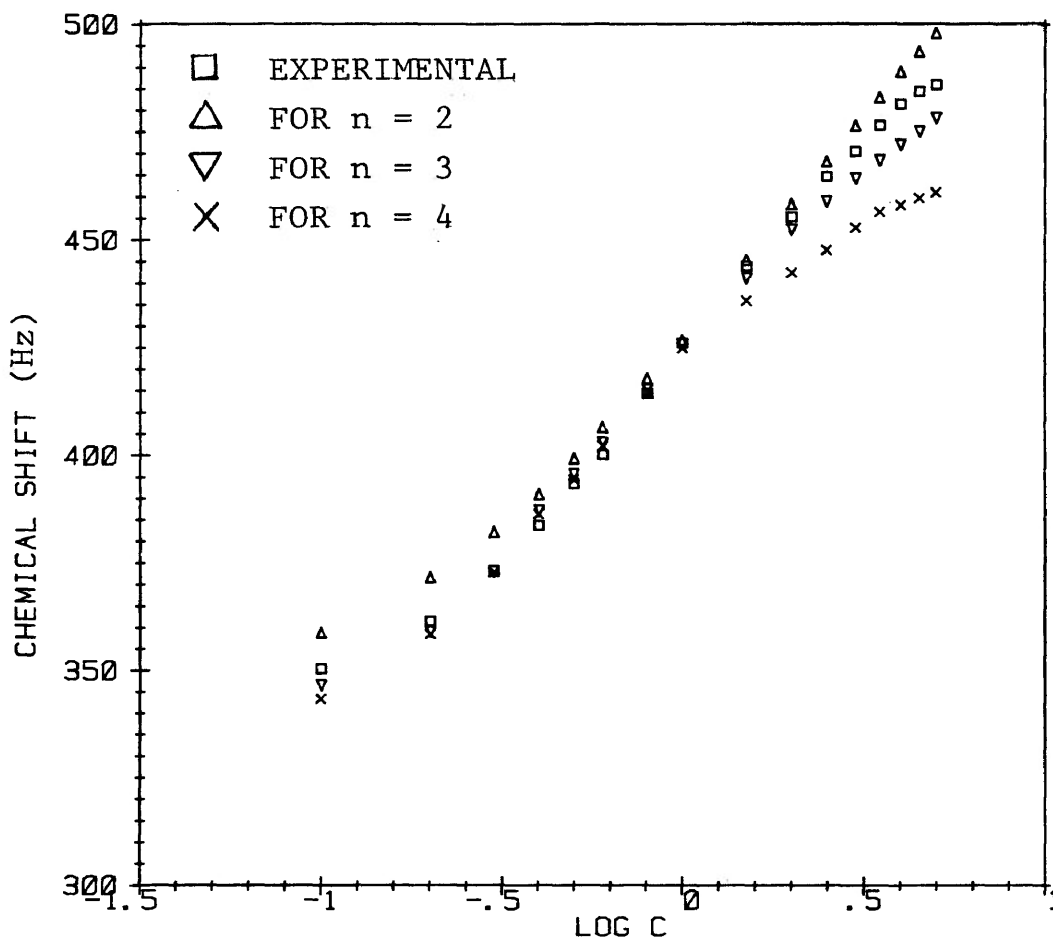


FIGURE IV.5. Plots of experimental and theoretical (for n = 2,3 and 4) chemical shifts versus log C for o-cresol.

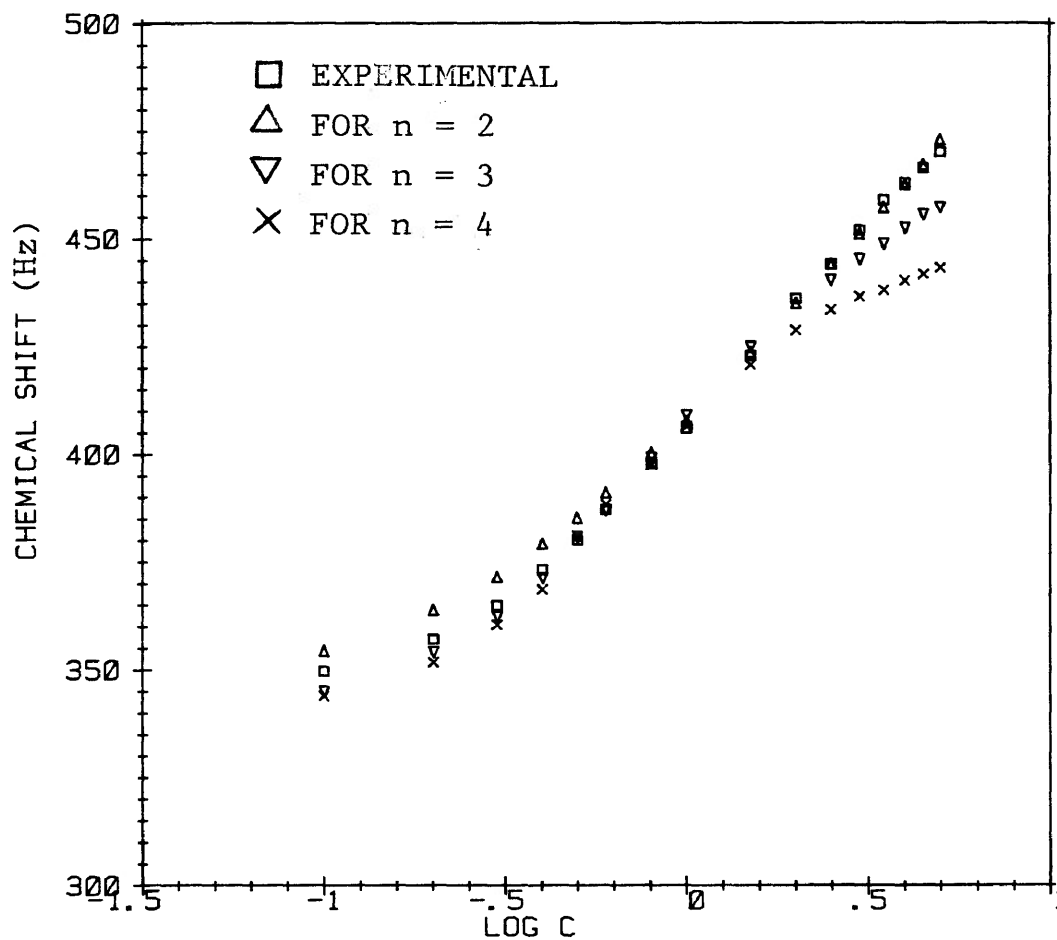


FIGURE IV. 6. Plots of experimental and theoretical (for n = 2,3, and 4) chemical shifts versus log C for 2-ethylphenol.

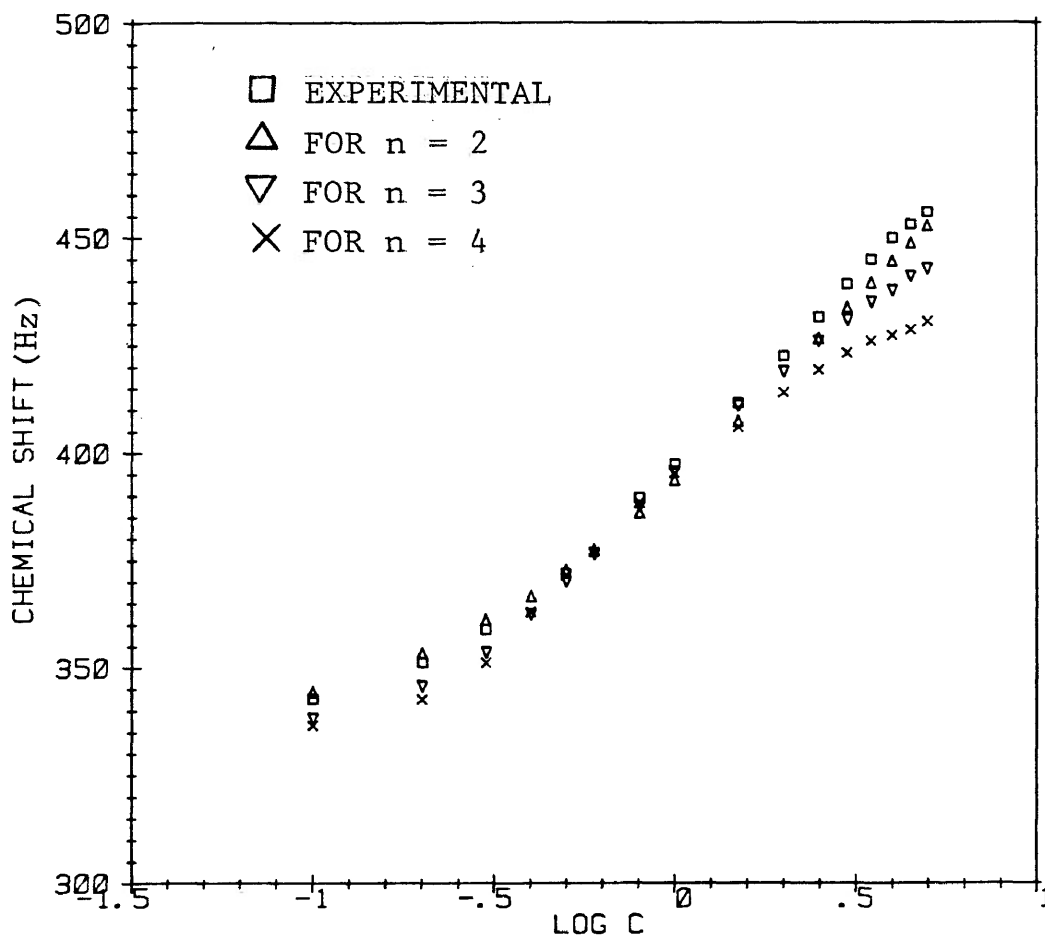


FIGURE IV.7. Plots of experimental and theoretical (for n = 2,3 and 4) chemical shifts versus log C for 2-isopropylphenol.

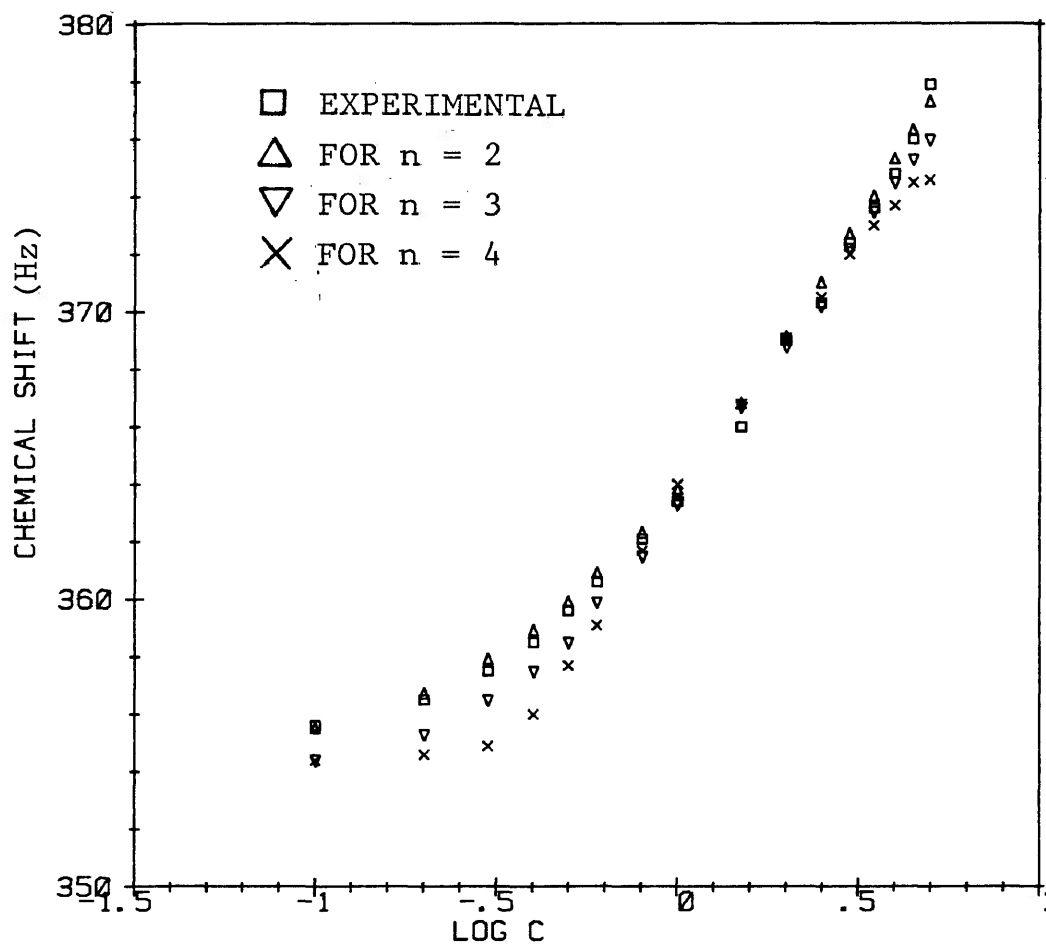


FIGURE IV.8. Plots of experimental and theoretical (for $n = 2, 3$ and 4) chemical shifts versus $\log C$ for 2-t-butylphenol.

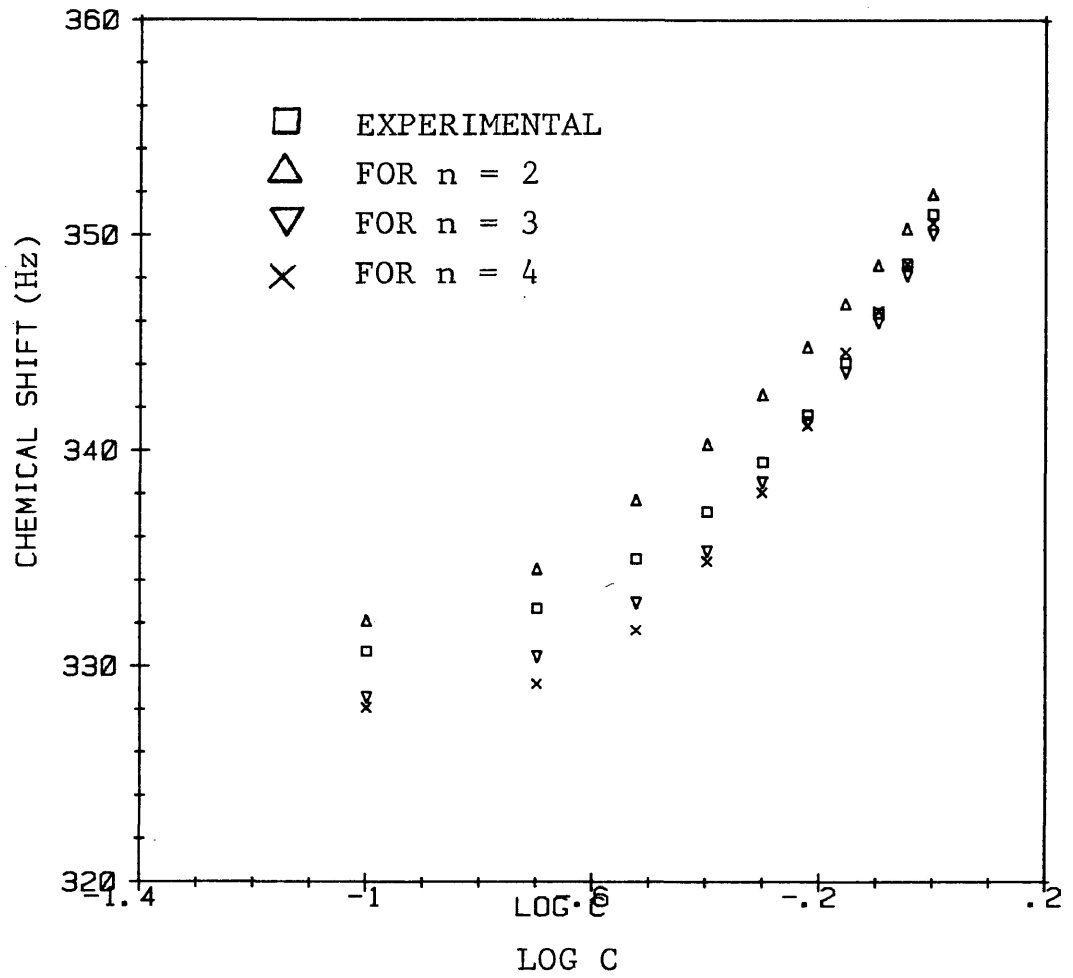


FIGURE IV.9. Plots of experimental and theoretical (for n = 2,3 and 4) chemical shifts versus log C for 2,4,6-trimethylphenol.

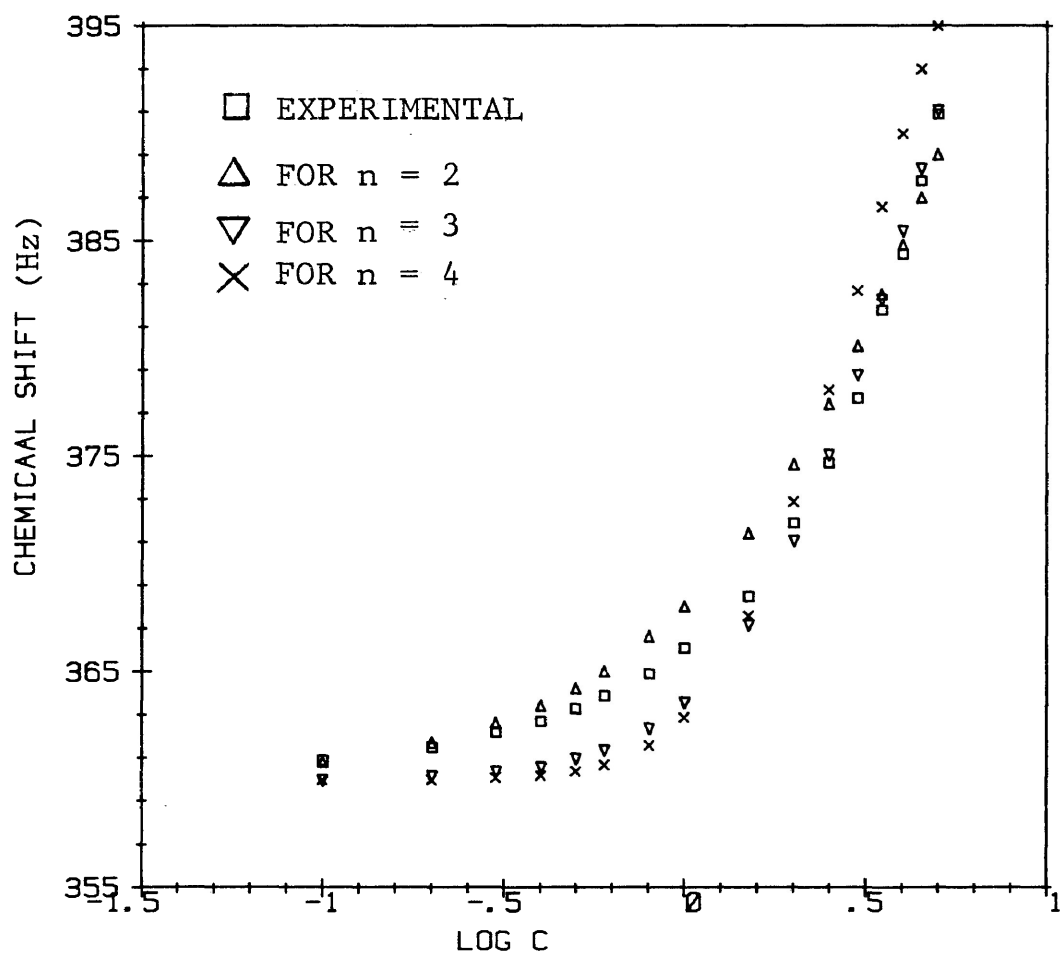


FIGURE IV.10. Plots of experimental and theoretical (for n = 2, 3 and 4) chemical shifts versus log C for 2,6-diisopropylphenol.

CHAPTER V:

DIELECTRIC RELAXATION STUDIES ON
SOME PHENOLS AND RELATED COMPOUNDS

INTRODUCTION

Compounds containing hydroxyl groups, especially the aliphatic alcohols and aromatic phenols as well as their solutions have been studied by various dielectric-absorption techniques. Studies (1-5) on primary and secondary alcohols in the pure liquid state indicate that the dielectric dispersion may be described by three relaxation times, with the dominating low-frequency process of Debye type. Studies (6-11) on alcoholic solutions in nonpolar solvents show that the contribution from the low frequency process (τ_1) is diminished gradually on dilution and becomes insignificant at high dilution. Despite diverse interpretations (12,13) by different workers, they seem to concur at one point that the absorption process (τ_3) having the shortest relaxation time is due to the reorientation of the OH group in the free monomers around the C-O bond. In case of phenolic solutions in nonpolar solvents, the dielectric data have been analyzed in terms of two relaxation times with respect to the molecular and an intramolecular process. In dielectric absorption studies the latter process having a very short

relaxation time (≈ 3 p s.) has been invariably interpreted as hydroxyl group relaxation, as for example, by Fong and Smyth (14) in the study of 1-naphthol, 4-hydroxybiphenyl and 2,6-dimethylphenol. For 2,6-dimethylphenol, the overall absorption was dominated by the contribution from the group rotation, and therefore the authors suggested that the OH group is prevented from intermolecular interaction by the o-substituted methyl groups. In a later and more detailed study using dielectric relaxation, proton magnetic resonance and infrared spectroscopy, Fong et al (15) concluded that substitution of alkyl groups (particularly the bulky t-butyl group) at 2,6-positions of phenols provide effective screening of the OH group from interaction. Similar conclusions were also arrived at by Gough and Price (16) from their dielectric absorption study over a wide frequency range on a number of cryptophenols (2,4,6-tri-t-butyl phenol, deuterioxy 2,4,6-tri-t-butyl phenol, 2,6-di-t-butyl phenol, 2,4,6-tri-t-pentyl phenol and 2,6-di-t-butyl 4-formyl phenol) both in the solid state and in decalin solution. With the exception of 4-formyl derivative, all these compounds appeared to show two absorptions, the higher frequency absorption being attributed to the phenolic OH group rotation. This

relaxation process for t-butyl phenols in decalin involved an activation energy of 9.2 to 11.7 kJ mol⁻¹. In the solid state of 2,4,6-tri-t-butyl phenol, however, the activation energy was found to be significantly lower (4.6 ± 2.1 kJ mol⁻¹), the reason for which could be greater experimental uncertainty inherent in the measurements of solid samples.

Further studies with 2,4,6-tri-t-butyl phenol and tricyclohexyl carbinol in pure solids (17) and in decalin solution (18) provided important results. In solid state study both compounds gave simple Debye curves, representing single relaxation times corresponding to OH group rotation around C-O bond. The energy barriers for such relaxation was found to be 9.2 and 18.4 kJ mol⁻¹ for 2,4,6-tri-t-butyl phenol and tri-cyclohexyl phenol respectively. The higher energy barrier for the latter compound was thought to be due to more highly hindered rotation about the C-O bond than in the former molecule. Davis and Meakins (18), while studying these two compounds in decalin solution, observed two separate absorptions: in both cases the higher frequency ones being suggested to be corresponding to the OH group relaxation. For 2,4,6-tri-t-butyl phenol the observed activation energy was

found to be 11.7 kJ mol^{-1} as compared to the value of 9.2 kJ mol^{-1} obtained in the solid state (17).

Regarding the energy barrier, one particular point should be mentioned here, that the barrier determined by the dielectric absorption technique is an Eyring enthalpy of activation (ΔH_E); this is to be contrasted with the one obtained from microwave or infrared spectra which is based on the cosine formula:

$$V = \frac{V_1}{2} (1 - \cos \theta) + \frac{V_2}{2} (1 - \cos 2\theta) + \frac{V_3}{2} (1 - \cos 3\theta) + \dots$$

where V_1, V_2, V_3, \dots represent Fourier potential terms determined by the structure of the molecule and θ is the angle of rotation of the rotatable part of the molecule about the bond concerned.

Phenol itself has a planar structure which is stabilized by delocalization of the p-type lone-pair electrons to the π -electrons of the ring resulting in some double-bond character of the C-O bond. The energy barrier, ΔH_E or V_2 (assuming $V_4 = 0$) has to be surmounted for the orientation of the hydrogen atom from one planar

position to the other. The planar structure of the ground state of phenol is supported by both microwave and infrared spectra. Various spectroscopic studies (19-22) indicate a (V_2) barrier of 14-15 kJ mol^{-1} for rotation of the OH group of phenols.

Davis and Edwards (23) studied dielectric absorption of β -naphthol molecularly dispersed in a polystyrene matrix. Their high-frequency absorption data provided a ΔH_E value of $2.1 \pm 1.3 \text{ kJ mol}^{-1}$ for hydroxyl group relaxation which did not reflect any appreciable double bond character in the C-O linkage. In the cases of some appropriately *o*-substituted phenols the hydroxyl rotational barrier can be appreciably increased owing to the intramolecular hydrogen bonding. Thus, a much higher activation enthalpy ($\sim 35 \text{ kJ mol}^{-1}$) has been obtained by Tay et al (24) for the OH group relaxation in phenols having nitrosubstitutents in both 2- and 6-positions. Recently, Mazid et al. (25) have carried out dielectric absorption studies on a series of 2,4,6-tri and penta-substituted phenols. The low temperature process for all halogenophenols was identified as hydroxyl group relaxation. The ΔH_E for this intramolecular process

was found to be proportional to the strength of the intramolecular H bonds formed with o-substituents. Thus, the intramolecular ΔH_E value increased from 15 ± 2 kJ mol^{-1} for 2,4,6-trichlorophenol to 26 ± 1 kJ mol^{-1} for pentachloro phenol which corresponds with the more protonic character and consequently stronger intramolecular H bond in the latter molecule. The ΔH_E value for the intramolecular process in pentachlorobenzenethiol is 12 kJ mol^{-1} less than pentachlorophenol, which has been related, at least in part, to the weak intramolecular hydrogen bond formed by the SH relative to the OH group.

In view of such points as those in the discussion, it would appear that the energy barrier to hydroxyl group relaxation in phenols and other hydroxy-compounds is dependent on the steric and probably the inductive effects of the substituents as well as on the strength of intramolecular hydrogen bonding. Barriers to molecular relaxation of such systems may be affected similarly by intermolecular hydrogen bonding. The aim of the present work is to extend the polystyrene matrix technique of dielectric absorption measurements to a wider variety of hydroxy compounds, including a few alkylsubstituted phenols.

naphthols and a few keto-enol tautomeric systems, in order to obtain energy barriers for hydroxyl-group relaxation as well as for molecular relaxation of these systems.

One particular aspect of the intramolecular process which, in general, has rarely been considered by dielectric-absorption workers is to examine whether the intramolecular process in phenols and other hydroxy compounds may be attributed to proton tunneling as opposed to hydroxyl-group relaxation. Energy barriers for hydroxyl and methoxy-group relaxation in non-intramolecularly hydrogen-bonded phenols (17,26) and aromatic $-OCH_3$ systems have been found to be of the same order (27,28). The value of ΔH_E of 9.6 kJ mol^{-1} for methoxy group relaxation (27) in 3,5-dimethylanisole was virtually the same as ΔH_E value (9.1 kJ mol^{-1}) which Meakins (17) found for hydroxyl group in pure and solid 2,4,6-tri-*t*-butylphenol. These results appear to negate the possibility of proton tunneling in non-intramolecularly hydrogen-bonded phenols. Mazid et al (25) did not find any evidence of proton tunneling in the intramolecular processes of 2,4,6-trihalogen and pentahalogenophenols. Gough and Price (16) in their work with deuterioxy 2,4,6-tri-*t*-

butylphenol found that the relaxation time of the high frequency absorption due to hydroxyl group relaxation increased over that in the undeuterated molecule by a factor of 1.2 ± 0.4 for both decalin solution and in the solid state. This ratio was similar to the normal isotopic mass factor, which strongly suggested the absence of any significant amount of proton tunneling associated with the high frequency relaxation process. Further, the activation energy for the motion of the deuterated phenolic group was the same as that of the undeuterated molecule.

Recent spectroscopic study (infrared and microwave) has demonstrated proton tunneling in the intramolecularly hydrogen bonded systems of tropolone (29) and malonaldehyde (30) in the gaseous phase. A number of other studies have also been made on tunneling in the solid state, as in, for example, the work of Phillips (31). Investigations of the possibility of proton tunneling have also been made with a few other hydroxy compounds such as acetylacetone (32), Phenols (25) and meso-tetraphenylporphine (33). In the light of recent development in proton tunneling studies, these molecules

seem to provide potential systems in which proton tunneling may be involved in their inter- and/or intramolecular processes. The experimental evidence for proton tunneling in a nonaqueous solution is extremely scarce and as yet, there does not appear to be any convincing case obtained from dielectric studies. Thus, one definite interest was to apply dielectric-absorption techniques to some of these suitable molecules in order to investigate the possibility of proton tunneling as an intramolecular process in these systems.

EXPERIMENTAL RESULTS

The following compounds were included in the present study:

- V.1 o-Cresol
- V.2 2-Ethylphenol
- V.3 2-Isopropylphenol
- V.4 2-t-Butylphenol
- V.5 2,6-Dichlorophenol
- V.6 4-Phenylphenol
- V.7 Triphenylmethanol
- V.8 1-Naphthol
- V.9 2-Naphthol
- V.10 6-Bromo-2-naphthol
- V.11 2-Methoxynaphthalene
- V.12 Tropolone
- V.13 2,4-Pentanedione
- V.14 3,3-Deutero-2,4-pentanedione
- V.15 Dibenzoylmethane

All of the compounds were studied in polystyrene matrices except 4-phenylphenol which was studied as a compressed solid disc; triphenylmethanol and 1-naphthol were examined both in polystyrene matrices and in compressed solid discs.

Results of Fuoss-Kirkwood analyses, the ϵ_{∞} values and experimental dipole moments for the above compounds are listed in Table V.2. Results of Eyring analyses for these compounds are presented in Table V.3. The relaxation times (τ) and the free energies of activation (ΔG_E) are given at wide temperature intervals, i.e. at 100 K, 200 K and 300 K since some of these molecules showed two separate families of absorption peaks covering such a temperature range. Sample plots of dielectric loss ($\epsilon'' = \epsilon''_{\text{obs}} - \epsilon''_{\text{polystyrene}}$) versus \log_{10} frequency are shown in Fig. V.1-4 while Fig. V.5-9 represents plots of $\log_{10} T\tau$ versus $\frac{1}{T}$ for some of the compounds under consideration.

DISCUSSION

In view of the results obtained from IR studies (Chapter III) and from PMR investigations (Chapter IV) on o-alkylphenols it was of interest to study the relaxation behaviour of these molecules by dielectric absorption techniques. Results (Tables V.2 and 3) of the present investigation shows that each of these molecules gave only one absorption peak characterized by different activation parameters. From Table V.3 it is found that with the increase of size of the alkyl substituent both

the free energy of activation (ΔG_E) and the enthalpy of activation (ΔH_E) increased.

From earlier works (14-18) on phenols and related hydroxy compounds two relaxation processes need to be considered; one due to the rotation of the -OH group and the other due to the whole molecule relaxation. Fong et al (15) showed that substitution of even a bulky alkyl (t-butyl) group in 2- and 6-positions of phenol does not hinder the OH group rotation around the C-bond. Thus, it seemed likely that ortho-alkyl substitution would not significantly affect such an intramolecular process in the molecules under consideration. However, Fong and Smyth (14), Meakins (17) and Davis and Meakins (18) observed the OH group relaxation in 2,4,6-trialkylphenols at frequencies around 10^{10} Hz. Mazid et al (25) in their recent investigation on 2,4,6-tri-t-butylphenol in a polystyrene matrix as well as in a pure solid disk could detect only the tail-end of the absorption due to the OH group relaxation at the highest frequencies (around 10^7 Hz) of their measurement. It is thus highly improbable that the only low temperature process for o-cresol involving $\Delta H_E = 16 \text{ kJ mol}^{-1}$ could be due to the OH group relaxation, although the ΔH_E value is fairly similar to that (12 - 15 kJ mol^{-1}) observed for OH group rotation around the C-bond.

Finally, the total absence of any such low temperature process in 2-ethylphenol, 2-isopropylphenol and 2-*t*-butylphenol strongly negates the possibility of OH group reorientation to be observed in the frequency range ($10^2 - 10^5$ Hz) at present employed. The observed absorption in each of these molecules under consideration should then be assigned to their respective molecular relaxation processes .

o-Cresol molecule can be compared with the similarly-sized rigid molecule *o*-dichlorobenzene for which the rotational energy barrier (ΔE) of $12.21 \text{ kJ mol}^{-1}$ was observed by Davis and Meakins (18) as compared to $\Delta H_E = 16 \text{ kJ mol}^{-1}$ for the former molecule. For a little larger rigid molecule, *o*-chlorobromobenzene, the ΔH_E and $\Delta G_{E100 \text{ K}}$ were found (34) to be 16 kJ mol^{-1} and 15.1 kJ mol^{-1} respectively as compared to the corresponding values of 16 kJ mol^{-1} and 18.3 kJ mol^{-1} for *o*-cresol. The latter molecule absorbed at a higher temperature region (108 K - 141 K) than the absorption region (88 K - 120 K) for the former. Again, the relaxation time, ($\tau_{100 \text{ K}} = 1.8 \times 10^{-3}$) for *o*-cresol was much longer than that observed ($\tau_{100 \text{ K}} = 3.6 \times 10^{-5}$ s) for *o*-chlorobromobenzene. These results appear to indicate that the observed activation parameters

for o-cresol were not due solely to the relaxation of simple unassociated monomer molecules. It would thus be reasonable to suggest that the molecular relaxation was restricted by intermolecular H-bonding requiring additional energy to break the H-bond before the molecule could relax.

The molecular size of 2-ethylphenol is similar to that of the rigid molecule, o-chloriodobenzene, for which the observed (34) values of ΔH_E , ΔG_{E200K} and τ_{200K} were respectively 16 kJ mol^{-1} , 20.3 kJ mol^{-1} and $4.8 \times 10^{-8} \text{ s}$ as compared to the corresponding values of 23 kJ mol^{-1} , 30.4 kJ mol^{-1} , and $2 \times 10^{-5} \text{ s}$ observed for the former molecule. These results suggest that the molecular relaxation was significantly hindered by intermolecular H-bonding as in the case of o-cresol. It is not unlikely that the associated species (dimers and/or multimers) contributed to the observed relaxation process.

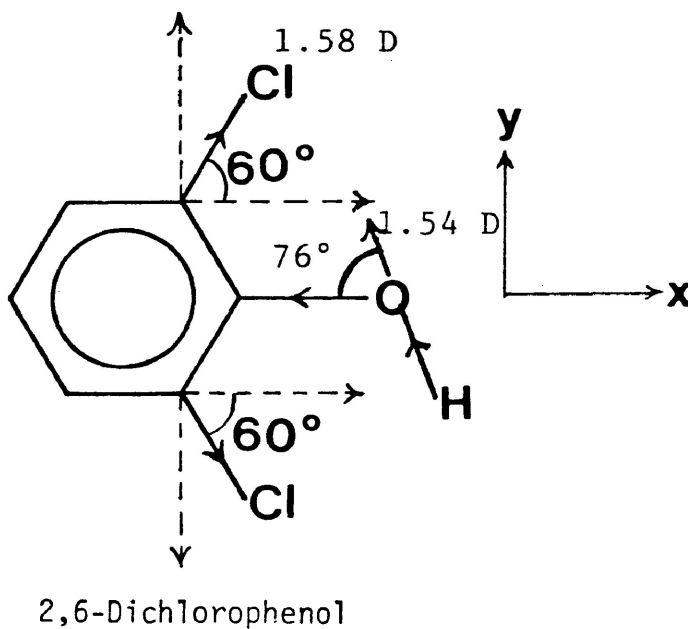
Results obtained with 2-isopropylphenol and 2-t-butylphenol indicated that they exhibited similar behaviour. 2-Isopropylphenol being slightly larger than o-chloriodobenzene yielded $\Delta H_E = 42 \text{ kJ mol}^{-1}$, $\Delta G_{E200K} = 33.5 \text{ kJ mol}^{-1}$ and $\tau_{200K} = 1.3 \times 10^{-4} \text{ s}$ as compared to the corresponding values of 16 kJ mol^{-1} , 20.3 kJ mol^{-1} and

4.8×10^{-8} s observed (34) for the latter molecule. The observed ΔH_E and $\Delta G_{E200\text{ K}}$ values for 2-t-butylphenol were 47 kJ mol^{-1} and 36.2 kJ mol^{-1} respectively as compared to the corresponding values of 20 kJ mol^{-1} and 25.6 kJ mol^{-1} for the similarly-sized rigid molecule α,α,α -trichlorotoluene (35). The relaxation time ($\tau_{200\text{ K}} = 6.8 \times 10^{-4}$ s) for the former molecule was again much longer than that ($\tau_{200\text{ K}} = 1.2 \times 10^{-6}$ s) for the latter. These results strongly support the involvement of intermolecular H bonding in the relaxation behaviour of these molecules in question.

From the above discussion one could possibly generalize that the intramolecular H bonding caused the enhancement of the energy barrier to molecular relaxation encountered by o-alkylphenols under investigation. It is, however, uncertain whether any associated species (dimers and/or multimers) contributed to the enhanced energy barriers for the respective molecules. It was shown by other methods (IR and n.m.r.) that polymer species exist in equilibrium with the monomers of these phenols. These should thus contribute to the dielectric absorption unless they happen to be nonpolar.

The molecule 2,6-dichlorophenol gave only one absorption in the temperature range of 110 - 140 K yielding ΔH_E of $\sim 16 \text{ kJ mol}^{-1}$ and ΔG_{E200} of 21.3 kJ mol^{-1} . The corresponding values for a similarly sized rigid molecule, m-dichlorobenzene, were found (34) to be 16.0 kJ mol^{-1} and 22.2 kJ mol^{-1} , respectively. In a similar experiment with 2,4,6-trichlorophenol, Mazid et al observed two absorption peaks where the low temperature absorption (92 K - 111 K) due to OH group relaxation yielded a ΔH_E of 15.0 kJ mol^{-1} and ΔG_{E200K} of 16.1 kJ mol^{-1} . The observed relaxation time τ_{200} for 2,6-dichlorophenol was $8.9 \times 10^{-8} \text{ s}$ as compared to the values of $1.5 \times 10^{-7} \text{ s}$ for m-dichlorobenzene and $3.7 \times 10^{-9} \text{ s}$ for 2,4,6-trichlorophenol (low temperature absorption). Further, the observed ΔS_E of $-29.0 \text{ J K}^{-1} \text{ mol}^{-1}$ for 2,6-dichlorophenol is fairly similar to those of $-30.0 \text{ J K}^{-1} \text{ mol}^{-1}$ for m-dichlorobenzene and $-5.0 \text{ J K}^{-1} \text{ mol}^{-1}$ for 2,4,6-trichlorophenol. All these results strongly indicate that both the molecular and the OH group relaxation could be potential candidates for the observed dielectric absorption. The most likely situation could be such that both the molecular and intramolecular processes would overlap in the said absorption region. The observed low β -value (~ 0.2) is consistent with this suggestion.

An approximate estimate of the weight factors, C_1 and C_2 , respectively, for molecular and the OH group relaxation in 2,6-dichlorophenol can be attempted using the following model structure which ignores intramolecular H bonding.



Calculated dipole moment components based on this structure are given in Table V.1.

TABLE V. 1: Calculated Dipole Moment Components for
2,6-Dichlorophenol

Substituent	μ_x (D)	μ_y (D)
2-Cl	$+1.58\cos 60^\circ = +0.79$	$+1.58\sin 60^\circ = +1.38$
6-Cl	$+1.58\cos 60^\circ = +0.79$	$-1.58\sin 60^\circ = -1.38$
OH	$-1.54\cos 76^\circ = -0.37$	$+1.54\sin 76^\circ = +1.49$

$$\mu_1 = 1.21$$

$$\mu_2 = 1.49$$

In the above calculations it has been assumed that the OH group moment of 1.54 D (36) acts at 76° (37) from the direction of O-C bond while two moment vectors (1.58 D) (38) due to Cl-atoms act along C-Cl bonds forming an angle of 120° with each other. The resultant component along x-direction (μ_1) is responsible for molecular reorientation while the component along y-direction results in the OH group rotation. According to the above calculations the weight factors for these processes will be:

$$C_1 = \frac{\mu_1^2}{\mu_1^2 + \mu_2^2} \quad 0.40 \quad \text{V.2 (a)}$$

$$C_2 = \frac{\mu_2^2}{\mu_1^2 + \mu_2^2} \quad 0.60 \quad \text{V.2 (b)}$$

The total moment ($\mu = \sqrt{\mu_1^2 + \mu_2^2}$) for the molecule, according to the above calculation is 1.92 D as compared with the literature value (39) of 1.60 D at 298 K. The discrepancy may be attributed to the oversimplified geometry of the model structure which will definitely be distorted owing to intramolecular OH bonding. Experimental values of effective dipole moments, while extrapolated to 300 K yielded a value of 1.54 D which is fairly close to the literature value.

Three molecules, namely, 4-phenylphenol, triphenylmethanol, and 1-naphthol studied in the compressed solid disks were found to give only one absorption each. This is what may be expected to be due to the OH group relaxation since it is highly unlikely that any molecular

relaxation could occur in the crystalline solid state. The observed ΔH_E values of 13 kJ mol^{-1} for 4-phenylphenol and $\sim 17 \text{ kJ mol}^{-1}$ for triphenyl-methanol are quite comparable to the barrier (V) of $14\text{-}15 \text{ kJ mol}^{-1}$ for the OH group rotation in phenols obtained by spectroscopic studies (19-22). Fong and Smyth (14) estimated the ΔH_E for OH group rotation in 4-phenylphenol and 1-naphthol in benzene solution which was negligibly small. This estimate appears to be unreasonable in view of the results of spectroscopic (19-22) and dielectric absorption (17,18,25) studies. The environment of the OH group in 4-phenylphenol molecule is almost similar to that in the 2-naphthol molecule. The latter molecule, while studied in a polystyrene matrix, yielded a ΔH_E of 12 kJ mol^{-1} for OH group relaxation (to be discussed later) as compared with the value of 13 kJ mol^{-1} for the former. These values are quite harmonious with those reported for OH group relaxation.

The triphenylmethanol molecule is comparable to the tricyclohexylearbinol molecule for which the reported values of ΔH_E are 12.4 kJ mol^{-1} in decalin solution (18) and 18.4 kJ mol^{-1} in the compressed solid state (17). Present investigation on triphenylmethanol in the solid state yielded

a ΔH_E of 16.7 kJ mol^{-1} which is fairly close to the solid state ΔH_E -value obtained with tricyclohexylcarbinol. These values appear to be a little higher than what is normally observed for OH group rotation. Davis and Meakins (18) suggested that the observed higher energy barrier to the OH group rotation in tricyclohexylcarbinol (in compressed solid) could be partly due to the interaction with neighbouring molecules in the crystal. The same argument might hold good in the case of triphenylmethanol where the proposed interaction would be intermolecular H bonding. Another possibility could be the effect of conjugation which might result in the enhanced energy barrier to OH group rotation by increasing the double bond character of the C-O linkage.

Results obtained with 1-naphthol in the compressed solid presented an interesting situation in that the observed ΔH_E of 35 kJ mol^{-1} and $\Delta G_{E200 \text{ K}}$ of $\sim 42.0 \text{ kJ mol}^{-1}$ were too high to be accounted for by the OH group relaxation alone. The molecule absorbed at a much higher temperature region (254 K - 287 K) as compared with those of 4-phenylphenol (90 K - 120 K) and triphenylmethanol (85 K - 102 K). The observed relaxation time ($\tau_{300 \text{ K}} =$

1.2×10^{-5} s) was also much higher than the corresponding values of 4-phenylphenol ($\tau_{300\text{ K}} = 2.3 \times 10^{-9}$ s) and triphenylmethanol ($\tau_{300\text{ K}} = 7.1 \times 10^{-12}$). By no means can these results be correlated with the only possible intramolecular process due to the OH group relaxation. On the other hand, as mentioned earlier, it was most unlikely that there could be any molecular rotation in the solid crystalline state. (As such, one possible explanation could be that the OH group rotation was strongly hindered by a fairly strong intermolecular H bond such that the OH group could relax only after the breakage of such bonds). The energy involved in the breakage of a moderately strong H bond may be assumed to be of the order of $\sim 20 \text{ kJ mol}^{-1}$. This amount of energy, when added up to the energy barrier of $\sim 15.0 \text{ kJ mol}^{-1}$ for OH group rotation, could then satisfactorily account for the observed ΔH_E (35 kJ mol^{-1}) for the absorption process in question. In the infrared spectrum of solid 1-naphthol a strong and broad absorption band was observed (Ch. III) around 3300 cm^{-1} which clearly indicated the formation of fairly strong intermolecular H bonds.

While studied in polystyrene matrices both triphenylmethanol and 1-naphthol showed only one absorption peak, but the absorption region for the former molecule

(273 K - 316 K) was much higher than that for the latter (120 K - 150 K). The observed relaxation parameters for these two molecules were also widely separated (Table V.2). For triphenylmethanol these parameters ($\Delta H_E = 44 \text{ kJ mol}^{-1}$, $\Delta G_{E300 \text{ K}} = 49.2 \text{ kJ mol}^{-1}$ and $\tau_{300 \text{ K}} = 5.8 \times 10^{-5} \text{ s}$) could hardly be assumed to be due to the OH group relaxation. The infrared spectrum of the compound did not seem to indicate any significant intermolecular hydrogen bonding which could account for the observed high relaxation parameters. Thus, the only process which might cause the observed absorption could be the whole molecule relaxation. To the knowledge of the author relaxation data on any similarly-sized rigid molecules are lacking in the literature. The molecule in question is, however, approximately of similar length ($\sim 12.6 \text{ \AA}$) to p-chlorobiphenyl (triphenylmethanol and p-chlorobiphenyl from the Courtauld model). The latter molecule (35) absorbed in the temperature region of 283 K - 305 K yielding a ΔH_E of 76 kJ mol^{-1} , $\Delta G_{E300 \text{ K}}$ of 48 kJ mol^{-1} and $\tau_{300 \text{ K}}$ of $3.6 \times 10^{-5} \text{ s}$. Considering some dissimilarities in size and shape of the two molecules, their relaxation parameters appear to be fairly comparable and consequently the occurrence of molecular relaxation giving rise to the dielectric absorption in question seems to be very likely.

For 1-naphthol the observed ΔH_E and $\Delta G_{E100\text{ K}}$ were respectively 17 kJ mol^{-1} and 20.4 kJ mol^{-1} as compared with the corresponding values of 16.4 kJ mol^{-1} and 19.0 kJ mol^{-1} observed (41) for the similarly-sized rigid molecule 1-bromonaphthalene which absorbed in a similar temperature region (108 K - 137 K). The observed ΔH_E of 17 kJ mol^{-1} is also very close to those obtained for the OH group rotation, viz., $\sim 17\text{ kJ mol}^{-1}$ in tri-phenylmethanol as a compressed solid. Thus, the observed absorption in question could be assigned either to the whole molecule relaxation or to the OH group relaxation. A very likely situation could be such that both the processes would overlap in the said absorption region.

The OH group moment of 1.54 D (38) in 1-naphthol may be assumed to act almost in the same direction (76° (37) from the O-C bond) as in phenol such that the component along the O-C bond ($\mu_1 = 1.54\text{ D} \cdot \cos 76^\circ$) will give rise to molecular rotation while the other component ($\mu_2 = 1.54\text{ D} \cdot \sin 76^\circ$) perpendicular to the O-C bond will be responsible for the OH group relaxation. Accordingly the weight factors for these two processes will be:

$$C_1 = \frac{\mu_1^2}{\mu_1^2 + \mu_2^2} = 0.16 \quad \text{V.3(a)}$$

$$C_2 = \frac{\mu_2^2}{\mu_1^2 + \mu_2^2} = 0.94 \quad \text{V.3(b)}$$

This approximate estimate indicates that the absorption process under consideration was overwhelmingly dominated by the OH group relaxation process. The experimental values of apparent dipole moment on regression yielded a value of 1.15 D which is significantly lower than the literature value of 1.46 D (39). Possible reasons for such a discrepancy could be the steric effects of perihydrogen (40) and the effect of intermolecular H bonding which might influence the molecular geometry.

While studied in polystyrene matrices, the molecules 2-naphthol, 6-bromo-2-naphthol, and 2-methoxy-naphthalene each showed two widely separated absorption peaks. The absorption regions, relaxation data, and the Eyring activation parameters all appear to suggest

consistently that the lower temperature absorption in each case could be corresponding to some intramolecular process while the higher temperature processes might presumably be due to the corresponding whole molecule relaxation. The only possible intramolecular process in these molecules should be the OH/OMe group reorientation.

In the case of 2-naphthol the low temperature process yielded a ΔH_E of 12 kJ mol^{-1} and $\Delta G_{E100 \text{ K}} = 17.9 \text{ kJ mol}^{-1}$ as compared with the corresponding values of 13 kJ mol^{-1} and 16.2 kJ mol^{-1} observed for the OH group relaxation in 4-phenylphenol. The relaxation time in the former case ($1.0 \times 10^{-3} \text{ s}$) was also fairly close to that of the latter ($1.3 \times 10^{-4} \text{ s}$) despite the fact that the two molecules were studied in two different media. These results appear to suggest that the dielectric absorption under consideration was due to the OH group relaxation around the C-O bond without any significant interaction whatsoever. The observed ΔH_E values for 6-bromo-2-naphthol and 2-methoxynaphthalene in the low temperature process were $\sim 8 \text{ kJ mol}^{-1}$ and $\sim 9 \text{ kJ mol}^{-1}$, respectively, while the corresponding $\Delta G_{E100 \text{ K}}$ -values were 15.0 kJ mol^{-1} and 15.3 kJ mol^{-1} . These values are fairly close to the corresponding values for 2-

naphthol. Nevertheless, there is some significance of the effect of substitution in the ring system but the estimation of such effects (conjugation, +I, -I, resonance, etc.) is extremely difficult. Infrared study indicated (Ch. III) that Br-substitution in 6-position of 2-naphthol reduces its H bonding ability. With these facts in mind, small differences in the Eyring activation parameters of the three molecules under consideration seem to be quite explicable. The energy barriers to OH and OMe group rotations are generally of similar order of magnitude (27,28). The observed ΔH_E ($\sim 9 \text{ kJ mol}^{-1}$) in 2-methoxynaphthalene appear to be in good agreement with the values ($9-11 \text{ kJ mol}^{-1}$) reported (27) for OMe group rotation in several molecules.

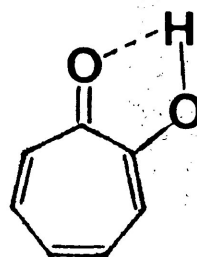
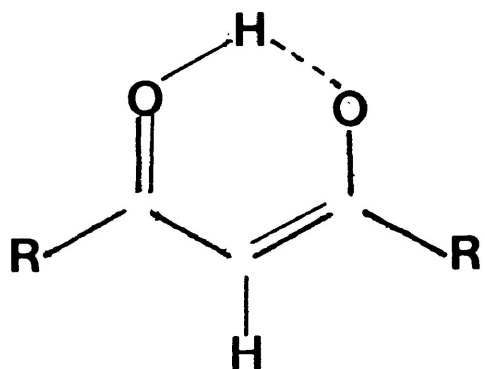
The second set of absorptions observed at higher temperatures for hydroxy/methoxy naphthalenes under consideration were assumed to be due to the corresponding molecular relaxation processes. But the observed activation parameters for these molecules do not appear to correspond to their relative sizes as might be expected for simple molecular rotation. The experimental ΔH_E of 52 kJ mol^{-1} for 2-naphthol was significantly higher than the corresponding value of 41 kJ mol^{-1} for the larger molecule, 6-bromo-2-naphthol. The 2-naphthol molecule can be compared with the

similarly sized rigid molecule 2-chloronaphthalene. In a similar measurement (41) with the latter molecule a ΔH_E of $\sim 35.0 \text{ kJ mol}^{-1}$ and a $\Delta G_{E200 \text{ K}}$ of $\sim 34.0 \text{ kJ mol}^{-1}$ were obtained as compared to the corresponding values of 52.0 kJ mol^{-1} and $\sim 41.0 \text{ kJ mol}^{-1}$ obtained with the former. The relaxation time for 2-naphthol ($\tau_{200 \text{ K}} = 1.3 \times 10^{-2} \text{ s}$) was also much longer than that for 2-chloronaphthalene ($\tau_{200 \text{ K}} = 2 \times 10^{-4} \text{ s}$). These results appear to indicate that the molecular relaxation of 2-naphthol was significantly hindered by intermolecular H bonding while such interaction was not prominent in the case of 6-bromo-2-naphthol in the concentration range in the polystyrene matrix. Infrared studies of these molecule (Ch. III) are consistent with this suggestion in that H bonding in 6-bromo-2-naphthol was less prominent than in 2-naphthol. Further, the observed ΔH_E (41 kJ mol^{-1}) and $\Delta G_{E200 \text{ K}}$ (42.3 kJ mol^{-1}) for 6-bromo-2-naphthol are fairly harmonious with the corresponding values (42.5 kJ mol^{-1} and 36.0 kJ mol^{-1} , respectively) of 2-bromonaphthalene (41) for its molecular relaxation.

The higher temperature absorption of 2-methoxynaphthalene yielded a ΔH_E of 138 kJ mol^{-1} , a $\Delta G_{E200 \text{ K}}$ of 42.0 kJ mol^{-1} and a $\tau_{250 \text{ K}}$ of $1.0 \times 10^{-4} \text{ s}$ as compared to the values of $\Delta H_E = 42.5 \text{ kJ mol}^{-1}$, $\Delta G_{E200 \text{ K}} = 36.0 \text{ kJ mol}^{-1}$

and $\tau_{200\text{ K}} = 5.0 \times 10^{-4}$ s obtained for a similarly sized rigid molecule, 2-bromonaphthalene (41). Although the ΔG_E -values and relaxation times for these molecules are fairly comparable the ΔH_E of ~ 138.0 kJ mol⁻¹ for 2-methoxynaphthalene is exceptionally large and, by no means, can be explained in terms of molecular relaxation. This unusually high ΔH_E -value could possibly be associated with some kind of cooperative process.

The three molecules namely, tropolone, 2,4-pentanedione (enol form) and dibenzoylmethane (enol form) were of special interest to the present investigation in that they are characterized by intramolecular H bonding as shown on page 156; the H atom of the OH group in each of these molecules is equally probable to be bonded to either of the O atoms while hydrogenbonded to the other and consequently, proton-jumping can be a potential intramolecular process. It should be mentioned here that the relative amounts of enol forms of 2,4-pentanedione and dibenzoylmethane have been estimated (42) to be $\sim 80\%$ and $\sim 100\%$ respectively.



a: Tropolone

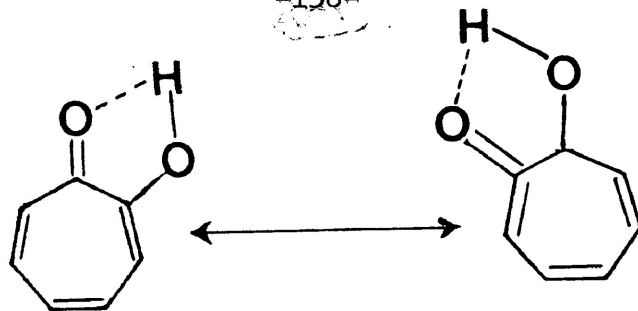
b. $R = \text{Me}$: 2,4-Pentanedione

c. $R = \text{Ph}$: Dibenzoylmethane

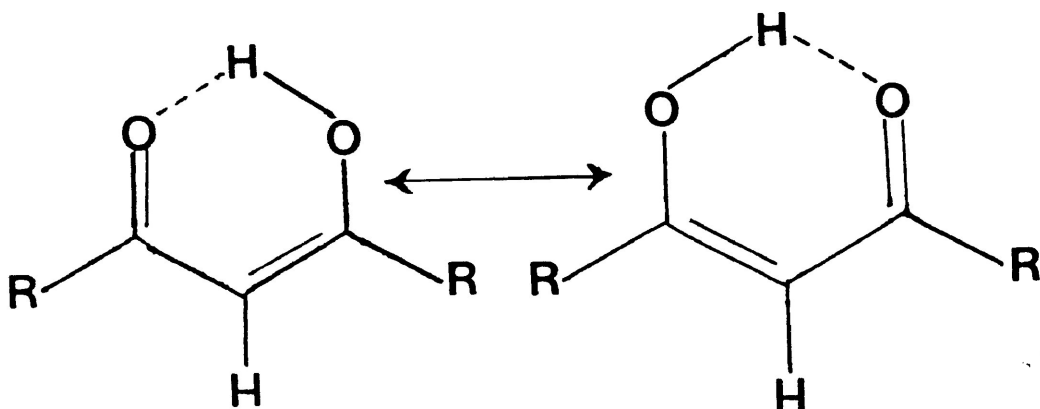
Each of these molecules, while studied in polystyrene matrices showed only one absorption which could be assigned to one or the other of the following processes: (i) respective molecular rotation, (ii) the OH group relaxation and (iii) proton jumping involving proton tunneling. In case of the first possibility the observed activation parameters (ΔH_E , ΔG_E and τ) should be dependent upon the size and shape of the respective molecules while the second possibility (OH group relaxation) would require that these parameters be of similar order of magnitude. On the basis of this generalization the involvement of the OH group relaxation

appears to be unlikely since the experimental parameters for the molecules in question seemed to be dependent on molecular size. Although the observed ΔH_E -values of $\sim 13 \text{ kJ mol}^{-1}$ and $\sim 15 \text{ kJ mol}^{-1}$ respectively for tropolone and 2,4-pentanedione (lower temperature region) are fairly similar to the value (12 - 15 kJ mol^{-1}) generally observed for unhindered OH group relaxation, one should be aware of the fact that the process in these molecules would require the breakage of fairly strong intramolecular H bonds and consequently the energy barrier would be much higher than the observed values.

The proton-jumping process can be shown in the following resonance structures (page 158) in which the OH proton can occupy two equilibrium positions in the same molecule. In these molecules the lighter atom H is attached to a much heavier atom O and the energy barrier separating the two equilibrium positions of the H atom appears to be fairly low such that proton tunneling could reasonably be involved in these equilibrium processes. The same arguments should be applicable to 2,6-dichlorophenol the results of which have been discussed earlier.



a: Tropolone



b. $R = \text{Me}$: 2,4-Pentanedione

c. $R = \text{Ph}$: Dibenzoylmethane

The effects of tunneling are generally shown by the reaction rate constants and the presence of appreciable tunneling can be identified by one or more of the following criteria (43):

- 1) Tunneling usually leads to greatly enhanced isotope effects (k_H/k_D);
- 2) The Arrhenius plots (plots of $\log k$ versus $\frac{1}{T}$) are generally curved at lower temperatures and at very low temperatures, if the tunneling rate is large enough, the rate constant is essentially temperature independent.

3) Tunneling usually lowers the energy barrier for equilibrium processes and unexpectedly large differences in effective activation energies for H and D species are observed.

It is to be noted that the $\log \tau T$ versus $\frac{1}{T}$ plots (Fig. V.7-9) for tropolone, dibenzoylmethane, and 2,6-dichlorophenol are all linear and by no means parallel to $\frac{1}{T}$ axis at lower temperatures. This evidence seems to negate the possible involvement of proton tunneling as intramolecular processes in these molecules.

The only absorption (80 K - 103 K) of tropolone yielded a ΔH_E of $\sim 13 \text{ kJ mol}^{-1}$, a $\Delta G_{E100 \text{ K}}$ of 15.8 kJ mol^{-1} and a $\tau_{100 \text{ K}}$ of $8.4 \times 10^{-5} \text{ s}$. This molecule can be compared in size with o-fluorochlorobenzene for which the corresponding quantities were found (34) to be 12.0 kJ mol^{-1} , 14.7 kJ mol^{-1} , and $2.3 \times 10^{-5} \text{ s}$. In view of the excellent agreement between the two sets of values the said absorption for tropolone could reasonably be assigned to the whole molecule relaxation.

The maximum length of dibenzoylmethane (enol form) is similarly comparable to that of p-fluorobiphenyl. The single absorption by the former molecule yielded

a ΔH_E of 61 kJ mol^{-1} and a $\Delta G_{E300 \text{ K}}$ of 39.6 kJ mol^{-1} as compared to the corresponding values of 59 kJ mol^{-1} and 42 kJ mol^{-1} for the latter obtained in a similar experiment (35). Dibenzoylmethane absorbed in the temperature region of $293 \text{ K} - 270 \text{ K}$ yielding a $\tau_{300 \text{ K}}$ of $1.3 \times 10^{-6} \text{ s}$ as against the corresponding value of $3.0 \times 10^{-6} \text{ s}$ for p-fluorobiphenyl which absorbed in a similar temperature region ($256 \text{ K} - 298 \text{ K}$). These results would tend to suggest that the only absorption observed with dibenzoylmethane could be associated to the molecular reorientation rather than to any intramolecular process.

The absorption process for 2,4-pentanedione presented an interesting situation in that an inflection was observed in the $\log \tau T$ versus $\frac{1}{T}$ plot (Fig. V. 8). The absorption itself was characterized by a wide temperature region ($85 \text{ K} - 130 \text{ K}$) and a very low β -value (.15) which seem to indicate an overlap of more than one absorption process. Experiments with deuterated 2,4-pentanedione presented almost similar results. In both cases the $\log \tau T$ versus $\frac{1}{T}$ plot (Fig. V. 8) could be considered to present two intersecting lines corresponding to two separate processes and accordingly, Eyring analyses were done with two separate

sets of data (Table V-3).

The lower temperature data yielded ΔH_E -value of $\sim 15 \text{ kJ mol}^{-1}$ and 16 kJ mol^{-1} for undeuterated and deuterated molecules respectively, while the respective values obtained with higher temperature data were $\sim 4 \text{ kJ mol}^{-1}$ and $\sim 9 \text{ kJ mol}^{-1}$. It seems unusual that the lower temperature data yielded higher ΔH_E -values. However, the higher values of enthalpy of activation appear to correspond to the relaxation of the respective molecules in the enol form. In this form the maximum length of 2,4-pentanedione would be approximately similar to that (8.2 \AA) of chlorobenzene. In a similar measurement with the latter molecule (34) a ΔH_E of 11 kJ mol^{-1} , $\Delta G_{E100 \text{ K}} = 16.7 \text{ kJ mol}^{-1}$, and $\tau_{100 \text{ K}} = 2.3 \times 10^{-5} \text{ s}$ were obtained. These parameters are fairly comparable to the corresponding values of $\sim 15 \text{ kJ mol}^{-1}$, 15.6 kJ mol^{-1} and $6.8 \times 10^{-5} \text{ s}$ obtained for 2,4-pentanedione. These parameters obtained for the deuterated molecule ($\Delta H_E = 16 \text{ kJ mol}^{-1}$, $\Delta G_{E100 \text{ K}} = 15.5 \text{ kJ mol}^{-1}$ and $\tau_{100 \text{ K}} = 6.0 \times 10^{-5}$) are also of similar orders of magnitudes. These results are fairly consistent with the suggestion of molecular relaxation of both the molecules in the lower temperature region.

The lower energy process yielding ΔH_E -values of $\sim 4 \text{ kJ mol}^{-1}$ and $\sim 9 \text{ kJ mol}^{-1}$ respectively for H and D species of 2,4-pentanedione has to be assigned to some other molecular or intramolecular motion which is not clearly understood. In view of the existence of keto forms ($\sim 20\%$) of these molecules one could possibly think of their relaxation. Segmental motion in these keto tautomers could be another possibility. One should appreciate the fact that for overlapping processes the activation parameters lose much of their significance, and consequently their interpretation becomes very difficult.

Fig. V_r8 could alternatively be assumed to present the bending of the same lines rather than two intersecting pairs (A and B) of straight lines representing the Arrhenius plots for H- and D-species of 2,4-pentanedione. This bending or inclination towards the $\frac{1}{T}$ axis may apparently indicate the involvement of proton tunneling in the observed absorption for the molecules in question. But one should carefully note the following points which seem to negate such a possibility:

1. The bending of the lines towards the $\frac{1}{T}$ axis occurs at the higher temperature side; for proton tunneling this should

be observed at lower temperature side (43).

2. The ratio $\frac{k_H}{k_D}$ (τ_D/τ_H) for the bent parts (B) of the lines comes out to be ~ 1.8 (100 K) which is not very much different from the normal isotope effect; Gough and Price (16) reported a value of 1.2 for OH group relaxation in a substituted phenol molecule.

3. The total absence of any similar absorption process (at lower temperatures) in dibenzoyl methane provides indirect evidence against the possibility of proton tunneling. The molecule exists exclusively in enol form ($\sim 100\%$) (42) while 2,4-pentane dione exists in keto form (20%) (42) which is likely to contribute to the observed absorption as anticipated above.

In view of the above arguments the author favours the suggestion of more than one overlapping process giving rise to the said absorptions in deuterated and undeuterated 2,4-pentanediones.

REFERENCES

1. W. Dannhauser, L. W. Bahe, R. Y. Liu and A. F. Fluekinger, *J. Chem. Phys.*, 43(1965)257.
2. S. K. Garg and C. P. Smyth, *J. Phys. Chem.* 69(1965)1294.
3. S. K. Garg and C. P. Smyth, *J. Chem. Phys.*, 46(1967)373.
4. W. Dannhauser, *J. Chem. Phys.*, 48(1968)1918.
5. P. Bordewijk, F. Gransch and C. J. F. Bottcher, *J. Phys. Chem.*, 73(1969)3255.
6. G. P. Johari and C. P. Smyth, *J. Am. Chem. Soc.*, 91(1969)6215.
7. J. Crossley, L. Glasser and C. P. Smyth, *J. Chem. Phys.*, 52(1970)6203.
8. J. Crossley, *Can. J. Chem.* 49(1971)712.
9. J. Crossley, *J. Phys. Chem.* 75(1971)1790.
10. L. Glasser, J. Crossley and C. P. Smyth. *J. Chem. Phys.*, 57(1972)3977.
11. J. Crossley, *Can. J. Chem.* 56(1978)352.
12. J. Crossley, *Adv. Mol. Relax. Processes*, 2(1970)69.
13. E. Jakusek and L. Sobezyk, *Dielectric and Related Molecular Processes (Specialist Periodical Reports)*, The Chemical Society, 3(1976)108.
14. F. K. Fong and C. P. Smyth, *J. Am. Chem. Soc.*, 85(1963)1565.
15. F. K. Fong, J. P. McTague, S. K. Garg and C. P. Smyth, *J. Phys. Chem.* 70(1966)3567.
16. S. R. Gough and A. H. Price, *Trans. Faraday Soc.*, 61(1965)2435.

REFERENCES continued...

17. R. J. Meakins, *Trans. Faraday Soc.*, 52(1956)320.
18. M. Davis and R. J. Meakins, *J. Chem. Phys.*, 26(1957)1584.
19. H. Forest and B. P. Dailey, *J. Chem. Phys.*, 45(1966)1736.
20. T. Pedersen, N. W. Larsen and L. Nygaard, *J. Mol. Structure*, 4(1969)59.
21. H. D. Bist and D. R. Williams, *Bull. Am. Phys. Soc.*, 11(1966)826.
22. L. Radom, W. J. Hehre, J. A. Pople, G. L. Carlson and W. G. Fatel, *J.C.S. Chem. Commn.*, (1972)308.
23. M. Davis and A. Edwards, *Trans. Faraday Soc.*, 63(1967)2163.
24. S. P. Tay, J. Draft and S. Walker, *J. Phys. Chem.*, 80(1976)303.
25. M. A. Mazid, M. A. Enayetullah and S. Walker, *Faraday Trans. II*, 77(1981)1143.
26. W. G. Fatel, G.H.L. Carlson and F. F. Bently, *J. Phys. Chem.*, 79(1975)199.
27. M. A. Mazid, J. P. Shukla and S. Walker, *Can. J. Chem.*, 56(1978)1800.
28. T. B. Grindley, A. R. Katritzky and R. D. Topsom, *J. Chem. Soc. Perkin Trans. II*, (1974)289.
29. R. L. Redington and T. E. Redington, *J. Mol. Spectrosc.*, 78(1979)229.
- 30(a) W. F. Rowe Jr., R. W. Querst and E. B. Wilson, *J. Am. Chem. Soc.*, 98(1976)4021.
- (b) C. J. Seliskar and R. E. Hoffmann, *J. Mol. Spectrosc.*, 88(1981)30.

REFERENCES continued...

- 31(a) W. A. Phillips, *J. Low Temp. Phys.*, 17(1976)3/4;
11(1973)5/6.
- (b) W. A. Phillips, *J. Non-Cryst. Solid*, 31(1978)267.
32. P. Schuster, *Chem. Phys. Lett.*, 3(1969)433.
33. P. Stilbs and M. E. Moseley, *J. C. S. Faraday II*,
76(1980)729.
34. M. A. Mazid, M.Sc. Thesis, Lakehead University,
Canada, 1978.
35. H. A. Khwaja and S. Walker, *Adv. Mol. Relax. and
Interact. Processes*, 19(1981)1.
36. J. H. Richards and S. Walker, *Trans. Faraday Soc.*,
57(1961)406.
37. J. W. Smith, "Electric Dipole Moments", Butterworths,
London, 1955.
38. C. P. Smyth, "Dielectric Behaviour and Structure",
McGraw-Hill Book Company, Inc., 1955.
39. A. L. McClellan, "Tables of Experimental Dipole
Moments", W. H. Freeman and Company, 1963.
40. V. I. Minkin, O. A. Osipov and Y. A. Zhadanov,
"Dipole Moments in Organic Chemistry", Plenum
Press, New York-London, 1970, p. 221.
41. S. P. Tay, Ph.D. Thesis, University of Salford,
England, 1977.
42. G. Allen and R. A. Dwek, *J. Chem. Soc., (B)*, (1966)161.
43. M. D. Harmony, *Quart. Rev. Chem. Soc.*, (1972)211.

TABLE V.2

Tabulated Summary of Fuoss-Kirkwood Analysis
Parameters and Effective Dipole Moments (μ)
for Phenols and Related Compounds

T(K)	$10^6 \tau$ (s)	$\log f_{\max}$	β	$10^3 \epsilon''_{\max}$	ϵ_{∞}	μ (D)
<u>0.77M o-Cresol in Polystyrene Matrix</u>						
108.0	381.3	2.62	0.18	0.23	2.82	0.41
115.0	118.3	3.13	0.16	5.68	2.82	0.47
119.8	64.2	3.39	0.19	5.98	2.82	0.45
124.6	42.2	3.58	0.18	6.31	2.82	0.49
129.8	12.8	4.09	0.16	6.67	2.81	0.54
135.8	6.7	4.38	0.17	7.07	2.81	0.55
140.5	5.7	4.45	0.19	7.23	2.82	0.54
<u>0.70M 2-Ethylphenol in Polystyrene Matrix</u>						
172.2	228.4	2.84	0.20	7.22	2.68	0.63
178.1	116.0	3.14	0.23	7.45	2.69	0.60
182.6	98.6	3.21	0.20	7.75	2.68	0.67
187.9	53.2	3.48	0.19	7.78	2.69	0.70
192.3	38.2	3.62	0.20	8.05	2.69	0.70
196.6	24.8	3.81	0.20	8.14	2.69	0.71
200.2	20.9	3.88	0.22	8.37	2.70	0.69
<u>0.63M 2-Isopropylphenol in Polystyrene Matrix</u>						
187.7	743.6	2.33	0.16	8.31	2.73	0.82
192.9	282.5	2.75	0.17	8.50	2.77	0.81
198.7	181.5	2.94	0.15	8.72	2.72	0.89
202.9	101.4	3.20	0.15	8.88	2.72	0.91
208.7	47.1	3.53	0.16	9.08	2.73	0.90
214.6	20.1	3.90	0.23	7.29	2.38	0.84
222.4	9.7	4.22	0.26	7.46	2.39	0.72
<u>0.56M 2-t-Butylphenol in Polystyrene Matrix</u>						
212.5	138.3	3.06	0.22	4.46	2.185	0.65
216.7	65.4	3.39	0.24	4.60	2.190	0.64
219.6	47.5	3.53	0.25	4.66	2.197	0.64
222.2	33.8	3.67	0.25	4.67	2.205	0.64
227.8	18.8	3.93	0.29	4.82	2.210	0.61
232.1	12.7	4.10	0.32	4.93	2.230	0.59

TABLE V.2. continued...

T(K)	$10^6 \tau$ (s)	$\log f_{\max}$	β	$10^3 \epsilon''_{\max}$	ϵ_{∞}	μ (D)
<u>0.53M 2,6-Dichlorophenol in Polystyrene Matrix</u>						
113.3	182.9	2.94	0.20	11.87	2.75	0.73
118.5	96.8	3.22	0.20	12.71	2.75	0.78
121.9	69.9	3.36	0.20	14.29	2.99	0.80
126.3	29.3	3.74	0.19	13.39	2.74	0.84
131.7	15.3	4.02	0.22	15.54	2.99	0.83
138.2	9.0	4.25	0.24	14.82	2.75	0.84
<u>7.435M 4-Phenylphenol in Compressed Solid</u>						
90.5	693.5	2.36	0.30	1.29	3.18	0.04
93.6	366.7	2.64	0.29	1.33	3.18	0.04
99.0	167.2	2.98	0.30	1.41	3.18	0.05
103.7	72.8	3.34	0.34	1.48	3.18	0.05
107.8	44.1	3.56	0.27	1.51	3.18	0.05
116.0	14.3	4.05	0.33	1.59	3.17	0.05
<u>0.33M Triphenylmethanol in Polystyrene Matrix</u>						
281.9	192.2	2.92	0.21	2.48	2.78	0.66
291.5	101.3	3.20	0.23	2.54	2.78	0.65
299.3	56.3	3.45	0.18	2.57	2.77	0.75
306.3	42.9	3.57	0.19	2.62	2.77	0.74
316.3	21.9	3.86	0.23	2.72	2.77	0.70
<u>4.97M Triphenylmethanol in Compressed Solid</u>						
85.5	499.1	2.50	0.27	2.50	2.89	0.08
87.7	252.2	2.80	0.25	2.60	2.88	0.09
90.2	138.1	3.06	0.27	2.69	2.86	0.09
94.2	49.1	3.51	0.26	2.82	2.87	0.09
96.8	25.3	3.80	0.27	2.94	2.87	0.09
99.8	13.2	4.08	0.29	3.05	2.87	0.09
102.0	10.6	4.18	0.31	3.05	2.87	0.09

TABLE V.2 continued...

T(K)	$10^6 \tau$ (s)	$\log f_{\max}$	β	$10^3 \epsilon''_{\max}$	ϵ_{∞}	μ (D)
<u>0.70M 1-Naphthol in Polystyrene Matrix</u>						
123.1	433.6	2.56	0.22	6.74	2.80	0.48
129.0	149.5	3.03	0.23	7.09	2.80	0.49
134.0	91.2	3.24	0.23	7.46	2.80	0.51
138.5	51.7	3.49	0.22	7.63	2.80	0.54
143.6	29.0	3.74	0.22	8.02	2.80	0.57
148.3	21.1	3.88	0.24	8.33	2.80	0.56
<u>10.426M 1-Naphthol in Compressed Solid</u>						
254.7	181.8	2.94	0.39	7.45	2.86	0.15
263.4	92.2	3.24	0.34	8.16	2.85	0.16
268.5	67.3	3.37	0.32	8.50	2.85	0.17
272.8	52.5	3.48	0.29	8.81	2.85	0.18
278.3	38.3	3.62	0.26	9.51	2.84	0.20
282.0	34.1	3.67	0.23	10.09	2.83	0.22
286.8	24.1	3.82	0.23	11.06	2.83	0.23
<u>0.57M 2-Naphthol in Polystyrene Matrix</u> <u>Low Temperature Absorption</u>						
109.4	170.0	2.97	0.23	2.89	2.72	0.33
117.1	129.0	3.09	0.17	3.19	2.71	0.41
123.4	60.3	3.42	0.16	3.38	2.72	0.45
126.5	35.0	3.66	0.19	3.56	2.72	0.43
132.5	22.2	3.85	0.18	3.67	2.74	0.45
137.8	15.3	4.02	0.19	3.84	2.73	0.46
<u>High Temperature Absorption</u>						
223.3	517.5	2.49	0.19	8.98	2.66	0.91
229.0	188.7	2.93	0.20	8.48	2.67	0.87
233.5	111.3	3.16	0.21	8.60	2.68	0.87
238.5	60.3	3.42	0.23	8.71	2.69	0.84
244.0	38.1	3.62	0.23	8.44	2.69	0.83
248.6	21.9	3.86	0.24	8.73	2.70	0.84
253.2	14.8	4.03	0.24	8.67	2.70	0.84

TABLE V.2 continued....

T (K)	$10^6 \tau$ (s)	$\log f_{\max}$	β	$10^3 \epsilon''_{\max}$	ϵ_{∞}	μ (D)
<u>0.38M 6-Bromo-2-Naphthol in Polystyrene Matrix</u>						
<u>Low Temperature Absorption</u>						
88.4	115.7	3.14	0.24	1.24	2.42	0.25
94.0	77.2	3.31	0.25	1.31	2.42	0.26
98.6	40.8	3.59	0.25	1.37	2.42	0.27
102.4	23.5	3.83	0.26	1.40	2.43	0.27
107.2	18.8	3.93	0.29	1.42	2.42	0.26
112.4	10.1	4.20	0.30	1.44	2.42	0.27
<u>High Temperature Absorption</u>						
242.9	265.1	2.78	0.30	9.30	2.41	1.00
253.6	115.8	3.14	0.28	9.64	2.40	1.08
258.6	89.2	3.25	0.26	9.84	2.40	1.14
262.7	62.7	3.40	0.17	9.89	2.38	1.43
265.1	53.1	3.48	0.17	9.94	2.38	1.44
272.6	25.2	3.80	0.17	10.29	2.37	1.48
287.1	9.4	4.22	0.18	10.79	2.37	1.52
294.0	7.7	4.31	0.20	10.86	2.38	1.46
<u>0.53M 2-Methoxy Naphthalene in Polystyrene Matrix</u>						
<u>Low Temperature Absorption</u>						
82.6	484.0	2.52	0.23	0.62	2.38	0.15
88.6	182.6	2.94	0.21	0.68	2.38	0.17
93.2	126.0	3.10	0.24	0.70	2.38	0.16
98.0	66.5	3.38	0.21	0.72	2.38	0.18
104.6	24.0	3.82	0.18	0.74	2.38	0.20
109.9	18.1	3.94	0.19	0.76	2.38	0.21
<u>High Temperature Absorption</u>						
244.1	609.8	2.42	0.31	36.73	2.36	1.69
248.6	164.0	2.99	0.34	35.86	2.36	1.58
250.6	107.5	3.17	0.34	34.32	2.36	1.55
253.7	49.2	3.51	0.35	34.11	2.37	1.53
255.7	32.8	3.72	0.34	32.8	2.36	1.53
258.5	13.2	4.08	0.36	33.17	2.37	1.51
261.0	7.6	4.32	0.38	32.62	2.37	1.46
263.1	3.6	4.64	0.38	32.21	2.37	1.46

TABLE V.2 continued...

T(K)	$10^6 \tau$ (s)	$\log f_{\max}$	β	$10^3 \epsilon''_{\max}$	ϵ_{∞}	μ (D)
<u>0.68M Tropolone in Polystyrene Matrix</u>						
80.0	1253.2	2.10	0.13	15.50	2.54	0.81
82.4	606.3	2.42	0.13	16.08	2.54	0.83
86.0	213.5	2.87	0.14	17.00	2.54	0.84
88.3	151.3	3.02	0.15	17.77	2.53	0.85
90.2	120.5	3.12	0.13	17.37	2.53	0.90
91.6	79.3	3.30	0.15	18.59	2.53	0.88
93.0	61.1	3.42	0.14	17.91	2.54	0.90
94.4	47.0	3.53	0.15	19.22	2.52	0.91
97.0	26.2	3.78	0.16	18.89	2.55	0.88
99.5	14.7	4.03	0.17	19.97	2.54	0.89
103.2	10.5	4.18	0.18	21.71	2.54	0.92
110.6	5.5	4.46	0.21	22.81	2.57	0.90

0.84M 2,4-Pentanedione in Polystyrene Matrix

86.1	1543.7	2.01	0.12	6.63	2.70	0.50
89.4	529.4	2.48	0.13	6.80	2.64	0.50
91.6	388.6	2.61	0.12	6.93	2.69	0.53
96.2	120.4	3.12	0.14	7.41	2.70	0.52
99.2	82.0	3.29	0.15	7.57	2.64	0.53
101.6	66.4	3.38	0.14	7.86	2.70	0.55
104.8	25.6	3.79	0.15	8.00	2.64	0.57
107.4	18.7	3.93	0.14	8.24	2.70	0.58
112.8	10.1	4.19	0.16	8.74	2.71	0.57
117.3	7.8	4.31	0.18	9.03	2.71	0.55
121.2	7.4	4.33	0.20	9.00	2.66	0.54
125.3	5.9	4.43	0.20	9.27	2.72	0.55
129.2	5.3	4.48	0.22	9.03	2.67	0.53

0.37M Dibenzoylmethane in Polystyrene Matrix

239.0	850.4	2.27	0.15	6.00	2.29	1.21
244.8	368.3	2.64	0.14	6.12	2.29	1.24
251.6	171.3	2.97	0.15	6.50	2.29	1.25
256.4	99.5	3.20	0.16	6.72	2.29	1.24
261.4	55.0	3.46	0.14	6.87	2.29	1.35
270.3	20.3	3.89	0.16	7.44	2.28	1.34

TABLE V.2 continued...

T (K)	$10^6 \tau$ (s)	$\log f_{\max}$	β	$10^3 \epsilon''_{\max}$	ϵ_{∞}	μ (D)
0.88 M 3,3-Deutero-2,4-pentanedione in Polystyrene Matrix						
89.5	750.30	2.33	0.11	8.28	2.56	0.60
94.9	152.48	3.02	0.13	8.74	2.57	0.58
99.6	67.79	3.37	0.13	0.16	2.56	0.61
103.1	30.52	3.72	0.13	9.40	2.57	0.63
106.7	17.40	3.96	0.14	9.73	2.55	0.63
199.3	11.31	4.15	0.15	9.96	2.53	0.62
113.4	9.03	4.25	0.18	10.30	2.55	0.59
116.9	7.00	4.36	0.19	10.47	2.55	0.59
121.3	4.25	4.57	0.19	10.70	2.55	0.60
125.2	3.40	4.67	0.20	10.84	2.57	0.60

TABLE V.3 EYRING ANALYSIS RESULTS FOR SOME PHENOLS AND RELATED COMPOUNDS

MOLECULE (*)	T (K)	τ (s)		ΔG_E (kJ mol ⁻¹)			ΔH_E (kJ mol ⁻¹)	ΔS_E (J K ⁻¹ mol ⁻¹)	
		100 K	200 K	300 K	100 K	200 K			300 K
o-Cresol (PS)	108-141	1.8x10 ⁻³	5.7x10 ⁻⁸	1.5x10 ⁻⁹	18.3	20.6	22.9	16	-23
2-Ethylphenol (PS)	170-200	4.7x10 ¹	2.0x10 ⁻⁵	1.3x10 ⁻⁷	26.8	30.4	34.0	23	-36
2-t-Butylphenol (PS)	212-232	2.6x10 ⁹	6.8x10 ⁻⁴	3.8x10 ⁻⁸	41.6	36.2	30.8	47	54
2,6-Dichlorophenol (PS)	110-140	2.0x10 ⁻³	8.9x10 ⁻⁸	2.6x10 ⁻⁹	18.4	21.3	24.2	~16	-29
4-Phenylphenol (CS)	90-120	1.3x10 ⁻⁴	4.0x10 ⁻⁸	2.3x10 ⁻⁹	16.2	20.0	23.9	13	-38
Triphenylmethanol (CS)	85-102	1.4x10 ⁻⁵	3.0x10 ⁻¹⁰	7.1x10 ⁻¹	14.3	11.9	7.5	~17	24
Triphenylmethanol (PS)	273-316	3.2x10 ¹¹	5.7x10 ⁻¹	5.8x10 ⁻⁵	45.6	47.4	49.2	44	-18
1-Naphthol (PS)	120-150	2.2x10 ⁻²	4.0x10 ⁻⁷	8.7x10 ⁻⁹	20.4	23.8	27.2	17	-34
1-Naphthol (CS)	254-287	4.8x10 ⁷	2.0x10 ⁻²	1.2x10 ⁻⁵	38.3	41.8	45.3	35	-35
2-Naphthol (PS)	109-137	1.0x10 ⁻³	3.9x10 ⁻⁷	2.4x10 ⁻⁸	17.9	23.8	29.7	12	-59
2-Naphthol (PS)	233-253	1.3x10 ¹²	1.3x10 ⁻²	2.4x10 ⁻⁷	46.8	41.1	35.4	54	57
6-Bromo-2-naphthol (PS)	88-12	3.4x10 ⁻⁵	1.6x10 ⁻⁷	2.3x10 ⁻⁸	15.0	22.3	29.6	~8	-73
6-Bromo-2-naphthol (PS)	240-295	2.6x10 ⁹	2.7x10 ⁻²	5.0x10 ⁻⁶	41.6	42.3	43.0	41	-7
2-Methoxynaphthalene (PS)	82-109	4.8x10 ⁻⁵	1.4x10 ⁻⁷	1.7x10 ⁻⁸	15.3	22.1	28.9	~9	-68
2-Methoxynaphthalene (PS)	244-263	1.0x10 ⁻⁴	at 250 K			42.0 at 250 K		138	55
Tropolone (PS)	80-103	1.9x10 ⁻⁵	8.1x10 ⁻⁹	5.2x10 ⁻¹⁰	14.5	17.3	20.1	~13	-19
2,4-Pentanedione (PS)	86-107	6.8x10 ⁻⁵	5.0x10 ⁻⁹	1.8x10 ⁻¹⁰	15.6	16.5	17.5	~15	-9
2,4-Pentanedione (PS)	112-129	1.9x10 ⁻⁵	9.9x10 ⁻⁷	3.1x10 ⁻⁷	14.5	25.3	30.0	~4	-108
3,3-Deutero-2,4-Pentamedione (PS)	89-106	6.0x10 ⁻⁵	1.6x10 ⁻⁹	3.9x10 ⁻¹¹	15.5	14.6	13.7	16	9
3,3-Deutero-2,4-Pentamedione (PS)	106-125	3.4x10 ⁻⁵	9.0x10 ⁻⁸	1.0x10 ⁻⁸	15.0	21.3	27.7	~9	-63
Dibenzoylmethane (PS)	239-270	7.5x10 ¹⁵	4.0x10 ⁻¹	1.3x10 ⁻⁶				61	72

PS - Molecules studied in polystyrene matrix

CS - Molecules studied in compressed solid disk

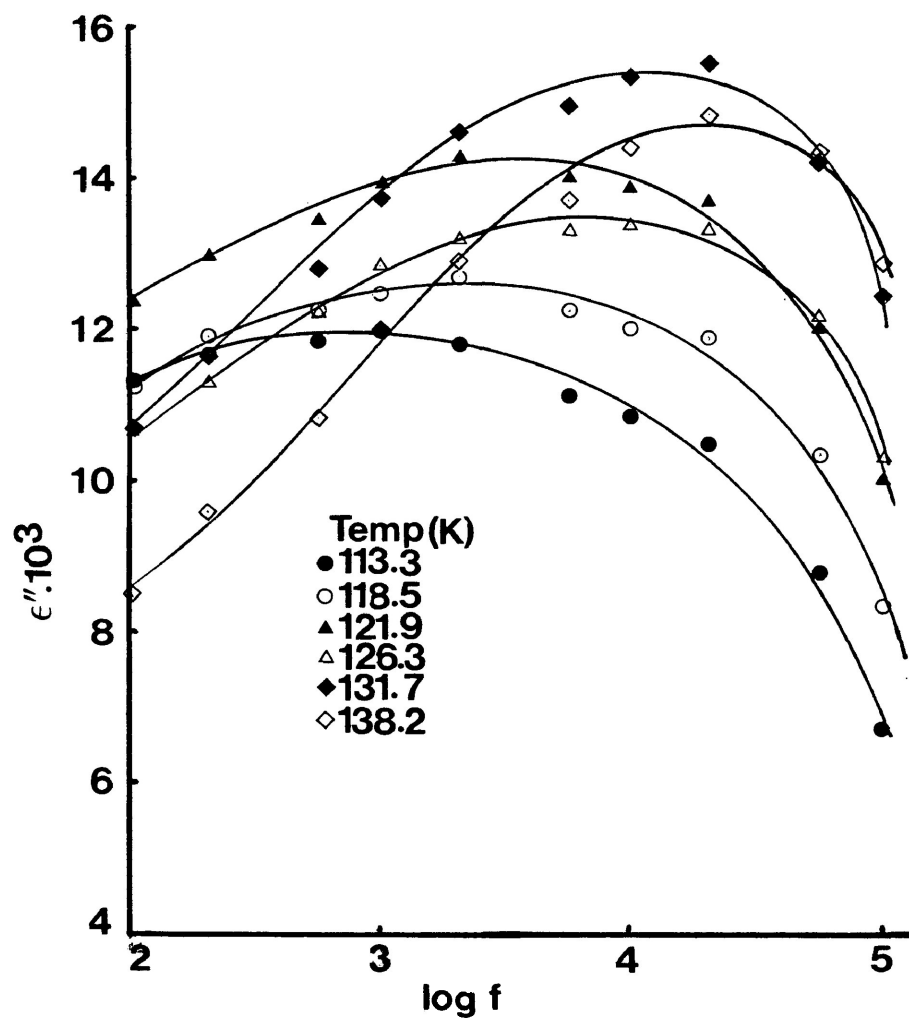


FIGURE V.1. PLOTS OF DIELECTRIC LOSS FACTOR (ϵ'') VERSUS LOG OF FREQUENCY FOR 2,6-DICHLOROPHENOL AT DIFFERENT TEMPERATURES.

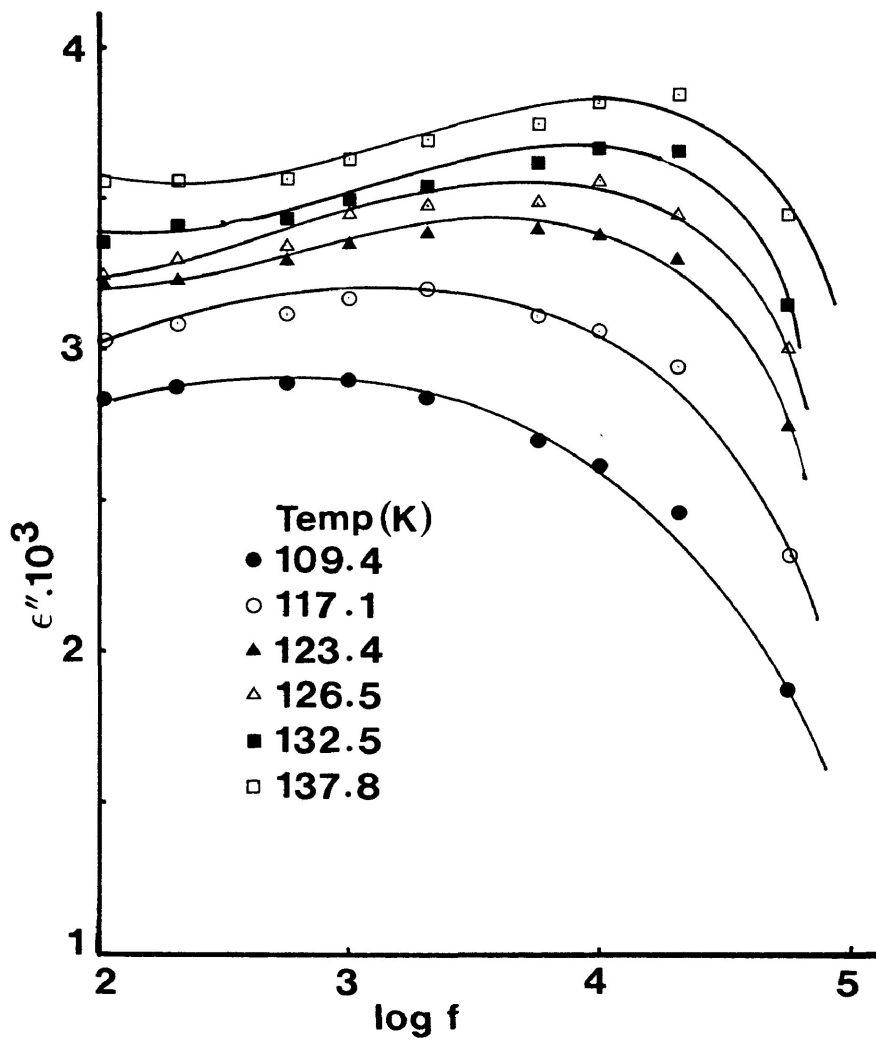


FIGURE V.2. PLOTS OF DIELECTRIC LOSS FACTOR (ϵ'') VERSUS LOG OF FREQUENCY FOR 2-NAPHTHOL AT DIFFERENT TEMPERATURES.

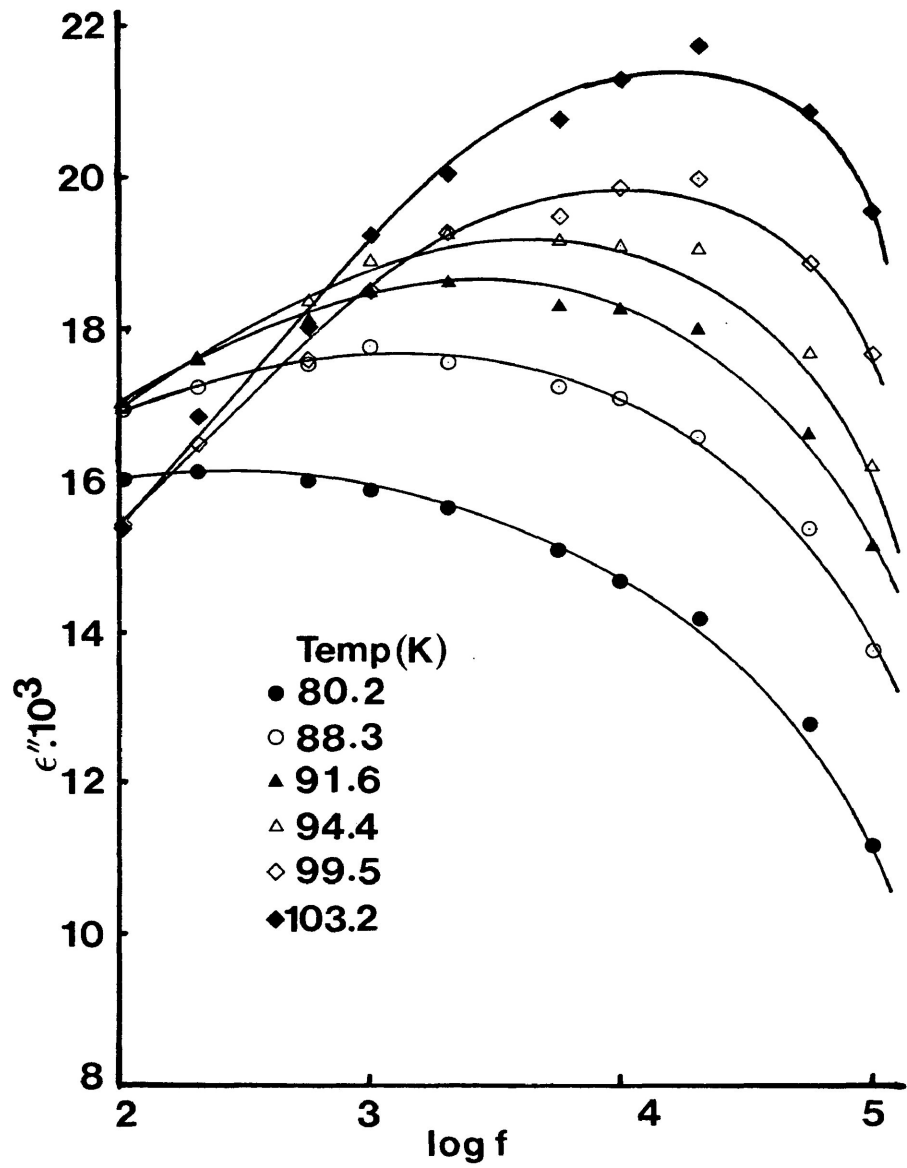


FIGURE V.3. PLOTS OF DIELECTRIC LOSS FACTOR (ϵ'') VERSUS LOG OF FREQUENCY FOR TROPOLONE AT DIFFERENT TEMPERATURES.

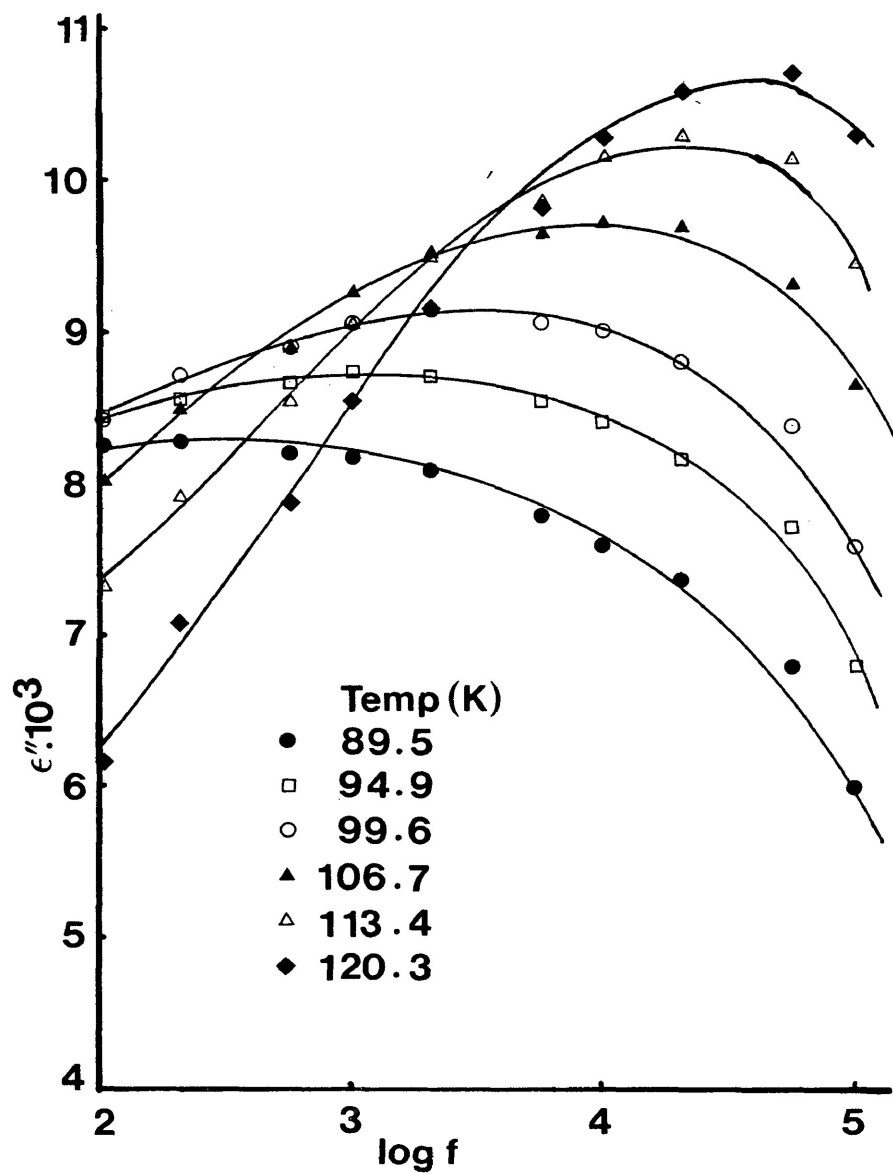


FIGURE V.4. PLOTS OF DIELECTRIC LOSS FACTOR (ϵ'') VERSUS LOG OF FREQUENCY FOR 3,3-DEUTERO-2,4-PENTANEDIONE AT DIFFERENT TEMPERATURES.

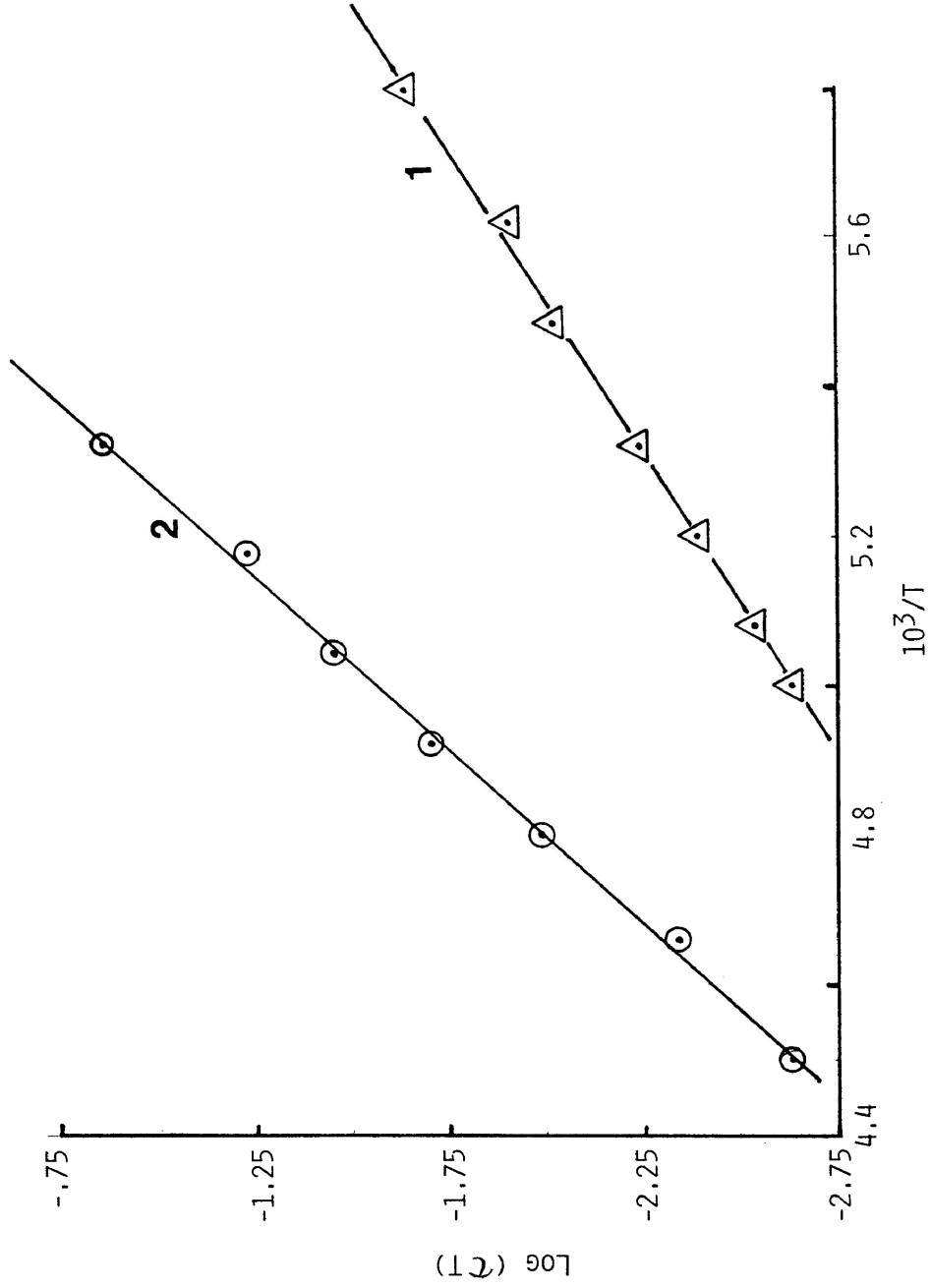


FIGURE V.5. EYRING PLOTS OF $\log(\tau T)$ VERSUS $\frac{1}{T}$ FOR 2-ETHYLPHENOL (1) AND 2-ISOPROPYLPHENOL (2).

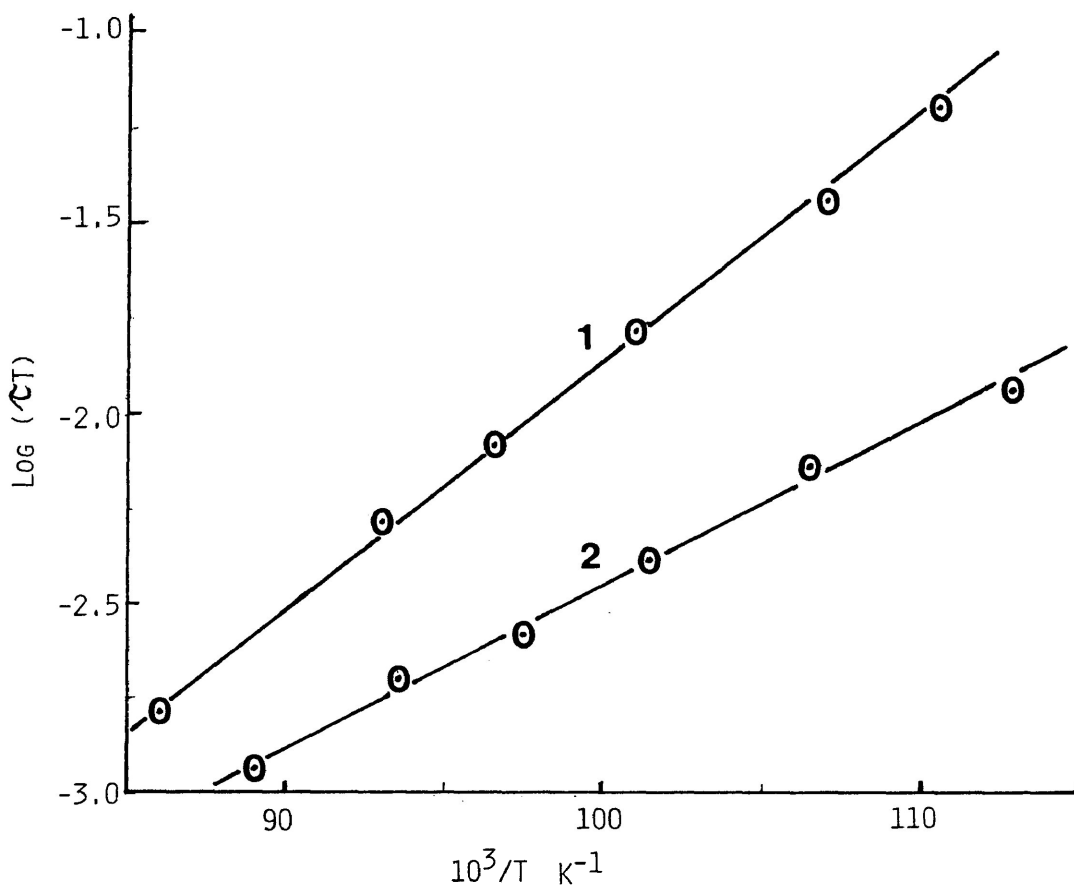


FIGURE V.6. EYRING PLOT OF LOG (τ) VERSUS $\frac{1}{T}$ FOR 4-PHENYL-PHENOL IN THE COMPRESSED SOLID (1) AND THE LOW TEMPERATURE PROCESS IN 6-BROMO-2-NAPHTHOL (2).

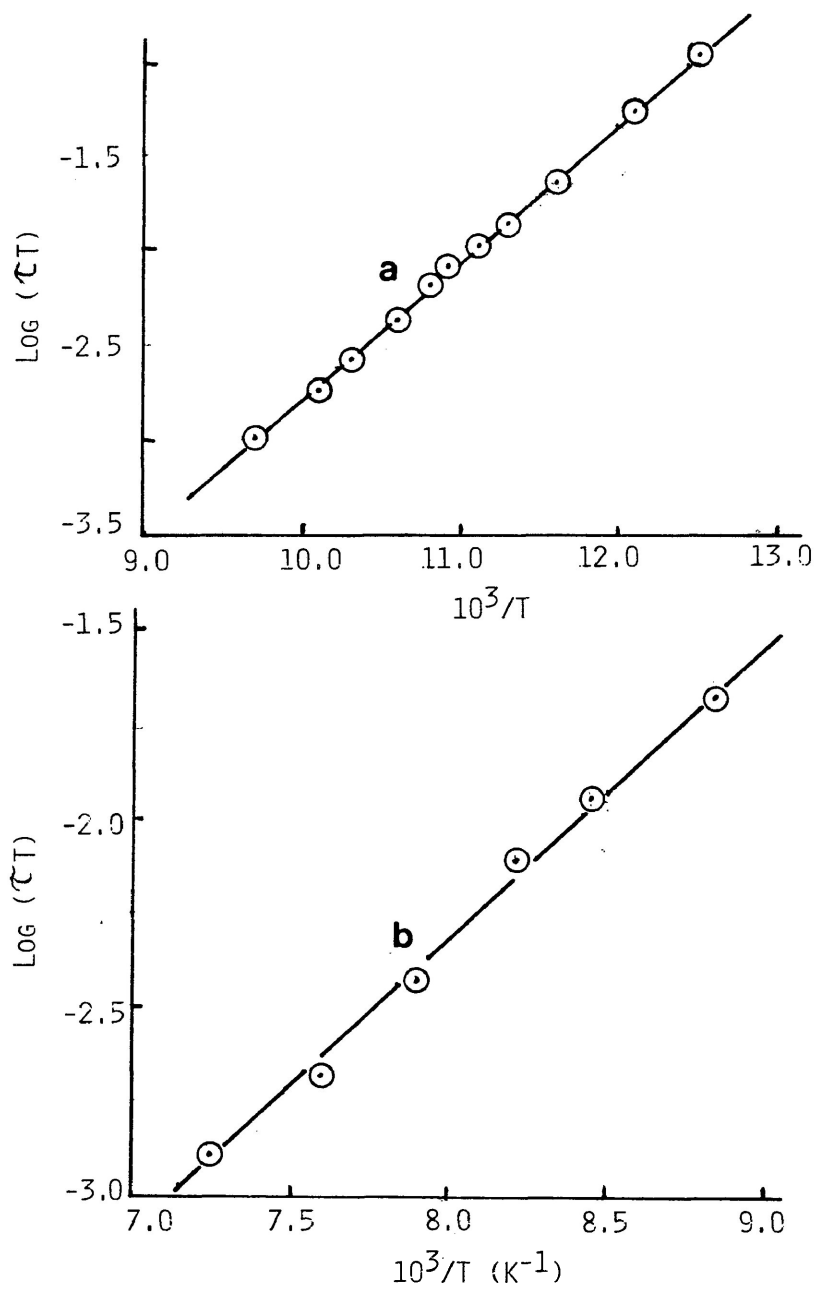


FIGURE V.7. EYRING PLOTS OF $\text{LOG}(\tau T)$ VERSUS $\frac{1}{T}$ FOR TROPOLENE (A) AND 2,6-DICHLOROPHENOL (B).

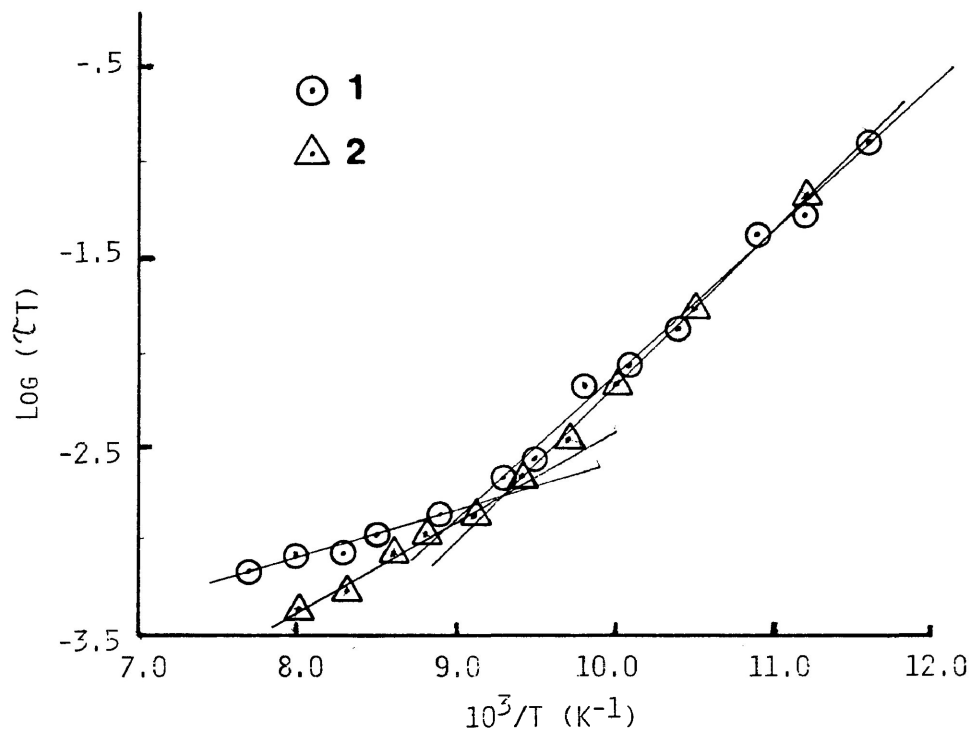


FIGURE V.8. EYRING PLOTS OF $\log(\tau T)$ VERSUS $\frac{1}{T}$ FOR 2,4-PENTANEDIONE (1) AND 3,3-DEUTERO-2,4-PENTANEDIONE (2).

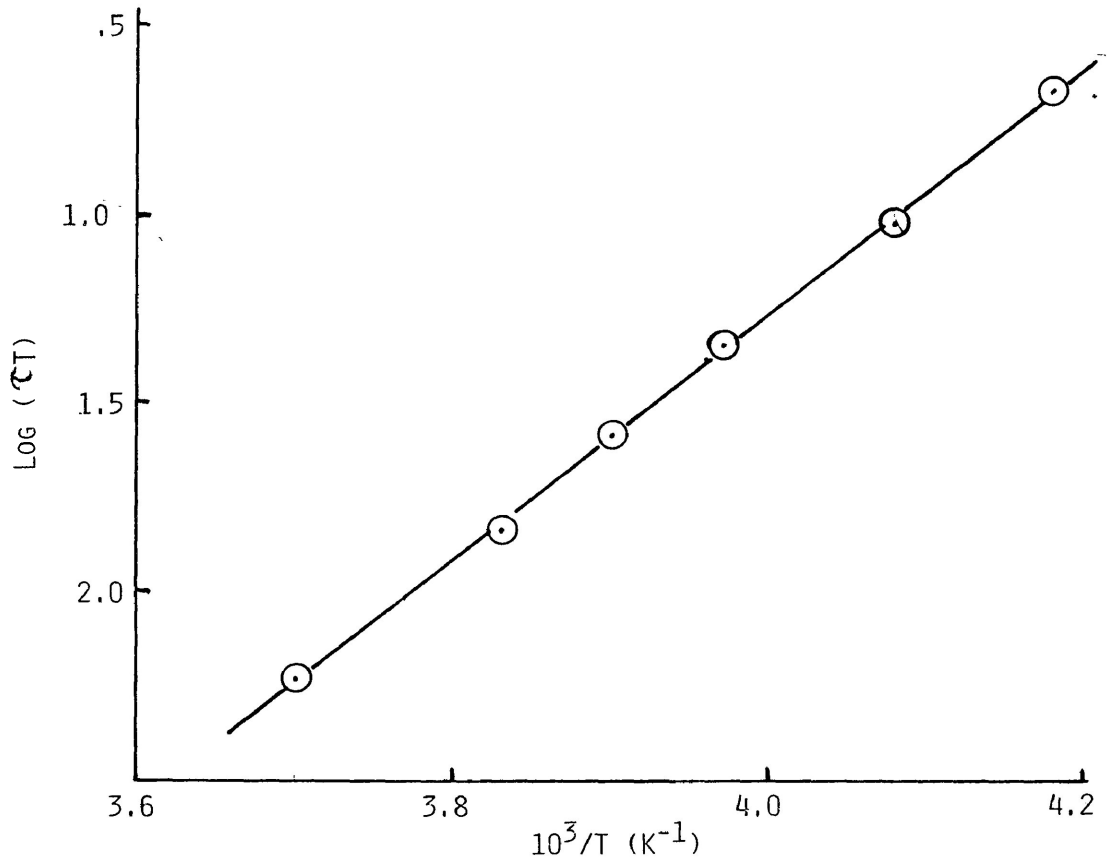


FIGURE V.9. EYRING PLOT OF LOG (τ) VERSUS $\frac{1}{T}$ FOR DIBENZOYLMETHANE

CHAPTER VI: DIELECTRIC RELAXATION STUDIES ON
SOME CARBOXYLIC ACIDS, ESTERS AND
SOME H BONDING ACID-BASE SYSTEMS

INTRODUCTION

Association of carboxylic acids through H-bonding has recently been the subject of extensive study by a variety of experimental and theoretical means. Various studies on pure acids in gas, liquid and solid phases as well as in solutions have resulted in the accumulation of a considerable body of quantitative data leading to conclusions which are often diverse and even, in a few cases, contradictory in nature which will be obviated by a subsequent survey. Results of earlier studies (up to the mid-sixties) have been reviewed and discussed by Allen and Caldin (1), Pimental and McClellan (2) and Ebersson (3). Despite diversity of the results these earlier works seem to converge on a few common aspects which are as follows:

- i) Carboxylic acids in general preferentially form the dimers. For example, the dimerization constants of acetic acid and benzoic acid in benzene are found (4) to be 4.00×10^2 and 8.9×10^3 respectively, which means that the relative amounts of the monomer:dimer would be approximately 1:14 and 1:66 respectively). The preferred structures of the dimers are found to be cyclic.

- ii) The H-bonds in carboxylic acids are stronger than those in alcohols, water or phenols, as may be expected from the tendency of the carbonyl group to withdraw electrons from the hydroxyl group and so to weaken the O-H bond and increase its polarity.

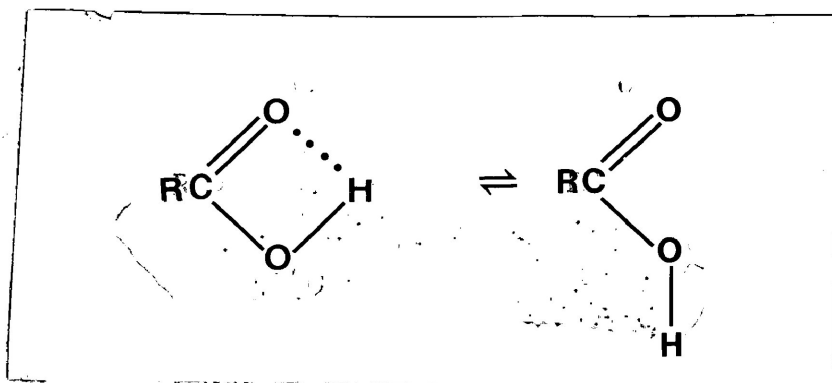
- iii) The heat of formation of H bond in the gas phase is around 30 kJ mol^{-1} .

Some recent studies (5-11) mostly favoured the cyclic structure for the acid dimers although the formation of open-chain dimers was not ruled out (6,9). The ΔH_d values (heat of dimerization), from ¹H n.m.r. study (6) and ΔE_{HB} values (energy of H bond formation) from a theoretical study (10), however, seems to markedly exceed the analogous parameters for the dimerization of carboxylic acids obtained by other physical methods (1,2).

Ultrasonic absorption studies on carboxylic acids provide some interesting results. Lamb and Pinkerton (12) measured the ultrasonic parameters for acetic acid in the frequency range 7.5 - 65 MHz and over the temperature range 283 - 333 K. Their results were found to fit a single re-

laxation which was attributed to the perturbation of monomer-dimer equilibrium. They arrived at a value of ΔH of $\sim 37 \text{ kJ mol}^{-1}$ and speculated that the process occurring involved the formation of only one H bond. Similar results were obtained for propionic acid by Lamb and Huddart (13). Freedman (14) estimated ΔH -values for the pure liquid acetic and propionic acids from vapor-state data; the values were $\sim 26 \text{ kJ mol}^{-1}$ and $\sim 39 \text{ kJ mol}^{-1}$ respectively. The calculated parameters were consistent with the view that ultrasonic absorption in acetic and propionic acid is caused by the perturbation of the monomer-dimer equilibrium.

With the evidences of his latter works on formic, butyric, and octanoic acids in the pure liquid state and in solution, Piercy (16) suggested that the ultrasonic absorption of carboxylic acids was due to the OH group rotation around the C-O bond which would lead to the following equilibrium system:



His argument appears to hinge on the value of 34.3 kJ mol^{-1} found for the activation energy for the reaction (whatever its nature be) occurring in carboxylic acids. Since spectroscopic evidence (16) pointed to a similar value (37.2 kJ mol^{-1}) for the barrier height to rotation about the C-O bond in acids, Piercy concluded that the same mechanism was responsible for the ultrasonic relaxation.

Dielectric investigations on H bonding in carboxylic acids are rather limited in the literature. In an early attempt (17) molecular polarization for monomeric and dimeric forms as well as dissociation constants of dimers of a number of acids in dilute solutions were estimated. Assuming cyclic structure for the dimers the calculated values of dipole moments (μ_d) were surprisingly high which were explained in terms of high atomic polarization. Relaxation studies in the liquid state showed (18) two dispersions (I and II) in formic acid and three (I, II and III) corresponding to the latter two regions of acetic acid observed at higher frequencies. The dispersion region (I) observed at the lowest frequency was thought to be related to the life time of chains linked through H bonds while the second and third dispersions (II and III) were attributed to the reorientation of the cyclic dimers with an opening of one hydrogen bond, and of free monomers.

Studies of dielectric relaxation led to the suggestion that the chain association dominates for formic acids and may be present in acetic acid while in higher carboxylic acids cyclic dimerization is predominant (19). Studies on very dilute solution of acetic acid in benzene (20) revealed two absorption regions. The relaxation time (τ_1) corresponding to the region I at lower frequency remained constant up to a concentration of 7 mol percent, and it was assigned to the reorientation of monomers. Beyond this concentration limit the relaxation time began to increase, suggesting an increase in the polar molecule concentration, most probably open-chain dimers and/or distorted cyclic dimers and possibly higher aggregates to a lesser extent. The relaxation time τ_2 corresponding to the higher frequency dispersion remained constant over the whole concentration range (up to 20 mol percent) and was considered to be due to some sort of very rapid internal motion. The possibility of hindered OH group rotation was put forward discarding the possible involvement of proton motion since the same relaxation time was found for deuterated acetic acid.

In view of the above discussion on the results obtained from diversified studies on carboxylic acids it was of interest to study the relaxation behaviour of these

molecules by the dielectric absorption method. Polystyrene matrix technique was employed in most cases which was of particular interest in view of the fact that such studies do not seem to appear in the literature. It was hoped that the present relaxation study would provide valuable information regarding the nature and strength of H bonding in carboxylic acids as well as regarding the nature and structure of associated species.

An important aspect of relaxation behaviour of carboxylic acids which has recently drawn considerable interest is the possible involvement of proton tunneling through H bonds in the cyclic dimers as one of the relaxation processes. Quite contradictory opinions have so far been put forward; while some authors (8,21-23) have supported the concept, others (20,24) have ruled out such a possibility and the problem seems yet to be unresolved. It was also hoped that the present study might provide some information on this aspect.

Studies of H-bonded complexes have been of considerable interest in recent years. The structure and interaction potential of a variety of H bonded complexes have recently been discussed in a comprehensive review by

Kohler and Huyskens (25). Lindemann and Zundel (26) have recently made an extensive infrared investigation on different H-bonded complexes of carboxylic acids with N-base. The authors, however, discussed aspects of polarizability, proton transfer, and symmetry of energy surfaces of the H bonds involved. Kraft et al (27) carried out some dielectric and spectroscopic studies on H-bonding of 2,4,6-trichlorophenol-complex with 1,4-diazabicyclo 2,2,2,-octane (DBO) in p-xylene. Both 1:1 and 2:1 complexes appeared to be formed, the concentration of the former being increased with the increase in the amine concentration. The authors suggested that the H-bond polarity increased considerably as a result of 'tautomeric' equilibrium appearing in the system under investigation. A dielectric relaxation study of several H-bonded complexes of the type N-H...N in polystyrene matrices was made by Shukla and Walker (28). The authors were able to separate the dielectric absorption of the complexes from that of the parent molecules and determined various activation parameters for different relaxation processes.

Dielectric studies of acetic acid-pyridine complexes were made by Davies and Sobczyk (29) and Gough and Price (30). Their results indicate that the dielectric absorption of a Debye type resulted from the reorientation

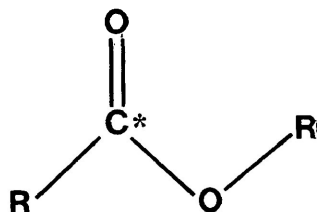
of complex species. For the $\text{CHCl}_2\text{COOH}\dots\text{B}$ and $\text{Cl}_3\text{CCOOH}\dots\text{B}$ complexes (18) some evidence was obtained which indicated the existence of a second absorption region related either to the intramolecular rotation or to the proton jumping.

None of the above studies gave an estimate of the H-bond energy. Very recently a theoretical approach by Remko (10) gave such an estimate for H-bonded complexes of several acids with pyridine. The author estimated for acid monomer...pyridine an E_{HB} (energy of H-bond formation) of around 50 kJ mol^{-1} . The lack of adequate experimental results revealing H-bond strength and the nature and size of the H-bonded complexes in the literature led the present relaxation study to be extended to a number of such systems dispersed in polystyrene matrices.

In order to elucidate the results obtained from the present study on carboxylic acids, it was felt necessary to investigate the relaxation behaviour of some related esters. Relaxation study of esters itself presents an interesting problem which would be apparent from the following discussion.

Relaxation studies on carboxylic acid esters have

recently been of considerable interest in that the possibility and the nature as well as the associated energy of intramolecular motions in these molecules of chemical interest have not, as yet, been established and different views on these aspects have been reported in the literature. McGreer et al (31), from their dielectric studies on esters in the pure liquid state, suggested the orientation of polar molecular segments presumably by rotation around C-C bonds while Crossley and Koizumi (32), from their dielectric absorption study of aliphatic esters RC^*OOR in cyclohexane solution, considered that the dipole orientation of the methoxy and ethoxy groups around C^*-O bonds is very important,



particularly in methyl and ethyl esters. Kano et al (33), from their dielectric absorption study on the same ester molecules, concluded that the dielectric relaxation of aliphatic esters is largely dominated by intramolecular rotation around the C-C bonds and/or the O-C bond rather

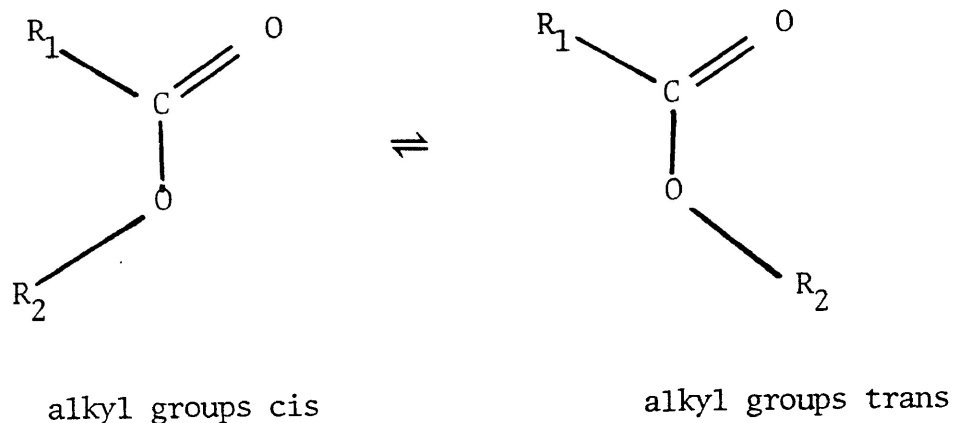
than around the C*-O bond.

Hassan et al. (34) explained their dielectric data on monocarboxylic esters in terms of both molecular and group relaxation; except for methyl and ethyl benzoate their data were consistent with a single relaxation process. It was proposed that the rotation of the -OR group around the C-OR linkage is inhibited owing to the double bond character of C-O bond caused by resonance.

Krishna and Upadhyay (35) proposed the possibility of restricted rotation of the -OR group from a dipole moment study of benzylbenzoate, 2-naphthyl benzoate, and o-hydroxybenzyl benzoate in benzene solution. For these molecules the authors obtained the energy barriers (ΔH_E) to such group rotation of 8.3 kJ mol^{-1} , 8.2 kJ mol^{-1} , and 8.8 kJ mol^{-1} respectively. Krishna et al. (36) in their dielectric study on methyl and ethyl esters of several nitro- and aminobenzoic acids did not find any intramolecular rotation except for methyl- and ethyl-m-nitrobenzoates.

From an extensive ultrasonic relaxation study of simple aliphatic mono- and diesters, Bailey and Walker (37) suggested that the -OR group relaxes between two

equilibrium positions corresponding to cis and trans forms of the molecules:



The authors observed a steady increase in ΔH (energy barrier) with the size of $R_1 + R_2$ from less than 4.2 kJ mol^{-1} for the formates to 33.4 kJ mol^{-1} for C_4 groups.

Dielectric relaxation data on some esters obtained by Saksena (38) supported by the viewpoint of Krishna and co-workers that $-OR$ group rotation about the $C-O$ bond is possible in spite of the rigidity introduced in it due to mesomerism. The estimated energy barriers (ΔH^*) for such group rotation ranged from 5.9 kJ mol^{-1} for $-OEt$ in

ethylisovalerate to 8.4 kJ mol^{-1} in -OBu in n-butyl benzoate.

Khwaja (39) studied the dielectric relaxation properties of a number of aromatic esters in polystyrene matrices in which the low temperature absorption attributed to intramolecular relaxation yielded ΔH_E values around 32 kJ mol^{-1} . The author was able to separate molecular relaxation processes from the corresponding intramolecular ones in several molecules. The intramolecular process was suggested to be due to the rotation of the whole ester group around the C-C bond.

Very recently Kashem (40) studied dielectric relaxation behaviour of a number of aliphatic and aromatic acid esters in different media, namely polystyrene, Santovac, (polyphenyl ether supplied by the Monsanto Company, St. Louis, U.S.A.), and glassy orthoterphenyl where considerably lower values of ΔH_E ($20-25 \text{ kJ mol}^{-1}$) were obtained as compared to those obtained by Khwaja for intramolecular processes.

In view of the points mentioned in the above survey it seemed worthy to extend the present study on carboxylic acids to some typical ester molecules.

EXPERIMENTAL RESULTS

In the present study the relaxation properities of the following compounds were investigated:

- VI.1 Formic acid
- VI.2 Acetic acid
- VI.3 Propionic acid
- VI.4 Butyric acid
- VI.5 Valeric acid
- VI.6 Trichloroacetic acid
- VI.7 Benzoic acid
- VI.8 p-Ethylbenzoic acid
- VI.9 4-Biphenylcarboxylic acid
- VI.10 2-Naphthoic acid
- VI.11 Salicylic acid
- VI.12 Methylsalicylate
- VI.13 Phenylsalicylate
- VI.14 Methylchloroformate
- VI.15 Ethylchloroformate
- VI.16 n-Butylchloroformate
- VI.17 iso-Butylchloroformate

Most of these compounds were studied in poly-

styrene matrices; 4-biphenylcarboxylic acid, 2-naphthoic acid and salicylic acid were studied as compressed solid discs while the methyl- and phenyl esters of salicylic acid were examined both in polystyrene matrices and as compressed solid discs.

Besides the acids and the esters listed above the following H bonding systems were also studied in polystyrene matrices.

- VI.18 Formic acid + Pyridine
- VI.19 Formic acid + 1,4-Dioxane
- VI.20 Formic acid + Methyl cyanide
- VI.21 Acetic acid + Pyridine
- VI.22 Acetic acid + 1,4-Dioxane
- VI.23 Acetic acid + Methyl cyanide
- VI.24 Benzoic acid + Pyridine
- VI.25 Benzoic acid + 1,4-Dioxane
- VI.26 Benzoic acid + Methyl cyanide

Results of Fuoss-Kirkwood analyses, the ϵ_{∞} values and the experimental dipole moments for the acids, the esters and the H bonding systems have been given in

separate tables viz. Tables VI.2, VI.3 and VI.4, respectively. Results of corresponding Eyring analyses are presented in Tables VI.5, VI.6 and VI.7, respectively. Results of salicylic acid have been tabulated with those of esters for comparison, due to its structural similarity with its esters, viz. methylsalicylate and phenylsalicylate. The relaxation times and the free energies of activation are given at 100 K, 200 K and 300 K since some of the molecular systems showed two separate families of absorption peaks around these temperatures. Several sample plots of dielectric loss versus $\log_{10} \nu$ are given in Figures VI.1 - VI.4. Figures VI.5 - VI.7 represent plots of $\log \tau$ versus $1/T$ for several compounds.

DISCUSSION

Acid Molecules

Results of Table VI.2 and VI.5 show that each of the acid molecules VI. 1-10 gave one common set of absorption peaks at a moderately high temperature region somewhere in between 190 K to 260 K, the absorption data yielding ΔH_E -values fairly close and ΔG_E -values approximately similar to one another. For convenience, this common absorption

process will be referred to as process A (say) in subsequent discussion.

The larger acid molecules, VI.4-8, studied in polystyrene matrices showed another set of absorption peaks at much lower temperature regions (in between ≈ 80 K to 190 K) in addition to the common one corresponding to the process A. p-Ethylbenzoic acid provided an exception which gave no such additional absorption. For these absorptions corresponding to a process B (say), the absorption region was shifted toward higher temperature and the observed ΔH_E -value appeared to increase roughly with the increasing size of the acid molecules. None of the smaller acid molecules (VI.1-3) showed any low temperature absorption except for propionic acid the tail end of an absorption was only detected around liquid nitrogen temperature.

Of the two separate families of absorption processes, process A observed for all the acid molecules (except salicylic acid) under investigation presented an interesting situation in that the process in different molecules was characterized by some common features which are as follows:

- i) the absorption regions for different molecules were fairly close to one another and lay between 190 K to 260 K;
- ii) the absorption process in different molecules yielded fairly close ΔH_E -values (37 - 57 kJ mol⁻¹) and approximately similar ΔG_E values (~ 34 - ~ 43 kJ mol⁻¹ at 200 K), while the ΔS_E -values for all the molecules were positive (5.0 - 90.0 J K⁻¹ mol⁻¹); and
- iii) the observed relaxation times (τ) for the processes in different molecules were also of fairly similar order of magnitude.

The only exception to the above findings was 4-biphenylcarboxylic acid which was studied as a compressed solid disc. Although the molecule absorbed in the temperature range of 176 K - 201 K the observed ΔH_E (26 kJ mol⁻¹) was considerably lower while ΔS_E (-24.0 J K⁻¹ mol⁻¹) was negative; the ΔG_E (30.7 kJ mol⁻¹ at 200 K) was also lower.

In view of the fact that the concentrations of the acid monomers are negligibly small as compared with those of corresponding dimeric species (as indicated

earlier), one could possibly think of the relaxation of the dimeric species giving rise to dielectric absorption corresponding to the process A. But the preferred structure of dimers being cyclic the resultant dipole moments would be too small to cause such an absorption. Moreover, various relaxation parameters for the process A appear to be fairly independent of the molecular size and shape, and consequently, the involvement of molecular reorientation or of the reorientation of any associated species in such an absorption process seems to be very unlikely. Evidently, this higher temperature process has to be attributed to some kind of intramolecular relaxation for which the following potential possibilities could be considered:

- a) relaxation of the whole carboxyl (-COOH) group around the adjacent C-C bond;
- b) relaxation of the OH group around C-O bond;
- c) the rate process of monomer \rightleftharpoons dimer equilibrium; and
- d) proton transfer through H bonds in the cyclic dimer involving quantum mechanical tunneling.

The first possibility viz., the carboxyl group rotation around the adjacent C-C bond could be thought to take place either in monomer molecules (if at all present in any appreciable amount) or in the dimeric species (cyclic). The observed energy barriers ($\Delta H_E = 40-55 \text{ kJ mol}^{-1}$ and $\Delta G_{E200 \text{ K}} \approx 40 \text{ kJ mol}^{-1}$) appear to be too high to be explained in terms of the carboxyl group rotation in acid monomers. There seems to be no reason to believe that the said C-C linkage in these monomer molecules has any appreciable double bond character which might induce rigidity into this bond and thus lead to such higher energy barriers to the said rotation. In cyclic dimers the carboxyl group rotation can occur only after the breakage of two H bonds involving a ΔH_E of $30-40 \text{ kJ mol}^{-1}$ (1,2,12-14). Such a process could possibly account for the observed energy barriers ($\Delta H_E \approx 40-55 \text{ kJ mol}^{-1}$) provided the COOH group relaxation involved an activation enthalpy of $10-15 \text{ kJ mol}^{-1}$. But the experimental results obtained with formic acid seem to rule out any possible involvement of the COOH group rotation around the adjacent C-C bond in the acid molecules under consideration irrespective of whether they exist as monomers or dimers. The question of such rotation in formic acid does not arise at all since there is no C-C bond adjacent to COOH group in this

molecule. Yet the molecule did absorb in the temperature region of 237 - 257 K and the observed activation parameters ($\Delta H_E = 46 \text{ kJ mol}^{-1}$ and $\Delta G_{E200 \text{ K}} = 42.2 \text{ kJ mol}^{-1}$) were very similar to the corresponding values for the process A in other acid molecules. Thus it would appear very unlikely that the carboxyl group rotation could represent the process A in question.

Assuming cyclic structure for the acid dimers the rate process of a monomer \rightleftharpoons dimer equilibrium (process C) would require the breakage of two H bonds and consequently could at best account for an activation enthalpy (ΔH_E) of $\sim 30\text{-}40 \text{ kJ mol}^{-1}$ (1,2,12-14) as opposed to the observed values of $\sim 40 - 55 \text{ kJ mol}^{-1}$ for the process A. It would thus be unreasonable to assume that the said rate process could be identified as the process A in acid molecules under consideration.

The process of proton transfer through H bonds (process D) would also involve the rupture of two H bonds in a cyclic acid dimer and consequently involve the similar amount of activation enthalpy ($30\text{-}40 \text{ kJ mol}^{-1}$) as that in process C. Should the proton tunneling be involved in such a process, the energy barrier would further

be significantly lowered. The experimental ΔH_E values for the process A in different acid molecules were rather higher than what would be required for the breakage of two H bonds in cyclic dimers. It would thus be highly improbable that the proton jumping process (involving proton tunneling) could result in the dielectric absorptions corresponding to the process A. Furthermore, involvement of such a process appears to be very unlikely in view of the following evidence:

a) none of the $\ln \tau T$ vs $\frac{1}{T}$ plots represented by Figure VI is, by any means, bent towards or parallel to the $\frac{1}{T}$ axis. As was mentioned in the previous chapter, such a plot should be curved at a lower temperature if proton tunneling is involved; and at very low temperatures, if the tunneling rate is large enough, the plot should become parallel to the $\frac{1}{T}$ axis indicating temperature-independence of the rate constant (41).

b) the frequency for a tunneling mechanism is very much dependent and consequently the relaxation times for deuterated and undeuterated acids differ greatly if proton jumping is involved in the process. Dicarlo and

Zurback (20), in their dielectric absorption study, observed the same relaxation time for deuterated and undeuterated acetic acid in benzene solution, and consequently, ruled out the possibility of proton-jumping as an intramolecular process.

The OH group rotation around the C-O bond in cyclic acid dimers could be a potential candidate for the higher temperature process (A). Such a rotational process in alcohols and phenols involving an activation enthalpy of $10-15 \text{ kJ mol}^{-1}$ is now well established (discussed in Chapter V). The present investigation with salicylic acid and its methyl and phenyl esters provided some interesting results (to be discussed later in this chapter) which would extend unequivocal support to the concept of OH group rotation in carboxylic acids. Such a relaxation process involving $\Delta H_E \sim 10-15 \text{ kJ mol}^{-1}$ only cannot, however, adequately explain the absorption process A yielding ΔH_E values of $\sim 40-55 \text{ kJ mol}^{-1}$. But considering the fact that the OH group relaxation in cyclic acid dimers would also be preceded by the breakage of two H bonds involving $\Delta H_E = \approx 30-40 \text{ kJ mol}^{-1}$ (1,2,12-14), one could reasonably account for the observed ΔH_E values ($40-55 \text{ kJ mol}^{-1}$) for the said process A. The occurrence of OH group relaxation seems to be equally likely

in all the acid molecules under consideration including formicaacid and the process in conjugation with the H bond breakage might be expected to yield energy barriers (ΔH_E or ΔG_E) of very similar orders of magnitude for various acid molecules. Thus, the suggestion of the OH group relaxation preceded by H bond breakage appears to be most plausible in view of the observed activation parameters, dominant dimer concentrations and cyclic structure of the dimers for different acid molecules under the present investigation.

Assuming the above suggestion to be valid, the observed energy barrier for the process A should be dependent upon (i) the energy of the H bonds in cyclic dimers and (ii) the extent of double bond character in the C-O linkage. These quantities are in turn affected by the acidity of the carboxyl proton, mesomeric effect of the C=O bond and the inductive effect of the R (R=H, alkyl or aryl) group adjacent to the carboxyl carbon. It is extremely difficult to estimate and sum up the effects of these factors in individual molecules. The small differences in the observed values of ΔH_E and ΔG_E corresponding to the process A in different acid molecules could, however, reasonably be attributed to these factors.

Each of the three acids, namely, biphenylcarboxylic acid, 2-naphthoic and salicylic acid, was found to give only one set of absorption peaks while studied as compressed solid disks. These absorptions must correspond to some intramolecular process since in the crystalline solidstate the possibility of molecular relaxation is negligibly poor. In the case of 2-naphthoic acid the absorption region (212-244 K), the ΔH_E (49 kJ mol⁻¹) and $\Delta G_{E200 K}$ (38.3 kJ mol⁻¹) are all comparable to the corresponding values (process A) for other acid molecules studied in polystyrene matrices. These experimental parameters could thus be reasonably explained in terms of OH group relaxation compounded by the breakage of two H bonds in a cyclic dimer. For biphenylcarboxylic acid the observed energy barrier ($\Delta H_E = 26$ kJ mol⁻¹ or $\Delta G_{E200 K} = 30.7$ kJ mol⁻¹) was, however, considerably smaller as compared to the corresponding values ($\Delta H_E = \sim 40-55$ kJ mol⁻¹ and $\Delta G_{E200 K} \approx 40$ kJ mol⁻¹) for the process A commonly observed with other acid molecules. For example, the process in benzoic acid and p-ethylbenzoic acid yielded ΔH_E values of 43 kJ mol⁻¹ and 41 kJ mol⁻¹, respectively as compared to the value of 26 kJ mol⁻¹ for biphenylcarboxylic acid. The relaxation time ($\tau_{200 K} = 2.5 \times 10^{-5}$ s) was also shorter by approximately

two orders of magnitude than that ($\tau_{200\text{ K}} = 3.3 \times 10^{-3}$ s) for the process A in benzoic acid. It would seem very unlikely that the conjugation effect of the phenyl group at the para position could affect the energy barrier (ΔH_E or ΔG_E) and relaxation time (τ) to such an extent, and there appears to be no other suitable explanation for such significant effects. One possibility could be that the acid dimer might be open chain rather than cyclic in the crystalline solid state and consequently only one H bond has to be broken before the OH group could relax.

Salicylic acid is significantly different from other acid molecules under consideration in that a chelated ring is formed in this molecule through intramolecular H bonding. The relaxation behaviour of this molecule will be discussed in the following section along with the results obtained with its methyl and phenyl esters for the sake of comparison and convenience.

Now, the other family of absorption peaks corresponding to the process B in larger acid molecules needs be considered. For this process observed at low temperature regions potential possibilities could be:

- a) the reorientation of the acid monomers;
- b) the intramolecular process due to the OH or COOH group relaxation;
- c) segmental motion around all the C-C bonds of the acid molecules which may be observed if the main COOH dipole accompanies such an intra molecular motion.

Each of these processes would require the monomeric species to be present in appreciable amounts in the systems under investigation. On the contrary, it has been pointed out earlier that the relative concentrations of the acid monomers in equilibrium with respective dimeric species are very small. One should, however, keep in mind that the process A (discussed earlier in this section) would lead to the formation of monomeric species since it involves the breakage of both the H bonds of the cyclic dimers. The process essentially includes continuous breakage and reformation of the cyclic dimers as a result of which the acid monomers might have finite life times in the dielectric field and undergo molecular and/or intramolecular relaxation. For convenient discussion of these processes approximate maximum lengths of various acid molecules and some rigid molecules (from Courtauld molecular models) along with their respective ΔH_E values are given in Table VI.

TABLE VI-1: Approximate lengths and ΔH_E values for several acids and rigid molecules.

Molecule	Maximum Length (Å)	ΔH_E (kJ mol ⁻¹)
Butyric acid	7.9	9 (Process B)
Valeric acid	9.5	10 "
Trichloroacetic acid	7.2	16 "
Benzoic acid	9.0	19 "
p-Ethylbenzoic acid	11.2	41 (Process A)
Fluorobenzene *	7.5	9 (Molecular Process)
Iodobenzene *	9.0	19 "
p-Ethylbromobenzene *	10.7	38 "

References 39 and 42

The process B in benzoic acid yielded a ΔH_E of 19 kJ mol⁻¹, a $\Delta G_{E200 K}$ of ~28 kJ mol and $\tau_{200 K} = 6.1 \times 10^{-6}$ s. These values are fairly comparable to the corresponding values of 19 kJ mol⁻¹, ~24 kJ mol⁻¹ and 3.6×10^{-7} s for the rigid molecule iodobenzene (42) which is of similar size to the benzoic acid molecule. In a similar experiment the former molecule absorbed in the temperature region of 134 K - 161 K while the latter (benzoic acid) absorbed in the range of

147 K - 190 K due to the process B. These results appear to suggest that the process in benzoic acid might be due to the rotation of monomer molecules. There is no possibility of any segmental motion (c) in this molecule. Only possible rotation around C-C bond could be due to the relaxation of -COOH group. The OH group rotation around the C-O bond would be another possibility, but in view of the total absence of the process B in p-ethylbenzoic acid such possibilities would seem to be most unlikely. If the process B were at all the COOH or OH group rotation, there is no reason why such a process would not occur in p-ethylbenzoic acid. On the other hand, the absence of any low temperature absorption process in this molecule could reasonably be explained in terms of overlap of the absorption due to the monomer relaxation with that corresponding to the process A which was observed in the range of 214 K - 245 K. This process in p-ethylbenzoic acid yielded a ΔH_E of 41 kJ mol⁻¹, a $\Delta G_{E200 K}$ of ~38 kJ and $\tau_{200 K} = 9.4 \times 10^{-4}$ s. A little smaller rigid molecule, p-bromoethylbenzene (39) was found to absorb in a similar temperature region (206 K - 254 K) and yielded $\Delta H_E = 38$ kJ mol⁻¹, $\Delta G_{E200 K} = 36$ kJ mol⁻¹ and $\tau_{200 K} = 6.9 \times 10^{-4}$ s. In view of close similarity between the two sets of values, it would be very reasonable to assume that the process B in p-ethylbenzoic acid due to monomer

relaxation would overlap with the process A in the said absorption region.

The possibility of the OH or COOH group rotation as a candidate for the process B in the acid molecules under consideration can further be ruled out with two experimental evidences. Firstly, the low temperature process (B) was totally absent in smaller acid molecules which cannot be explained if the process B were assumed to be COOH/OH group rotation. Secondly, the absorption region and the activation parameters for the process B in different acid molecules were considerably different which should not have been the case if the process were due to the OH or COOH group rotation.

In trichloroacetic acid no segmental motion of the type c is possible and thus the process B has to be identified with the relaxation of the monomeric acid molecule. The observed $\Delta H_E = 16 \text{ kJ mol}^{-1}$ for the molecule was, however, significantly larger than the value ($\Delta H_E = 9 \text{ kJ mol}^{-1}$) reported for fluorobenzene (39) although the two molecules are of approximately similar length (Table VI-1). The reason for this does not seem to be clear; the effect of intermolecular interaction viz., H bonding could possibly be a reasonable suggestion.

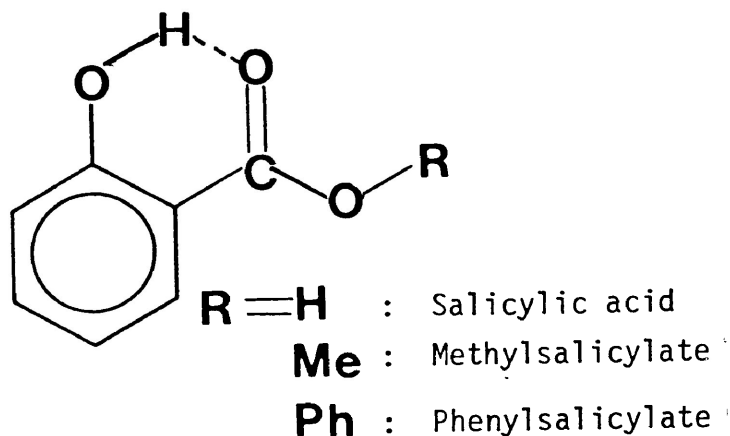
For butyric and valeric acids one possibility for the observed process (B) would be reorientation of the respective monomer molecules. But the observed $\Delta H_E = 10 \text{ kJ mol}^{-1}$ for valeric acid does not seem to correspond to its maximum length (9.5 \AA). The rigid molecule iodobenzene (42) having approximate length of 9.0 \AA yielded a ΔH_E of 19 kJ mol^{-1} for its molecular rotation. However, the latter molecule being more bulky would have a larger rotational volume which might be partly responsible for larger enthalpy barrier.

An alternative and very potential candidate for the process B in these two molecules could be segmental motion around C-C bonds in the long chain. In a similar experiment with a number of long chain aldehyde molecules such as process has been observed (43) in the temperature region around 100 K. The process in butanal and pentanal yielded the same ΔH_E (14 kJ mol^{-1}), and $\Delta G_{E200 \text{ K}}$ (14 kJ mol^{-1}). For butyric and valeric acids the corresponding values were $\sim 10 \text{ kJ mol}^{-1}$ and $\sim 15 \text{ kJ mol}^{-1}$. The observed relaxation times (τ) at 100 K for these acid and aldehyde molecules are also of very similar ($1.0 \times 10^{-5} \text{ s} - 3.6 \times 10^{-5} \text{ s}$). In view of these results it would not be unreasonable to suggest that the said segmental motion could represent the process B in the two acid molecules in question. A likely situation could, however, be such that both the processes do overlap

in the same absorption region.

Salicylic Acid and Ester Molecules

Salicylic acid and its methyl and phenyl esters are characterized by chelated ring systems formed by intramolecular H bonding as shown below:



Study of the relaxation properties of these molecules was of special interest in that it was expected to confirm whether or not the OH group relaxation could occur in carboxylic acid molecules discussed in the previous section.

While studied as compressed solid disks each of these molecules showed one set of absorption peaks which should correspond to some intramolecular process since molecular

relaxation in the crystalline solid state is most unlikely. The potential candidates for such intramolecular process could be either (a) the reorientation of the OR group around C-O bond, or (b) rotation of the whole COOR group around C-C bond. Infrared spectroscopy study of these molecules (Chapter III) indicated that the intramolecular H bonds forming the chelated ring is fairly strong. This bond had to be broken before the COOR group could relax and consequently the process (b) would involve an energy barrier much higher than what would be encountered for the carboxyl/ester group rotation only. The energy barrier for the process (a) should, on the other hand, be of similar order of magnitude to those observed for OH/OMe group relaxation in the previous chapter.

Salicylic acid absorbed in the temperature region of 113 K-146 K and yielded $\Delta H_E = 14 \text{ kJ mol}^{-1}$, $\Delta G_{E100 \text{ K}} \sim 19 \text{ kJ mol}^{-1}$ and $\tau_{100 \text{ K}} = 6.4 \times 10^{-3} \text{ s}$. These values are fairly comparable to the corresponding values for OH group relaxation in hydroxyl compounds (see Table V). For example, 4-phenylphenol in the compressed solid state absorbed (90 K-120K) due to the OH group relaxation yielding $\Delta H_E = 13 \text{ kJ mol}^{-1}$, $\Delta G_{E200 \text{ K}} \sim 16 \text{ kJ mol}^{-1}$ and $\tau_{100 \text{ K}} = 1.3 \times 10^{-4} \text{ s}$. These results would seem to be very consistent with .

the suggestion that the dielectric absorption for salicylic acid could be due to the OH group rotation around C-O bond. The absorption region (170 K-205 K), the activation parameters ($\Delta H_E = 21 \text{ kJ mol}^{-1}$ and $\Delta G_{E200 \text{ K}} \sim 31 \text{ kJ mol}^{-1}$) and the relaxation time ($2.5 \times 10^{-5} \text{ s}$) obtained with methylsalicylate were all approximately of the right order of magnitude as compared to the corresponding values for salicylic acid and consequently the absorption process in question could most likely be due to the OMe group relaxation. The observed ΔH_E and ΔG_E values, however, appear to be considerably higher than the reported values ($\Delta H_E = 10-16 \text{ kJ mol}^{-1}$ and $\Delta G_{E200 \text{ K}} = 16-21 \text{ kJ mol}^{-1}$) for the OMe group relaxation in several methoxy compounds (44) studied in the polystyrene matrices. The enhanced energy barrier could possibly be attributed at least partly to the mesomeric effect of the adjacent C=O bond and the conjugation effect of the benzene ring which might induce partial double bond character to the C-O linkage. Crystal packing in the compressed solid could be another reason which might cause some hindrance to the OMe group rotation, and thereby the associated energy barrier might be enhanced. For the whole ester group (COOMe) rotation in methylbenzoate Khwaja (39) obtained a ΔH_E of $\sim 31 \text{ kJ mol}^{-1}$ in a similar study

of the molecule in a polystyrene matrix. Such an intramolecular process in methylsalicylate would involve a ΔH_E considerably higher than 31 kJ mol^{-1} since some extra energy would be required for breaking the intramolecular H bond. The absorption process in question would thus appear to be most unlikely owing to the ester group rotation. Similar arguments could also be put forward in opposition to the possibility of COOH group relaxation in salicylic acid. For the aldehyde (-CHO) group rotation in some aromatic aldehyde molecules studied in different polymer matrices ΔH_E values around 30 kJ mol^{-1} have been reported (45) and therefore the COOH group rotation would involve a ΔH_E not smaller than 30 kJ mol^{-1} . The process in salicylic acid would further be preceded by the breakage of the intramolecular H bond and consequently the associated ΔH_E would by far be greater than 30 kJ mol^{-1} as opposed to the value of 14 kJ mol^{-1} only obtained by the present study. In ref. 45 no intramolecular process was observed in salicylaldehyde. All these evidences would appear to suggest that the COOH group relaxation would be highly unlikely candidate for the intramolecular process in salicylic acid which caused the observed dielectric absorption.

Phenylsalicylate, while studied in the compressed

solid absorbed in the region of 152 K - 211 K, and yielded a ΔH_E of 20 kJ mol⁻¹ and $\Delta G_{E200 K} \sim 30$ kJ mol⁻¹. In view of the above discussion on salicylic acid and its methyl ester the most likely candidate for the said absorption would appear to be the phenoxy (OPh) group rotation. The observed ΔH_E and ΔG_E values might appear to be a little smaller for the OPh group rotation when compared to the corresponding values ($\Delta H_E = 21$ kJ mol⁻¹ and $\Delta G_{E200 K} \sim 31$ kJ mol⁻¹) for OMe group rotation. These values are, however, in fair agreement with those ($\Delta H_E = 17 \pm 2$ kJ mol⁻¹ and $\Delta G_{E200 K} \approx 34$ kJ mol⁻¹) for phenoxy group relaxation in biphenyl phenyl ether which was studied in a polystyrene matrix by Desando and Walker (46). The authors obtained for the latter molecule a fairly high negative ΔS_E (-87 JJK⁻¹ mol⁻¹) and high β values (0.27-0.38). These values are quite comparable to the corresponding values ($\Delta S_E \approx -50$ J K⁻¹ mol⁻¹ and $\beta = 0.36 - 0.52$) obtained with phenylsalicylate in the compressed solid state. The results appear to be very much consistent with the suggestion that the phenoxy group rotation in the latter molecule caused the dielectric absorption in question.

When studied in polystyrene matrices both methylsalicylate and phenylsalicylate showed only one set

of absorption peaks for which the activation parameters and β values were significantly different from those for corresponding intramolecular processes in the respective molecules; the observed ΔH_E and ΔG_E values were larger, ΔS_E values were positive and the β value considerably smaller. Furthermore, these parameters for the two ester molecules were by no means of similar magnitude. In view of these results it would appear most unlikely that any intramolecular process might be involved in the said dielectric absorption. Molecular relaxation should thus be considered as the most likely candidate for the same.

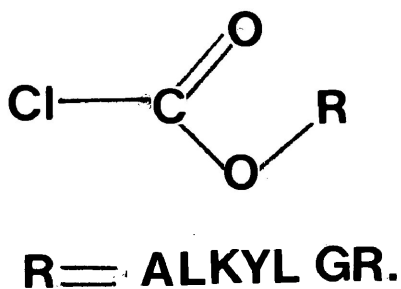
Methylsalicylate in a polystyrene matrix yielded a ΔH_E of 39 kJ mol⁻¹, $\Delta G_{E200 K} = 32 \text{ kJ mol}^{-1}$ and $\Delta S_E = 35 \text{ J K}^{-1} \text{ mol}^{-1}$. These values are very similar to the corresponding values ($\Delta H_E = 42.5 \text{ kJ mol}^{-1}$, $\Delta G_{E200 K} = 36 \text{ kJ mol}^{-1}$ and $\Delta S_E = 35 \pm 5 \text{ J K}^{-1} \text{ mol}^{-1}$) for a little larger rigid molecule 2-bromonaphthalene (47). Similarly, the observed $\Delta H_E = 58 \text{ kJ mol}^{-1}$ and $\Delta G_{E200 K} = 45 \text{ kJ mol}^{-1}$ and $\tau_{200 K} = 1.3 \times 10^{-1} \text{ s}$ for phenylsalicylate are in excellent agreement with the corresponding values ($\Delta H_E = 58 \text{ kJ mol}^{-1}$, $\Delta G_{E200 K} = 47 \text{ kJ mol}^{-1}$ and $\tau_{200 K} = 3.7 \times 10^{-1} \text{ s}$) obtained with the similarly-sized rigid molecule, o-hydroxy benzophenone (46). These results seem to bear out that molecular

relaxation should be responsible for the observed absorption in both the ester molecules.

The reason for the absence of any intramolecular process in these ester molecules is not clearly understood. One possibility could be the overlap of such a process (due to OR group rotation) with the observed one due to molecular relaxation. The absorption region (170 K - 205 K) for OMe group rotation in compressed solid methylsalicylate was very similar to that (178 K - 213 K) in which the molecule in a polystyrene matrix absorbed due to the proposed molecular relaxation. Therefore, it would appear very likely that both the processes could overlap in the latter experiment with polystyrene disks. The absorption region for phenylsalicylate in the compressed solid (152 K - 273 K) were but considerably separated such that the possibility of such overlap might appear unlikely. However, considering the absorption region (263 K - 301 K) for 4-biphenyl phenyl ether (46) in the polystyrene matrix (due to OPh group rotation) the possibility of overlap of intramolecular and molecular processes in phenylsalicylate cannot be totally ruled out when the molecule is studied in the polystyrene matrix.

Results obtained with different alkyl esters of

chloroformic acid were of particular importance in that they might be expected to provide an effective answer to the question as to whether the intramolecular process observed in acids and esters could be due to the proposed OR (R=H or alkyl group) group rotation around the adjacent C-O bonds as shown below:



Alkylchloroformate

In each case of the chloroformates only one set of absorption peaks was observed for which either or both of the following two processes could be held responsible:

- i) the reorientation of the whole ester molecule in which case the activation parameters would vary with molecular size;
- ii) rotation of the alkoxy (OR) group around the adjacent C-O bond.

The possibility of the ester group (COOR) rotation does not arise in the molecules under consideration since the adjacent

C-Cl bond is a part of the rigid portion of such a molecule.

Of the two possibilities, the first one, viz., the molecular process would appear to be less likely in view of the fact that the observed activation parameters (ΔH_E , ΔG_E and ΔS_E) for different ester molecules were approximately of similar magnitudes. Furthermore, the smallest ester molecule, methylchloroformate, would seem to be too small to show any absorption due to its rotation even in the lowest temperature region (around 85 K) of the present study. The maximum length of this molecule (from Courtauld molecular model) is only 6.6 Å as compared to that of the rigid molecule chlorobenzene (8.2 Å) which was found (42) to absorb in the range of 81 K - 111 K yielding a ΔH_E of 11 kJ mol⁻¹. It would thus appear almost impossible that the molecular relaxation of methylchloroformate could show up in the observed absorption region (127 K - 148 K). Moreover, the observed ΔH_E (23 kJ mol⁻¹) and ΔG_E (26 kJ mol⁻¹) would be exceedingly large for such a small molecule and, by no means, could they be associated with the molecular reorientation. As such, the said absorption has to be associated to some intramolecular process and obviously, the OMe group rotation could be the most likely one.

The intramolecular process in methylsalicylate (compressed solid) yielding $\Delta H_E = 21 \text{ kJ mol}^{-1}$ and $\Delta G_E = 26 \text{ kJ mol}^{-1}$ at 100 K has been explained in terms of OMe group rotation. The corresponding quantities ($\Delta H_E = 23 \text{ kJ mol}^{-1}$ and $\Delta G_{E100 \text{ K}} \approx 26 \text{ kJ mol}^{-1}$) for methylchloroformate would thus strongly suggest the involvement of the same process. The ΔH_E and $\Delta G_{E100 \text{ K}}$ values for the latter molecule, like those of the former, are significantly larger than the corresponding values ($\Delta H_E = 10-16 \text{ kJ mol}^{-1}$, $\Delta G_{E100 \text{ K}} = 16-21 \text{ kJ mol}^{-1}$) or methoxy group relaxation reported in reference 44. However, taking into consideration the mesomeric effect of the C=O bond and the inductive effect of the Cl atom, the larger energy barrier ($\Delta H_E/\Delta G_E$) for the process in methylchloroformate would appear to be fairly acceptable. For this molecule Kashem (40) obtained a ΔH_E of $\sim 24 \text{ kJ mol}^{-1}$ and $\Delta G_{E100 \text{ K}} \sim 24 \text{ kJ mol}^{-1}$ in a more viscous medium santovac. These values are in excellent agreement with those obtained by the present study.

In other ester molecules, namely, ethyl-n-butyl and isobutylchloroformates, the absorption processes could most possibly be due to the respective OR group rotations since the observed activation parameters (ΔH_E ,

ΔG_E & ΔS_E) for different molecules are of similar magnitudes irrespective of their size. However, the possibility of molecular relaxation in these cases should not be ruled out. Although none of these molecules showed any additional absorption, there appears to be no reason why the relaxation of these molecules would not show up in the temperature span covered by the present investigation. A possible explanation could be such that the molecular process might overlap with the intramolecular one (OR group rotation). In fact, Kashem (40) was able to separate the two processes in isobutylchloroformate by studying the molecule in santovac. The lower temperature process (130 K - 155 K) yielding a ΔH_E of 19 kJ mol^{-1} appear to represent the OR group rotation while the higher temperature process (184 K - 218 K) presumably due to the molecular reorientation yielded a ΔH_E of $\sim 38 \text{ kJ mol}^{-1}$. The single absorption process (143 K - 184 K) of the molecule in the present study (in a polystyrene matrix) yielded a ΔH_E of 25 kJ mol^{-1} . These results would tend to suggest that the molecular and the intramolecular processes for iso-butyl chloroformate in the polystyrene matrix might overlap in the said absorption region. Santovac being more viscous than polystyrene hindered the molecular relaxation significantly leaving the OR group relaxation almost unaffected and consequently the effective separation of the two processes was possible. In ethyl-

and n-butylchloroformates also similar overlap of molecular and intramolecular processes would seem to be fairly likely although their separation was not achieved in either of the media.

H Bonding Acid-Base Systems

Results of dielectric relaxation studies on several acid-base mixtures (Systems VI.18-VI.24, p.196) in polystyrene matrices are presented in Tables VI-4 and VI-7. These results clearly show that each of the H bonding systems exhibited at least one absorption peak while some of them absorbed in two different temperature regions. Due to the complex molecular compositions of the systems proper assignment of their absorption peaks is likely to be difficult. Before discussing any individual system it would to take a careful note of the following outlines:

(i) Of the three acid molecules, formic and acetic acids are too small to give rise to any dielectric absorption in the frequency and temperature ranges of the present study. With pure acids in polystyrene matrices no absorption peak corresponding to molecular relaxation was observed. The absorption due to molecular reorientation of benzoic acid has been well characterized (Table VI-2 and VI-4).

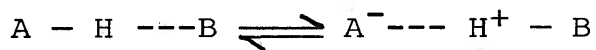
(ii) Each of the three acids was found to exhibit a common absorption due to a common process identified as the

O-H group relaxation preceded by H bond-breakage in cyclic dimers (referred to as process A in the earlier discussion). The same process is likely to show up in the acid-base mixture provided the cyclic acid dimer remains in the system at appreciable concentration.

(iii) Of the three organic base molecules, viz. pyridine, 1,4-dioxane and methylcyanide, pyridine is the biggest; this molecule in a polystyrene matrix was found (28) to absorb due to its molecular reorientation at temperatures around 84-88 K ($\Delta H_E = 3 \text{ kJ mol}^{-1}$) in a similar study in this laboratory. Obviously, there is no way the base molecules can cause only absorption in the mixed acid-base systems under consideration.

(iv) The formation of the acid-base complex is the most likely outcome of dispersing the acid and base molecules simultaneously in polystyrene matrices. There are overwhelming evidence in the literature (26,29,30, 48-50) supporting the formation of strongly H bonded complexes of carboxylic acids with organic bases. These complexes behave as rigid structures and are found to cause dielectric absorption in the solid state as well as in benzene solution (29,30). In polystyrene matrices these complexes will be most likely candidates to absorb due to their dipolar reorientation.

(v) Proton jumping processes in the equilibrium between the H bonded and ionic forms



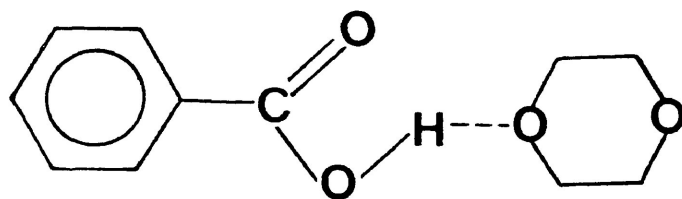
could also be considered as a potential possibility. But experimental evidence (28-30,48) has supported the formation of strongly H bonded complexes (A-H---B) simple carboxylic acid with pyridine (the strongest base among the three) rather than ionic or ion-pair species. Dielectric studies (29,30) of these complexes provided no evidence of proton jumping. Such a process thus appears to be highly unlikely to give rise to dielectric absorption in the H bonding systems of our interest.

Results of dielectric absorption studies on systems, (a) benzoic acid-pyridine and (b) benzoic acid - 1,4-dioxane, were very simple for interpretation. In both cases two absorption peaks were observed, the temperature regions of two absorptions in the same system being widely separated. The low temperature absorptions in both systems (a) and (b) were very similar to the one observed with (c) benzoic acid in polystyrene disc. The absorption regions, 148-183 K (a), 163-193 K (b), and 147-190 K (c), were almost similar; ΔH_E -values (17 kJ mol⁻¹, 23 kJ mol⁻¹ and 19 kJ mol⁻¹, respectively) were very close to one another and the ΔS_E values (-60 J K⁻¹ mol⁻¹, 31 J K⁻¹ mol⁻¹ and -45 J K⁻¹ mol⁻¹ respectively)

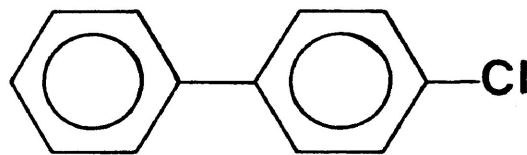
were all negative and fairly comparable. At 200 K the ΔG_E values (29.2 kJ mol^{-1} , 29.0 kJ mol^{-1} and 28.4 kJ mol^{-1} , respectively) were almost the same and the relaxation times, τ , ($10 \times 10^{-6} \text{ s}$, $8.9 \times 10^{-6} \text{ s}$ and $6.1 \times 10^{-6} \text{ s}$ respectively for systems (a), (b) and (c)) were of the same order of magnitude. All these results very definitely suggest that the low temperature absorptions in these three systems are due to the same process which has been suggested to be the molecular reorientation of the benzoic acid molecule.

The high temperature absorptions for systems (a) and (b) yielded ΔH_E of 114 kJ mol^{-1} and 77 kJ mol^{-1} respectively as compared to 43 kJ mol^{-1} for system (c). Absorption regions, relaxation times and Eyring activation parameters are all widely different for three systems. The process involved in the high temperature absorption in systems (a) and (b), could not, therefore, be identified as the process A (discussed earlier) in the system (c). The most likely process responsible for the absorption in question could be the relaxation of the H bonded complex. Should this be true, various relaxation parameters for the H bonded complex would be comparable to those observed with a similarly-sized rigid molecule. The H bonded complex, $A - H \cdots B$ of benzoic acid and 1,4-dioxane is fairly comparable in size with the rigid molecule p-chlorobiphenyl. The latter molecule, while studied in a polystyrene disk (39) absorbed in the temperature

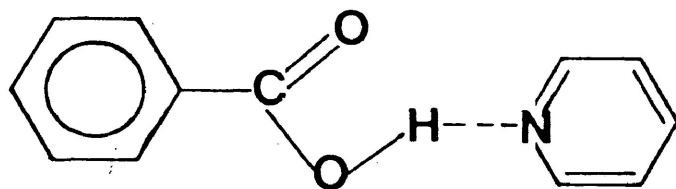
region of 283-305 K yielding a ΔH_E of 76 kJ mol^{-1} , $\Delta G_{E300 \text{ K}}$ of 48 kJ mol^{-1} and ΔS_E of $93 \text{ J K}^{-1} \text{ mol}^{-1}$. The corresponding values obtained for the high temperature (290 - 317 K) absorption in system (b) were respectively 77 kJ mol^{-1} , $\sim 55 \text{ kJ mol}^{-1}$ and $74 \text{ J K}^{-1} \text{ mol}^{-1}$. Similarly the size of the benzoic acid-pyridine complex appears to be comparable to that of the rigid molecule p-iodobiphenyl.



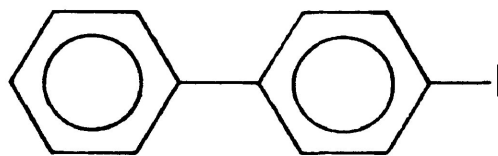
Benzoic acid-Dioxane complex



p-Chlorobiphenyl



Benzoic acid-Pyridine complex



p-Iodobiphenyl

The latter molecule, in a similar study was found (39) to absorb in the temperature region of 313-331 K yielding ΔH_E of 102 kJ mol^{-1} as compared with 114 kJ mol^{-1} obtained for high temperature (308-327 K) absorption of system 'a'.

Close similarities of these experimental results would thus strongly suggest that the high temperature absorptions in systems (a) and (b) could be due to the dipolar re-orientation of the respective acid-base complexes.

Results obtained with the systems of formic acid-base and acetic acid-base were apparently puzzling in the sense that while some systems showed only one absorption each, others exhibited two sets of absorption peaks. For latter systems, viz. formic acid-pyridine, formic acid-1,4-dioxane and acetic acid-1,4-dioxane, the low temperature absorptions (due to process I, say) occurred in the temperature range of 185-230 K while the high temperature process (II, say) gave absorptions in the temperature range of 240-315 K.

Following the outlines given in the beginning of this section one could figure out two possible candidates for either of the processes I and II. These are: the process A as discussed earlier and the relaxation of H-bonded complex $A - H \cdots B$. One of these two processes should be identified as process I while the other should automatically be assigned to the absorption process II. Let us arbitrarily suppose that the relaxation of H bonded complex represents the process I while the process A corresponds to process II. Should these assumptions be correct various experimental

parameters for the process II would be in good agreement with those for the process A observed with the pure acid molecules in polystyrene matrices. On the other hand such parameters for the process I supposedly due to the relaxation of the complex species should be comparable to those obtained with similarly-sized rigid molecules since the H bonded complexes are believed to behave as rigid structures (29,30). The desired comparisons are provided in Tables VI-8 and VI-9

Comparative results in Table VI-8 would strongly support the arbitrary suggestion that the dipolar reorientation of the H bonded complexes should be identified as the process I. The agreement of the results in Table VI-9, however, appear to be relatively poor. In general, the process II in acid-base systems yielded $\Delta G_{E200 K}$ and ΔH_E values significantly higher and $\tau_{200 K}$ considerably longer than the corresponding values for the process A in pure acids in polystyrene matrices. These enhancements of ΔG_{E200} and ΔH_E values and elongation of $\tau_{200 K}$ could, however, be adequately explained in terms of interactions of the O-H proton in the acids with the electron donor atoms (O/N) in the base molecules. The process A, as explained earlier, is the relaxation of the carboxylic O-H groups after severing H bonds in the cyclic acid dimers. In the presence of any base molecule in the neighbourhood, the

relaxation of the OH group is very likely to be hindered due to the interaction of the acidic proton with the lone-pair orbital of N or O of the base molecule and consequently the energy barrier will be higher and the relaxation time will be longer. Thus the arbitrary suggestion of process II being identified as the process A appears to be fairly explicable and harmonious.

The relaxation parameters and Eyring activation parameters obtained for the single absorption of formic acid-methyl cyanide system appear to be lower to those for the process I than to those for the process II. Consequently, the process involved is more likely to be the reorientation of H bonded complex (process I). The process II (or A) was apparently missing in the system as in benzoic acid-base systems. In the present case one possibility could be the overlap of the processes I and II in the same absorption region. Alternatively, absence of cyclic acid dimer at appreciable concentration could also account for the missing of the process II, although such a reasoning is open to question. In the systems, acetic acid-pyridine also the single absorption yields relaxation parameters and Eyring activation parameters very similar to those for the process I (Table VI-8) suggesting that the relaxation of the H bonded complex could be responsible for the absorption in question.

The absence of the process II in this system could be accounted for with the same arguments as in the case of formic acid-methylcyanide system.

Many more of similar H-bonding systems of interest could not be studied due to time limitations. Such investigations on a good number of systems would provide more clear information regarding the relaxation behaviour of H-bonded complexes. Nevertheless, the results of the present study were quite interesting to motivate further work in this intriguing area.

REFERENCES

1. G. Allen and E. F. Caldin; *Quart. Rev.* 1953, 7, 255.
2. G. C. Pimentel and A. L. McClellan, "The Hydrogen Bonding", W. H. Freeman and Co., San Francisco, 1960.
3. L. Ebersson, in "The Chemistry of Carboxylic Acids and Esters", S. Patai Ed., Interscience Publishers, 1969, p. 211.
4. Maier, *J. Chem. Phys.*, 1964, 61, 239; Ref. 2, p. 368.
5. P. Exco-fon and Y. Marechal, *Spectrochim Acta.*, 1972, 28A, 269.
6. L. L. Kimtys and V. O. Balevicivs, *Adv. Mol. Relax. Interact. Processes*, 1979, 15, 151.
7. P. Hemmes, K. Sherr, Al. Jarmas and E. V. Morse, *Adv. Mol. Relax. Interact. Processes*, 1978, 12, 333.
8. W. A. Sokalski, H. Romanowski and A. Jaworski, *Adv. Mol. Relax. Interact. Processes*, 1977, 11, 29.
9. P. Schuster and Th. Funk, *Chem. Phys. Lett.*, 1968, 2, 587.
10. M. Remko, *Adv. Mol. Relax. Interact Processes*, 1979, 15, 193.
11. P. Bosi, G. Zerbi and E. Clementi, *J. Chem. Phys.*, 1977, 66, 3376.
12. J. Lamb and T. M. M. Pinkerton, *Proc. Roy. Soc. (London) Ser. A*, 1949, 199, 114.
13. J. Lamb and D. H. A. Huddart, *Trans. Faraday Soc.*, 1950, 46, 540.
14. E. Freedman, *J. Chem. Phys.* 1953, 21, 1784.
15. J. E. Piercy and J. Lamb. *Trans. Faraday Soc.*, 1956, 52, 930.

16. J. E. Piercy and M. G. S. Rao, *J. Acoust. Soc. Am.* 1967, 41, 1591.
17. H. A. Pohl, M. E. Hobbs and P. M. Gross, *J. Chem. Phys.*, 1941, 9, 408.
18. E. Jakusek and L. Sobczyk, *Dielect. and Related Mol. Processes*, 1977, 3, 129.
19. E. Constant and A. Lebrun, *J. Chim. Phys.*, 1964, 61, 163.
20. E. N. Dicarolo and E. P. Zurvack, *Chem. Phys. Lett.*, 1972, 15, 563.
21. w. G. Rothschild, *J. Chem. Phys.*, 1974, 61, 342.
22. H. R. Zelsman, Y. Marechal, A. Chosson and P. Faure, *J. Mol. Struct.* 1975, 29, 35.
23. S. Hayashi and J. Umemura, *J. Chem. Phys.*, 1975, 63, 1732.
24. S. W. Ginn and J. L. Wood, *J. Chem. Phys.*, 1967, 46, 2735.
25. F. Kohler and P. Huyskens, *Adv. Mol. Relax. Processes*, 1976, 8, 125.
26. R. Lindseman and G. Zundel, *J. C. S. Faraday Trans. II*, 1977, 73, 788.
27. J. Kraft, S. Walker and M. D. Magee, *J. Phys. Chem.*, 1975, 79, 881.
28. J. P. Shukla and S. Walker. *J.C.S. Faraday Trans. I*, 1978, 74, 2045.
29. M. Davies and L. Sobczyk, *J. Chem. Soc.*, 1962, 3000.
30. S. R. Gouph and A. H. Price, *J. Phys. Chem.*, 1969, 73, 459.
31. P. L. McGreer, A. J. Curtin, G. B. Rathman and C. P. Smyth, *J. Am. Chem. Soc.*, 1952, 74, 3451.
32. J. Crossley and N. Koizumi, *J. Chem. Phys.*, 1974, 60, 4800.

33. Y. Kano, R. Minami and H. Takahashi, Bull. Chem. Soc. Japan, 1980, 53, 642.
34. A. Hasan, A. Das and A. Ghatak; Indian J. Phys., 1971, 45, 443; 1973, 47, 701.
35. B. Krishman and R. K. Upadhyay; J. Chem. Soc. A., 1970, 3144.
36. B. Krishna, B. Prakash and S. V. Mahadane, J. Phys. Chem., 1969, 73, 3697.
37. J. Bailey, S. Walker, and A. M. North, J. Mol. Structure, 1970, 6, 53.
38. A. R. Saksena, Advan. Mol. Relax. Interact. Processes, 1977, 11, 159.
39. H. A. Khwaja, M.Sc. Thesis, Lakehead University, 1977.
40. M.A. Kashem, Personal Communication, This Laboratory.
41. M. D. Harmony, Quart. Rev., 1972, 211.
42. M. A. Mazid, M.Sc. Thesis, Lakehead University, 1977.
43. H. A. Khwaja and S. Walker
44. M. A. Mazid, J. P. Shukla and S. Walker, Can. J. Chem., 1978, 56, 1800.
45. A. Lakshmi, S. Walker, N. A. Weir and J. H. Calderwood, Adv. Mol. Relax. Interact. Processes, 1978, 13, 287.
46. M. A. Desando and S. Walker, J. Chem. Phys., 1980, 73, 3467.
47. S. P. Tay, Ph.D. Thesis, Salford University,
48. S. E. Odinkov, A. A. Mashkovsky, V. P. Glazunov, Spectrochim. Acta, 1976, 32, 1355.
49. N. Muller and P. Rose, J. Phys. Chem., 1965, 69, 2564.
50. H. Fujwara, J. Phys. Chem., 1974, 78, 1662.

TABLE VI.2

Tabulated Summary of Fuoss-Kirkwood Analysis
Parameters and Effective Dipole Moments (μ)
for Carboxylic Acids

T (K)	$10^6 \tau$ (s)	$\log f_{\max}$	β	$10^3 \epsilon''_{\max}$	ϵ_{∞}	μ (D)
<u>1.85 M Formic Acid in Polystyrene Matrix</u>						
237.4	283.74	2.75	0.18	2.66	2.74	0.29
241.7	179.39	2.95	0.21	2.67	2.74	0.27
246.7	107.45	3.17	0.22	2.66	2.74	0.27
252.3	67.21	3.37	0.24	2.67	2.74	0.26
257.3	42.95	3.57	0.24	2.64	2.74	0.26
<u>1.68 M Acetic Acid in Polystyrene Matrix</u>						
239.5	265.60	2.78	0.16	2.62	2.76	0.32
242.8	184.96	2.93	0.17	2.65	2.76	0.31
247.2	114.22	3.14	0.18	2.68	2.75	0.31
252.3	71.00	3.35	0.18	2.69	2.75	0.31
257.0	46.46	3.53	0.19	2.69	2.75	0.31
<u>1.14 M Propionic Acid in Polystyrene Matrix</u>						
192.8	690.76	2.36	0.18	3.03	2.81	0.35
199.2	225.76	2.85	0.22	3.47	2.80	0.34
203.6	108.96	3.16	0.24	3.45	2.80	0.33
207.9	56.16	3.45	0.24	3.42	2.80	0.33
212.8	31.99	3.70	0.35	1.77	2.45	0.22
217.8	14.43	4.04	0.25	1.94	2.45	0.27
<u>0.96 M Butyric Acid in Polystyrene Matrix</u> <u>Low Temperature Absorption</u>						
82.1	575.51	2.44	0.16	1.29	2.70	0.18
87.4	179.58	2.95	0.17	1.35	2.71	0.18
93.2	75.13	3.33	0.20	1.40	2.71	0.17
104.6	118.75	3.93	0.22	1.41	2.71	0.18
113.5	11.60	4.14	0.21	1.33	2.71	0.18
<u>High Temperature Absorption</u>						
205.1	156.81	3.01	0.25	0.81	2.39	0.19
209.2	95.59	3.22	0.27	0.82	2.39	0.18
213.9	72.23	3.34	0.29	0.83	2.39	0.18
219.3	41.64	3.58	0.26	9.81	2.39	0.19
224.2	25.21	3.80	0.29	0.84	2.38	0.19
231.0	11.68	4.13	0.33	0.86	2.38	0.18

TABLE VI.2

continued...

T(K)	$10^6 \tau$ (s)	$\log f_{\max}$	β	$10^3 \epsilon''_{\max}$	ϵ_{∞}	μ (D)
<u>0.82 M Valeric Acid in Polystyrene Matrix</u> <u>Low Temperature Absorption</u>						
88.9	375.78	2.63	0.21	1.27	2.74	0.17
93.9	138.29	3.06	0.22	1.31	2.74	0.17
99.0	53.60	3.47	0.20	1.34	2.74	0.18
104.2	35.12	3.66	0.24	1.37	2.74	0.18
108.2	19.45	3.91	0.21	1.34	2.73	0.19
113.2	14.94	4.03	0.21	1.32	2.74	0.19
<u>High Temperature Absorption</u>						
223.9	340.27	2.67	0.10	2.41	2.71	0.54
233.8	116.23	3.14	0.15	2.33	2.73	0.44
238.5	73.66	3.33	0.18	2.36	2.74	0.41
243.3	52.04	3.49	0.20	2.38	2.73	0.39
248.0	34.25	3.67	0.22	2.40	2.73	0.38
255.0	20.91	3.88	0.24	2.44	2.73	0.37
<u>0.53 M Trichloroacetic Acid in Polystyrene Matrix</u> <u>Low Temperature Absorption</u>						
105.8	746.67	2.33	0.19	4.43	2.78	0.45
112.4	245.12	2.81	0.19	3.99	2.44	0.47
119.6	94.35	3.23	0.20	4.22	2.44	0.49
125.5	43.37	3.56	0.19	4.36	2.43	0.52
131.8	19.32	3.92	0.19	4.54	2.43	0.54
137.5	8.98	4.25	0.18	4.71	2.43	0.58
141.6	6.67	4.38	0.18	4.81	2.43	0.60
<u>High Temperature Absorption</u>						
222.2	345.07	2.66	0.31	16.68	2.47	0.95
227.4	158.09	3.00	0.31	13.63	2.46	0.96
231.6	92.45	3.24	0.35	13.76	2.47	0.92
238.0	38.08	3.62	0.44	15.64	2.48	0.88
244.1	19.52	3.91	0.44	15.64	2.49	0.89
251.8	7.73	4.31	0.41	15.68	2.48	0.94

T(K)	$10^6 \tau$ (s)	$\log f_{\max}$	β	$10^3 \epsilon''_{\max}$	ϵ_{∞}	μ (D)
<u>0.68 M Benzoic Acid in Polystyrene Matrix</u> <u>Low Temperature Absorption</u>						
147.4	532.02	2.48	0.16	1.60	2.79	0.30
153.5	221.98	2.86	0.18	1.69	2.79	0.30
159.3	159.90	3.00	0.17	1.76	2.79	0.32
164.6	105.63	3.18	0.16	1.83	2.79	0.34
175.6	38.13	3.62	0.13	1.94	2.78	0.41
183.1	17.29	3.96	0.10	2.04	2.77	0.49
190.5	111.17	4.15	0.10	0.10	2.12	0.51

<u>High Temperature Absorption</u>						
218.9	350.03	2.66	0.14	2.71	2.77	0.52
223.1	197.03	2.91	0.16	2.72	2.78	0.49
228.6	116.03	3.14	0.17	2.83	2.28	0.49
233.6	68.01	3.37	0.17	2.84	2.77	0.50
239.0	39.69	3.60	0.19	2.89	2.77	0.48
245.8	23.98	3.82	0.21	2.96	2.77	0.47

<u>0.56 M p-Ethylbenzoic Acid in Polystyrene Matrix</u>						
214.0	194.23	2.91	0.22	1.17	2.45	0.32
219.6	86.15	3.27	0.22	1.20	2.45	0.33
244.0	58.62	3.43	0.23	1.22	2.45	0.32
229.2	34.38	3.67	0.21	1.21	2.45	0.34
231.7	31.27	3.71	0.22	1.24	2.44	0.33
238.7	14.10	4.05	0.22	1.27	2.45	0.35
245.9	8.12	4.29	0.17	1.25	2.44	0.40

<u>6.39 M 4-Biphenylcarboxylic Acid in Compressed Solid</u>						
176.8	226.57	2.85	0.40	0.53	3.25	0.00
180.5	144.57	3.04	0.43	0.55	3.25	0.00
188.3	69.72	3.36	0.48	0.55	3.25	0.00
194.8	41.83	3.58	0.37	0.55	3.25	0.04
201.9	21.52	3.87	0.48	0.55	3.24	0.00

<u>7.38 M 2-Naphthoic Acid in Compressed Solid</u>						
212.4	405.87	2.59	0.30	4.19	3.04	0.13
218.8	171.49	2.97	0.29	4.63	3.03	0.14
224.5	96.38	3.22	0.33	4.96	3.03	0.13
229.8	44.01	3.56	0.35	5.21	3.03	0.13
234.8	30.16	3.72	0.37	5.62	3.02	0.14
239.0	15.83	4.00	0.27	5.83	3.02	0.16
244.8	8.82	4.26	0.27	6.03	3.02	0.17

TABLE VI.3 Tabulated Summary of Fuoss-Kirkwood Analysis
Parameters and Effective Dipole Moments (μ)
for Salicylic Acid and Some Esters.

T(K)	$10^6 \tau$ (s)	$\log f_{\max}$	β	$10^3 \epsilon''_{\max}$	ϵ_{∞}	μ (D)
<u>9.50 M Salicylic Acid in Compressed Solid</u>						
113.5	787.39	2.31	0.83	0.15	2.95	0.00
120.8	266.30	2.78	0.59	0.17	2.95	0.00
127.8	129.59	3.09	0.51	0.18	2.95	0.00
134.5	51.12	3.49	0.42	0.18	2.95	0.00
141.5	29.40	3.73	0.32	0.15	2.95	0.00
145.5	24.20	3.82	0.40	0.15	2.95	0.00
<u>6.40 M Methylsalicylate in Compressed Solid</u>						
172.9	189.01	2.93	0.42	9.47	3.45	0.14
177.6	142.26	3.05	0.30	6.74	2.94	0.16
184.2	91.60	3.24	0.30	7.24	2.94	0.17
189.8	46.03	3.54	0.32	7.70	2.94	0.17
195.2	38.05	3.62	0.38	7.96	2.94	0.16
205.4	16.83	3.98	0.40	8.47	2.94	0.17
<u>0.56 M Methylsalicylate in Polystyrene Matrix</u>						
178.1	1053.10	2.18	0.19	15.82	2.42	1.14
184.9	451.07	2.55	0.19	16.49	2.42	1.19
189.8	191.93	2.92	0.20	17.04	2.42	1.19
193.9	119.04	3.13	0.20	17.65	2.42	1.23
199.1	65.06	3.39	0.20	18.14	2.41	1.26
205.0	27.77	3.76	0.20	18.71	2.41	1.30
213.2	12.42	4.11	0.20	19.30	2.40	1.35
<u>4.92 M Phenylsalicylate in Compressed Solid</u>						
152.7	684.54	2.37	0.52	3.59	3.26	0.09
160.4	259.84	2.79	0.56	3.83	3.26	0.09
170.0	147.32	3.03	0.51	4.35	3.24	0.10
178.5	61.54	3.41	0.39	4.51	3.24	0.12
187.7	34.62	3.66	0.42	4.74	3.24	0.12
196.2	15.14	4.02	0.39	4.86	3.22	0.13
202.7	10.16	4.20	0.39	4.98	3.22	0.14
211.0	6.94	4.36	0.36	5.05	3.22	0.15

TABLE VI.3

continued...

T(K)	$10^6 \tau$ (s)	$\log f_{\max}$	β	$10^3 \epsilon''_{\max}$	ϵ_{∞}	μ (D)
<u>0.39 M Phenylsalicylate in Polystyrene Matrix</u>						
233.5	685.00	2.37	6.16	9.39	2.54	1.29
238.0	471.19	2.53	0.15	9.57	2.53	1.36
242.7	226.39	2.85	0.17	9.83	2.54	1.30
247.8	140.02	3.06	0.17	10.01	2.54	1.33
253.6	75.55	3.32	0.17	10.22	2.53	1.36
259.1	40.18	3.60	0.17	10.50	2.53	1.39
265.3	17.03	3.97	0.16	10.88	2.52	1.48
272.6	8.83	4.26	0.16	11.29	2.52	1.53
<u>1.00 M Methylchloroformate in Polystyrene Matrix</u>						
150.4	763.82	2.32	0.34	3.51	2.59	0.27
157.7	296.53	2.73	0.35	3.73	2.59	0.28
165.6	92.47	3.24	0.41	4.05	2.59	0.28
171.4	74.40	3.33	0.34	4.23	2.59	0.32
177.9	32.32	3.69	0.41	4.58	2.59	0.30
183.2	23.74	3.83	0.36	4.90	2.59	0.34
<u>0.78 M Ethylchloroformate in Polystyrene Matrix</u>						
127.1	1126.90	2.15	0.14	2.67	2.18	.42
133.7	275.18	2.76	0.15	2.82	2.18	.43
138.7	159.49	3.00	0.15	2.97	2.18	.44
143.3	69.94	3.36	0.15	3.06	2.15	.46
147.5	44.87	3.55	0.15	3.19	2.17	.48
153.5	23.34	3.83	0.16	3.38	2.17	.48
<u>0.63 M Chloroformate in Polystyrene Matrix</u>						
158.6	864.51	2.27	0.18	16.84	2.58	1.04
165.8	319.86	2.70	0.18	17.62	2.58	1.14
172.0	164.89	2.98	0.18	18.71	2.57	1.19
177.8	75.12	3.33	0.18	19.65	2.57	1.23
183.5	37.97	3.62	0.18	20.43	2.56	1.36
190.3	21.56	3.87	0.17	21.39	2.44	1.38
196.9	10.65	4.17	0.18	22.62	2.45	1.46
205.3	5.94	4.43	0.17	23.49	2.46	1.46

TABLE VI.3

continued...

T(K)	$10^6 \tau$ (s)	$\log f_{\max}$	β	$10^3 \epsilon''_{\max}$	ϵ_{∞}	μ (D)
<u>0.66 M Isobutyl chloroformate in P.S.</u>						
143.4	765.42	2.32	0.19	14.83	2.52	0.89
150.2	305.76	2.72	0.18	15.58	2.51	0.96
156.0	152.70	3.02	0.19	16.35	2.43	1.00
159.1	94.19	3.23	0.18	16.85	2.42	1.05
164.4	48.30	3.52	0.18	17.53	2.42	1.10
171.9	20.85	3.88	0.19	18.59	2.43	1.14
178.5	11.02	4.16	0.20	19.57	2.44	1.13
184.2	6.14	4.41	0.20	20.28	2.44	1.17

Table VI-4: Tabulated Summary of Fuoss-Kirkwood Analysis
Parameters for H Bonding Acid-Base Systems

T(K)	$10^6 \tau$ (s)	$\log f_{\max}$	β	$10^3 \epsilon''_{\max}$	ϵ_{∞}
<u>Formic Acid + Pyridine in Polystyrene Matrix</u>					
<u>Low Temperature Absorption</u>					
188.3	693.84	2.36	0.20	10.07	2.87
194.5	300.75	2.72	0.20	10.50	2.86
203.2	102.65	3.19	0.21	11.23	2.86
210.5	39.76	3.60	0.18	11.72	2.80
218.4	18.47	3.94	0.18	12.63	2.80
225.6	9.09	4.24	0.21	13.06	2.81
<u>High Temperature Absorption</u>					
275.7	156.56	3.00	0.21	13.20	2.85
281.1	96.10	3.22	0.23	13.11	2.85
287.0	56.06	3.45	0.24	13.10	2.86
293.5	45.59	3.54	0.29	10.85	2.53
301.0	21.24	3.87	0.29	10.68	2.53
312.6	9.91	4.21	0.31	10.15	2.53
<u>Formic Acid + Dioxane in Polystyrene Matrix</u>					
<u>Low Temperature Absorption</u>					
184.0	796.22	2.30	0.21	2.01	2.70
189.8	323.95	2.69	0.23	2.06	2.70
195.0	177.16	2.95	0.23	2.11	2.70
199.0	109.88	3.16	0.24	2.10	2.70
202.6	82.82	3.28	0.25	2.04	2.72
207.9	65.00	3.39	0.25	2.09	2.70
<u>High Temperature Absorption</u>					
240.4	187.49	2.93	0.18	2.60	2.71
246.3	90.74	3.24	0.20	2.65	2.71
249.2	66.00	3.38	0.22	2.68	2.71
252.5	42.61	3.57	0.23	2.71	2.71
258.0	24.10	3.82	0.27	2.75	2.71

Table VI-4, cont'd....

T(K)	$10^6 \tau$ (s)	$\log f_{\max}$	β	$10^3 \epsilon''_{\max}$	ϵ_{∞}
<u>Formic Acid + Methyl Cyanide in Polystyrene Matrix</u>					
184.5	327.75	2.69	0.25	0.49	2.38
189.1	93.38	3.23	0.23	0.72	2.37
193.2	57.48	3.44	0.21	0.72	2.37
198.4	39.58	3.60	0.21	0.73	2.37
203.5	30.99	3.88	0.20	0.76	2.37
208.3	14.67	4.04	0.17	0.74	2.37
<u>Acetic Acid + Pyridine in Polystyrene Matrix</u>					
194.9	1244.80	2.11	0.23	9.29	2.68
200.1	668.21	2.38	0.23	9.58	2.68
205.0	378.00	2.62	0.22	9.75	2.68
209.7	205.28	2.89	0.23	10.07	2.68
214.4	135.06	3.07	0.21	10.23	2.67
219.4	82.27	3.29	0.18	10.48	2.66
226.7	35.24	3.65	0.17	10.78	2.66
233.9	17.79	3.95	0.19	11.16	2.66
<u>Acetic Acid + Dioxane in Polystyrene Matrix</u> <u>Low Temperature Absorption</u>					
204.4	444.55	2.55	0.18	1.19	2.53
208.2	251.81	2.80	0.20	1.19	2.53
212.6	126.58	3.09	0.18	1.20	2.53
217.0	82.25	3.29	0.24	1.21	2.53
221.8	59.69	3.43	0.24	1.20	2.53
226.7	36.81	3.64	0.24	1.19	2.53
232.3	22.78	3.84	0.32	1.19	2.53
<u>High Temperature Absorption</u>					
287.6	230.39	2.84	0.17	1.36	2.53
293.3	136.25	3.07	0.21	1.33	2.53
297.8	97.30	3.21	0.19	1.34	2.53
303.0	86.64	3.26	0.19	1.31	2.53
308.5	57.06	3.45	0.16	1.25	2.53
314.9	40.45	3.60	0.25	1.22	2.53

Table VI-4, cont'd....

T (K)	$10^6 \tau$ (s)	$\log f_{\max}$	β	$10^3 \epsilon''_{\max}$	ϵ_{∞}
<u>Acetic Acid + Methyl Cyanide in Polystyrene Matrix</u>					
147.0	569.68	2.45	0.41	0.67	2.47
164.0	150.11	3.03	0.37	0.84	2.47
171.9	84.73	3.27	0.47	0.91	2.47
179.2	66.23	3.38	0.28	0.95	2.47
189.3	42.89	3.57	0.31	1.04	2.47
<u>Benzoic Acid + Pyridine in Polystyrene Matrix</u> <u>Low Temperature Absorption</u>					
148.0	585.43	2.43	0.18	2.63	2.71
152.2	342.87	2.67	0.16	2.72	2.70
158.4	208.09	2.88	0.17	2.85	2.70
162.8	123.69	3.11	0.20	2.93	2.70
168.2	77.95	3.31	0.22	3.04	2.70
175.8	51.00	3.49	0.17	3.17	2.69
183.0	32.45	3.69	0.18	3.37	2.69
<u>High Temperature Absorption</u>					
308.8	1214.40	2.12	0.19	7.22	2.32
312.6	751.94	2.33	0.20	7.22	2.28
316.7	506.23	2.50	0.19	7.14	2.24
321.0	233.01	2.83	0.19	7.16	2.25
323.8	153.94	3.01	0.20	7.24	2.26
327.6	92.53	3.24	0.20	7.27	2.27
<u>Benzoic Acid + 1,4-Dioxane in Polystyrene Matrix</u> <u>Low Temperature Absorption</u>					
163.2	248.76	2.81	0.20	4.23	2.76
168.3	121.75	3.12	0.20	4.40	2.75
173.5	81.13	3.29	0.19	4.55	2.75
178.6	50.10	3.50	0.19	4.72	2.75
183.7	36.25	3.64	0.19	4.88	2.75
188.9	22.59	3.85	0.18	5.02	2.75

Table VI-4, cont'd....

T (K)	$10^6 \tau$ (s)	$\log f_{\max}$	β	$10^3 \epsilon''_{\max}$	ϵ_{∞}
<u>High Temperature Absorption</u>					
290.7	1480.9	2.03	0.16	1.95	2.43
297.3	803.92	2.30	0.16	1.90	2.43
302.5	429.25	2.57	0.18	1.87	2.43
307.7	280.63	2.75	0.19	1.85	2.43
313.3	136.98	3.07	0.16	1.86	2.43
317.4	96.60	3.22	0.13	1.87	2.43

TABLE VI.5
EYRING ANALYSIS RESULTS FOR SOME CARBOXYLIC ACIDS

MOLECULE	T (K)	τ (s)			ΔG_E (kJ mol ⁻¹)			ΔH_E (kJ mol ⁻¹)	ΔS_E (J K ⁻¹ mol ⁻¹)
		100 K	200 K	300 K	100 K	200 K	300 K		
Formic Acid (PS)	237-257	4.7×10^{10}	2.5×10^{-2}	1.7×10^{-6}	44.0	42.2	40.0	46	18
Acetic Acid (PS)	239-257	4.8×10^{11}	4.0×10^{-2}	1.5×10^{-6}	46.0	43.0	40.0	49	30
Propionic Acid (PS)	192-217	1.7×10^{10}	2.0×10^{-4}	3.8×10^{-9}	43.2	34.2	25.1	52	90
Butyric Acid (PS)	82-114	3.7×10^{-5}	9.1×10^{-8}	1.0×10^{-8}	15.1	21.4	27.6	9	-62
	205-231	2.1×10^{-4}	2.9×10^{-4}	1.3×10^{-7}	35.7	34.8	33.9	~37	9
Valeric Acid (PS)	88-113	6.0×10^{-5}	5.8×10^{-8}	4.8×10^{-9}	15.5	20.6	25.7	10	-51
	224-255	3.6×10^8	4.8×10^{-3}	9.5×10^{-7}	40.0	39.4	38.9	~41	53
Trichloroacetic Acid (PS)	105-141	2.3×10^{-3}	9.9×10^{-8}	2.9×10^{-9}	18.5	21.5	24.5	~16	-30
	222-252	2.3×10^{13}	1.2×10^{-2}	7.9×10^{-8}	49.2	40.9	32.7	57	82
Benzoic Acid (PS)	147-190	1.4	6.1×10^{-6}	8.4×10^{-8}	23.8	28.4	32.9	19	-45
	218-246	9.1×10^8	3.3×10^8	4.2×10^{-7}	40.7	38.8	36.9	43	19
p-Ethylbenzoic Acid (PS)	214-245	9.2×10^7	9.4×10^{-4}	1.8×10^{-4}	38.7	36.7	34.7	41.	20
Biphenylcarboxylic Acid (CS)	176-201	2.9×10^2	2.5×10^{-5}	9.4×10^{-8}	28.3	30.7	33.1	26	-24
2-Naphthoic Acid (CS)	212-244	3.1×10^{10}	2.5×10^{-3}	8.9×10^{-8}	43.7	38.3	33.0	49	53

TABLE VI.6 EYRING ANALYSIS RESULTS FOR SALICYLIC ACID AND SOME ESTERS

MOLECULE	T (K)	τ (s)				ΔG_E (kJ mol ⁻¹)				ΔH_E (kJ mol ⁻¹)	ΔS_E (J K ⁻¹ mol ⁻¹)
		100 K	200 K	300 K	300 K	100 K	200 K	300 K	300 K		
Salicylic Acid (CS)	113-146	6.4×10^{-3}	6.4×10^{-3}	2.5×10^{-8}	19.4	24.6	29.8	14	-52		
Methylsalicylate (CS)	170-205	1.3×10^1	2.5×10^{-5}	2.6×10^{-7}	25.7	30.7	35.7	21	-49		
Methylsalicylate (PS)	178-213	1.7×10^6	5.5×10^{-5}	1.5×10^{-8}	35.5	32.0	28.5	39	35		
Phenylsalicylate (CS)	152-211	3.7	1.3×10^{-5}	1.7×10^{-7}	24.7	29.6	34.6	20	-49		
Phenylsalicylate (PS)	234-273	3.5×10^{14}	1.3×10^{-1}	8.2×10^{-7}	51.4	45.0	35.5	58	65		
Methylchloroformate (PS)	150-183	1.2×10^1	5.5×10^{-6}	3.7×10^{-8}	25.6	28.2	30.8	23	-25		
Ethylchloroformate (PS)	127-154	5.2×10^{-1}	2.1×10^{-7}	1.3×10^{-9}	23.0	22.7	22.4	23	-3		
n-Butylchloroformate (PS)	158-205	3.1×10^2	8.6×10^{-6}	2.2×10^{-8}	28.4	28.9	29.5	27	-6		
Iso-Butylchloroformate (PS)	143-184	9.9	1.6×10^{-6}	7.3×10^{-9}	25.5	26.1	26.8	25	-6		

TABLE VI - 7: EYRING ANALYSIS RESULTS FOR SOME H BONDING ACID-BASE SYSTEMS

SYSTEM IN PS	TEMPERATURE RANGE (K)	Relaxation Time τ (s)			ΔG_E (kJ mol ⁻¹)			ΔH_E kJ mol ⁻¹	ΔS_E J K ⁻¹ mol ⁻¹
		100 K	200 K	300 K	100 K	200 K	300 K		
Formic acid + Pyridine	188 - 225	6.2×10^{16}	1.5×10^{-4}	3.6×10^{-8}	36.6	33.6	30.7	~40	29
	275 - 312	3.3×10^{13}	9.0×10^{-1}	2.3×10^{-5}	49.0	48.0	47.0	51	13
Formic acid + 1,4-Dioxane	184 - 202	6.2×10^5	1.0×10^{-4}	4.7×10^{-8}	34.7	33.0	31.4	36	16
	240 - 260	2.1×10^{14}	7.8×10^{-2}	4.7×10^{-7}	51.0	44.1	37.2	58	69
Formic acid + Methylcyanide	189 - 208	4.0×10^3	3.1×10^{-5}	5.2×10^{-8}	30.5	31.1	31.6	30	-6
Acetic acid + Pyridine	194 - 233	2.4×10^7	6.7×10^{-4}	1.7×10^{-7}	37.7	36.2	34.6	39	16
Acetic acid + 1,4-Dioxane	204 - 232	2.1×10^7	6.5×10^{-4}	1.7×10^{-7}	37.6	36.1	34.6	39	15
	287 - 314	4.1×10^{11}	8.8×10^{-1}	9.5×10^{-5}	45.8	48.1	50.4	~54	22
Benzoic acid + Pyridine	148 - 183	6.5×10^{-1}	1.0×10^{-5}	2.2×10^{-7}	23.2	29.2	35.3	17	-60
	308 - 327	-	-	-	-	-	-	114	-
Benzoic acid + 1,4-Dioxane	163 - 193	1.4×10^1	8.9×10^{-6}	6.3×10^{-8}	25.8	29.0	32.2	~23	-31
	290 - 317	1.2×10^{24}	4.4×10^3	5.7×10^{-3}	69.7	62.3	54.8	77	74

PS - Polystyrene matrix; blank space indicates the unavailability of information.

TABLE VI - 8: COMPARATIVE EYRING ANALYSIS RESULTS FOR THE PROCESS I* IN ACID-BASE SYSTEMS AND FOR MOLECULAR RELAXATION OF SOME RIGID MOLECULES

SYSTEM IN PS	ABSORPTION TEMP T (K)	$\tau_{200 \text{ K}}$ (s)	$\Delta G_{E200 \text{ K}}$ (kJ mol ⁻¹)	ΔH_E (kJ mol ⁻¹)	ΔS_E (J K ⁻¹ mol ⁻¹)
Formic acid + Pyridine	188 - 225	1.5×10^{-4}	33.6	~40	29
Formic acid + 1,4-Dioxane	184 - 202	1.0×10^{-4}	33.0	36	16
Acetic acid + 1,4-Dioxane	204 - 232	6.5×10^{-4}	36.1	39	15
Acetic acid + Pyridine	194 - 233	6.7×10^{-4}	36.2	39	16
p-Iodotoluene**	199 - 241	3.1×10^{-4}	35	42	33
p-Bromoethylbenzene**	206 - 254	6.9×10^{-4}	36	38	9
p-Tolunitrile‡	196 - 244	4.3×10^{-4}	35.4	37	7

* For definition see text; ** Ref. 39; ‡ Ref. 42; PS - Polystyrene matrix

TABLE VI-9: COMPARATIVE EYRING ANALYSIS RESULTS FOR THE PROCESS II* IN ACID-BASE SYSTEMS AND FOR THE PROCESS A* IN ACIDS

SYSTEM IN PS	ABSORPTION TEMP T (K)	$\tau_{200\text{ K}}$ (s)	$\Delta G_{E200\text{ K}}$ (kJ mol ⁻¹)	ΔH_E (kJ mol ⁻¹)	ΔS_E (J K ⁻¹ mol ⁻¹)
Formic acid + Pyridine	275 - 312	9.0×10^{-1}	48.0	51	13
Formic acid + 1,4-Dioxane	240 - 260	7.8×10^{-2}	44.1	58	69
Formic Acid	237 - 257	2.5×10^{-2}	42.2	46	18
Acetic acid + 1,4-Dioxane	287 - 314	8.8×10^{-1}	48.1	54	22
Acetic acid	239 - 257	4.0×10^{-2}	43	49	30
Trichloroacetic acid	222 - 252	1.2×10^{-2}	40.9	57	82

* For definition see text; PS - polystyrene matrix

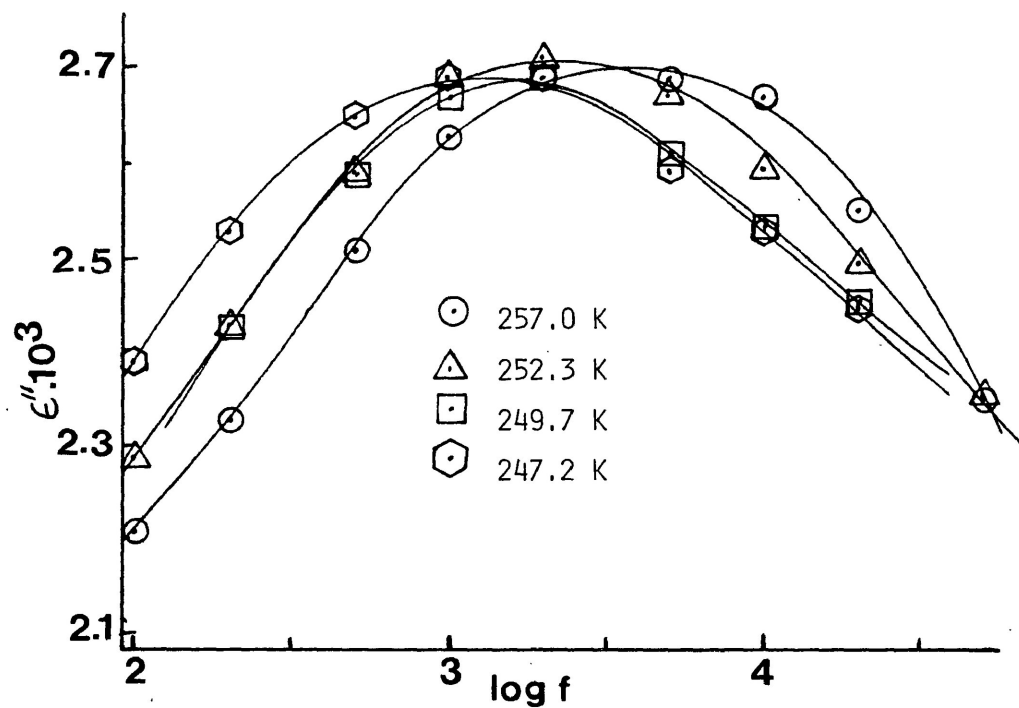


FIGURE VI.1. PLOTS OF DIELECTRIC LOSS FACTOR (ϵ'') VERSUS LOG OF FREQUENCY FOR ACETIC ACID AT DIFFERENT TEMPERATURES.

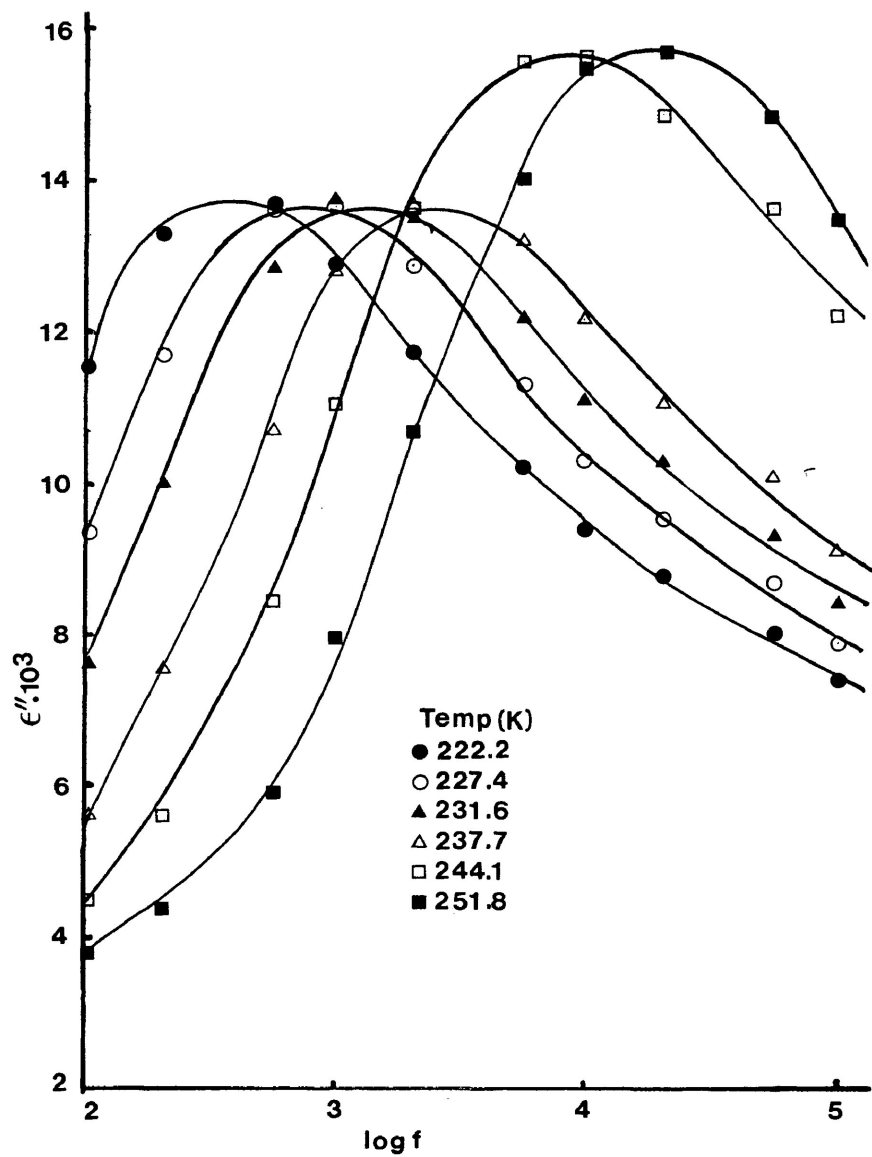


FIGURE VI.2. PLOTS OF DIELECTRIC LOSS FACTOR (ϵ'') VERSUS LOG OF FREQUENCY FOR TRICHLOROACETIC ACID AT DIFFERENT TEMPERATURES.

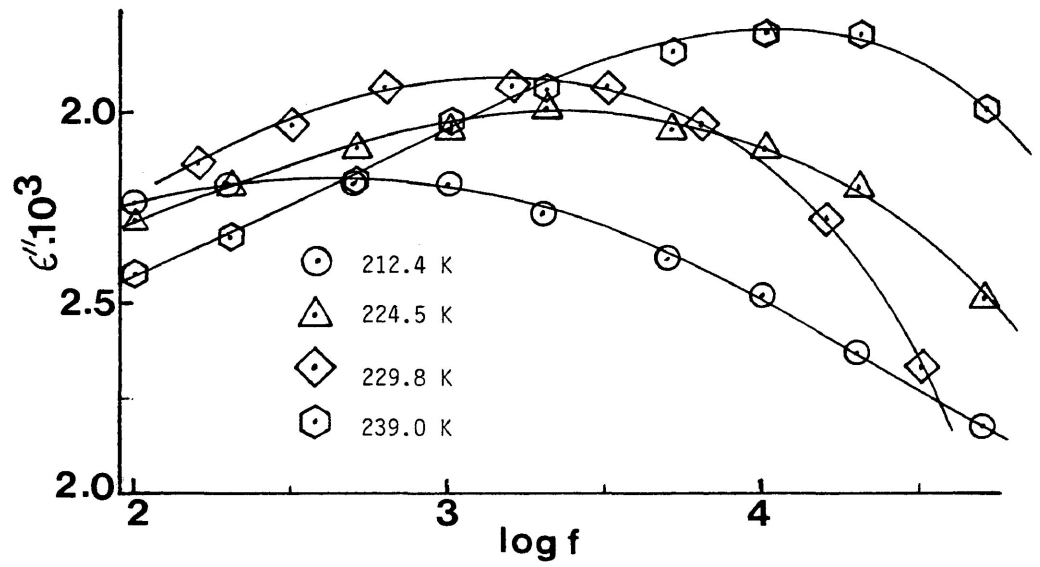


FIGURE VI.3. PLOTS OF DIELECTRIC LOSS FACTOR (ϵ'') VERSUS LOG OF FREQUENCY FOR 2-NAPHTHOIC ACID AT DIFFERENT TEMPERATURES.

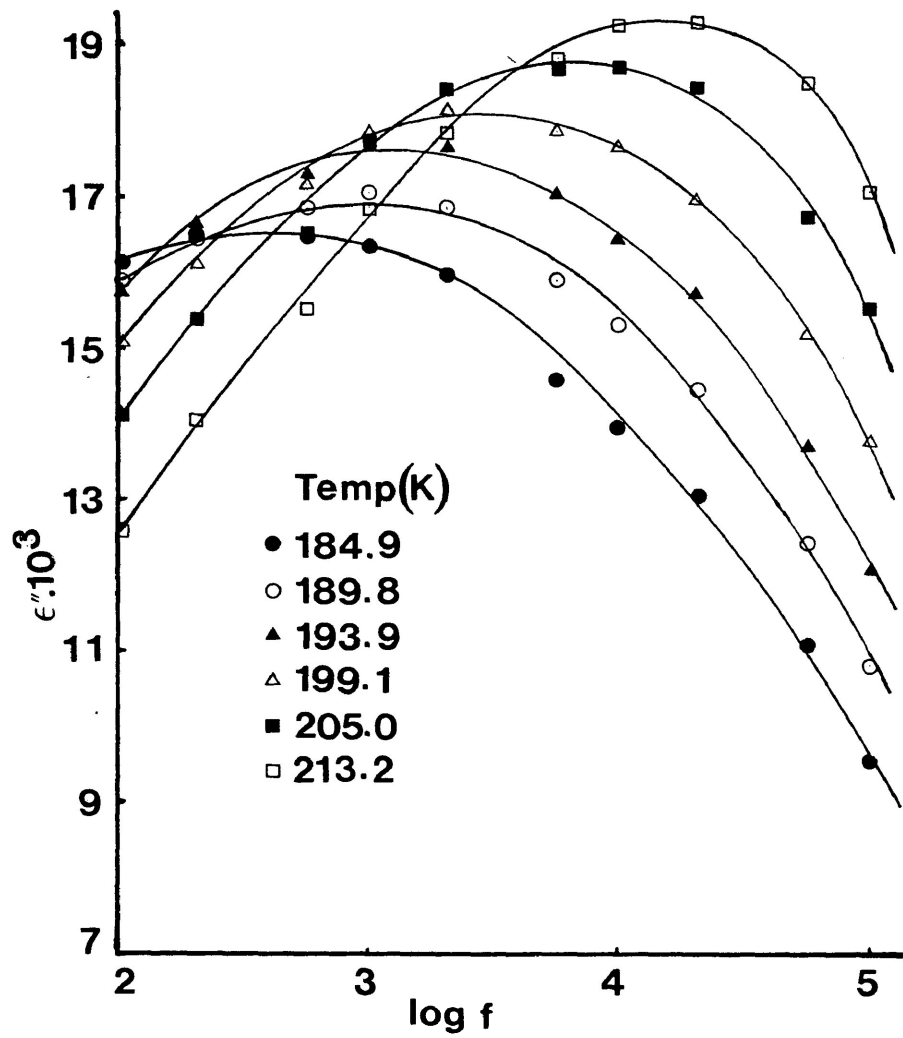


FIGURE VI.4. PLOTS OF DIELECTRIC LOSS FACTOR (ϵ'') VERSUS LOG OF FREQUENCY FOR METHYLSALICYLATE AT DIFFERENT TEMPERATURES.

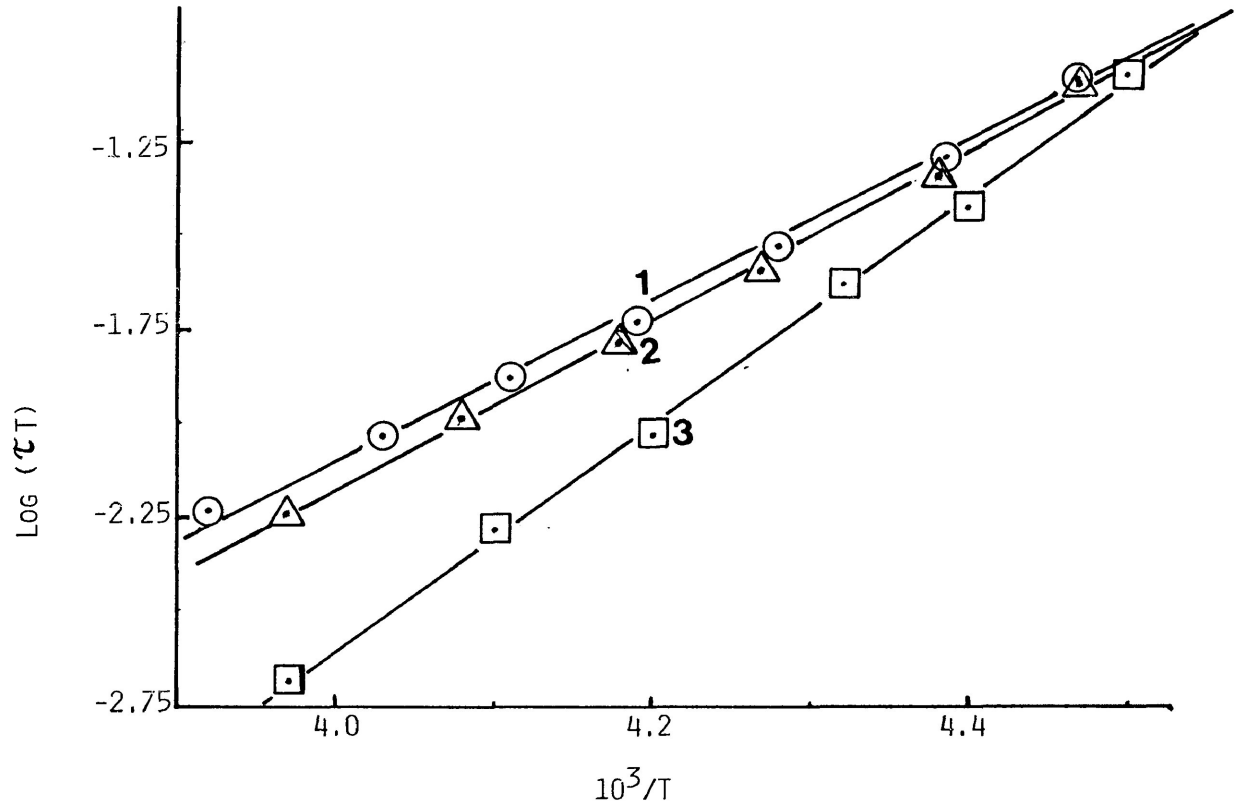


FIGURE VI.5. EYRING PLOTS OF $\log(\tau T)$ VERSUS $\frac{1}{T}$ FOR VALERIC ACID (1), TRICHLOROACETIC ACID (2) AND BENZOIC ACID (3).

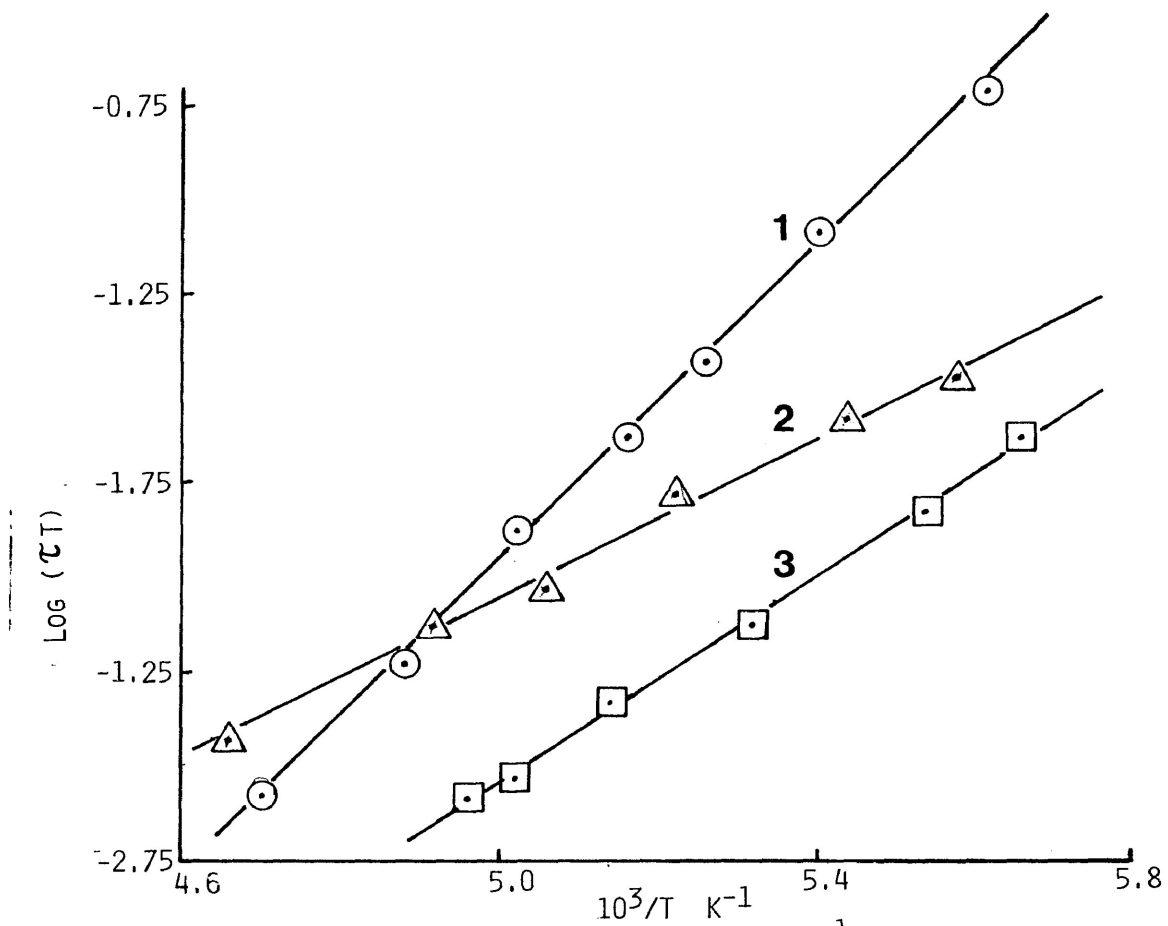


FIGURE VI.6. EYRING PLOTS OF $\log(\tau T)$ VERSUS $\frac{1}{T}$ FOR METHYLSALICYLATE IN A POLYSTYRENE MATRIX (1), IN COMPRESSED SOLID (2), AND IN 4-BIPHENYLCARBOXYLIC ACID.

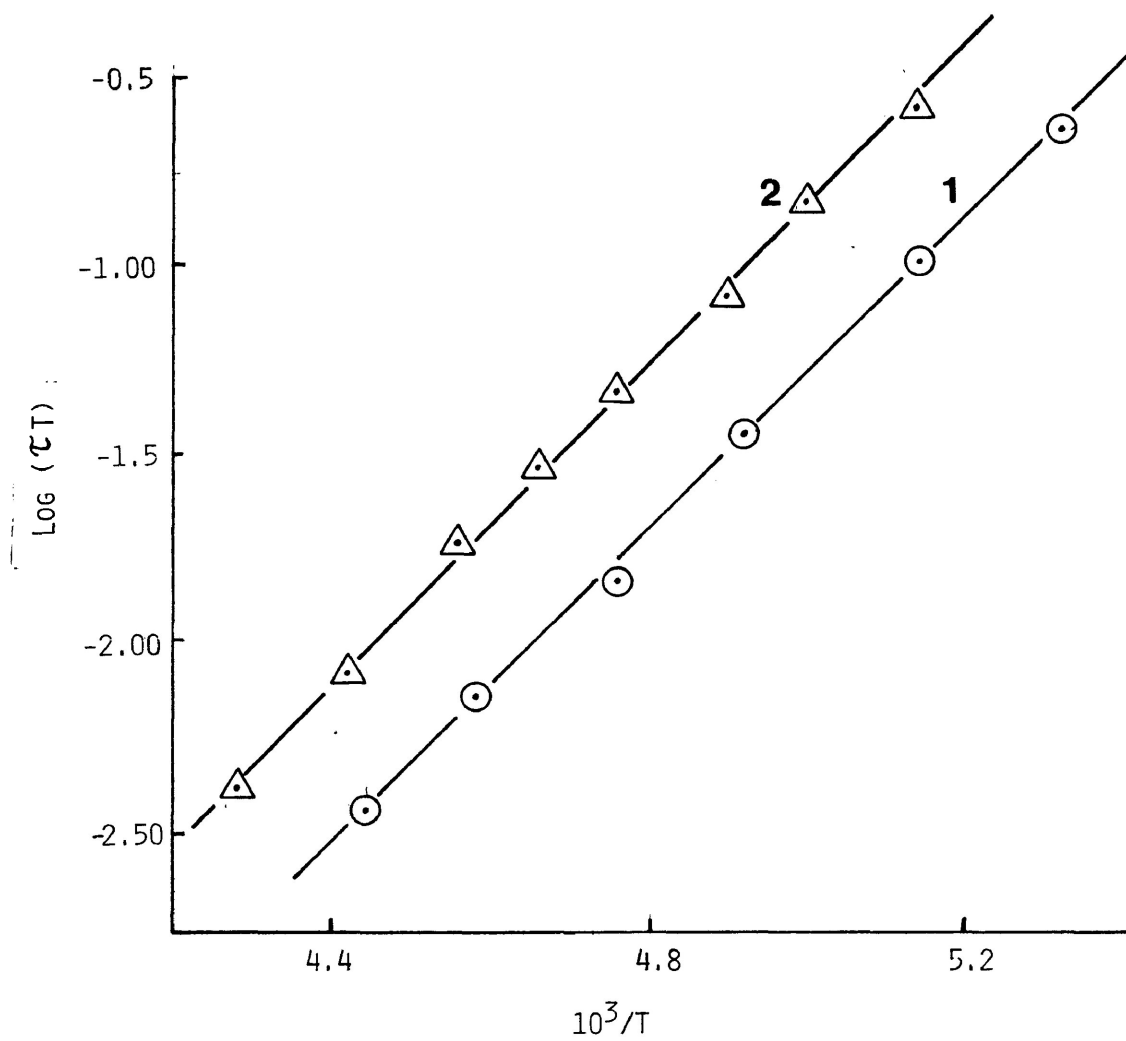


FIGURE VI.7. EYRING PLOTS OF $\log \tau T$ VERSUS $\frac{1}{T}$ FOR LOW TEMPERATURE PROCESSES IN FORMIC ACID+PYRIDINE (1) AND ACETIC ACID+PYRIDINE (2).